NUREG/CR-6439
BMI-2189

Design of the IPIRG-2 Simulated Seismic Forcing Function

Prepared by
R. Olson, P. Scott, G. Wilkowski

Battelle

Prepared for
U.S. Nuclear Regulatory Commission

AVAILABILITY NOTICE

Availability of Reference Materials Cited in NRC Publications

Most documents cited in NRC publications will be available from one of the following sources:

1. The NRC Public Document Room, 2120 L Street, NW., Lower Level, Washington, DC 20555-0001

2. The Superintendent of Documents, U.S. Government Printing Office, P. O. Box 37082, Washington, DC 20402-9328

3. The National Technical Information Service, Springfield, VA 22161-0002

Although the listing that follows represents the majority of documents cited in NRC publications, it is not intended to be exhaustive.

Referenced documents available for inspection and copying for a fee from the NRC Public Document Room include NRC correspondence and internal NRC memoranda; NRC bulletins, circulars, information notices, inspection and investigation notices; licensee event reports; vendor reports and correspondence; Commission papers; and applicant and licensee documents and correspondence.

The following documents in the NUREG series are available for purchase from the Government Printing Office: formal NRC staff and contractor reports, NRC-sponsored conference proceedings, international agreement reports, grantee reports, and NRC booklets and brochures. Also available are regulatory guides, NRC regulations in the *Code of Federal Regulations*, and *Nuclear Regulatory Commission Issuances*.

Documents available from the National Technical Information Service include NUREG-series reports and technical reports prepared by other Federal agencies and reports prepared by the Atomic Energy Commission, forerunner agency to the Nuclear Regulatory Commission.

Documents available from public and special technical libraries include all open literature items, such as books, journal articles, and transactions. *Federal Register* notices, Federal and State legislation, and congressional reports can usually be obtained from these libraries.

Documents such as theses, dissertations, foreign reports and translations, and non-NRC conference proceedings are available for purchase from the organization sponsoring the publication cited.

Single copies of NRC draft reports are available free, to the extent of supply, upon written request to the Office of Administration, Distribution and Mail Services Section, U.S. Nuclear Regulatory Commission, Washington, DC 20555-0001.

Copies of industry codes and standards used in a substantive manner in the NRC regulatory process are maintained at the NRC Library, Two White Flint North, 11545 Rockville Pike, Rockville, MD 20852-2738, for use by the public. Codes and standards are usually copyrighted and may be purchased from the originating organization or, if they are American National Standards, from the American National Standards Institute, 1430 Broadway, New York, NY 10018-3308.

DISCLAIMER NOTICE

NUREG/CR-6439
BMI-2189

Design of the IPIRG-2 Simulated Seismic Forcing Function

Manuscript Completed: January 1996
Date Published: February 1996

Prepared by
R. Olson, P. Scott, G. Wilkowski

Battelle
505 King Avenue
Columbus, OH 43201-2693

M. Mayfield, NRC Project Manager

Prepared for
Division of Engineering Technology
Office of Nuclear Regulatory Research
U.S. Nuclear Regulatory Commission
Washington, DC 20555-0001
NRC Job Code D2060

ABSTRACT

A series of pipe system experiments was conducted in IPIRG-2 that used a realistic seismic forcing function. Because the seismic forcing function was more complex than the single-frequency increasing-amplitude sinusoidal forcing function used in the IPIRG-1 pipe system experiments, considerable effort went into designing the function. This report documents the design process for the seismic forcing function used in the IPIRG-2 pipe system experiments.

CONTENTS

CONTENTS

CONTENTS

Page

LIST OF FIGURES

CONTENTS

CONTENTS

CONTENTS

Page

LIST OF TABLES

EXECUTIVE SUMMARY

The procedure for designing and scaling a "seismically inspired" forcing function for the IPIRG-2 simulated seismic pipe system experiments is presented. The objective of the study was to define the actuator motion for three load levels; a safe shut-down earthquake level which, if the current design procedures are conservative, should cause no apparent damage, a "test" level excitation which should cause test flaws in the IPIRG pipe system to propagate, and a "decision tree" excitation to be applied if the "test" level loading does not grow the test flaws.

The design process used design tools and modeling assumptions that are consistent with nuclear plant analysis and design details. Ground acceleration served as the driving force for a simple nuclear plant model, which was then assumed to be coupled to the IPIRG pipe system. The resulting pipe motion was then modified and scaled to define time histories of actuator displacement for the IPIRG-2 simulated seismic pipe system experiments. In contrast to typical plant design, however, the analyses focussed on the time domain, because in the IPIRG-2 experiments we are concerned about a significantly nonlinear event involving the growth of large cracks.

The data assumed for the analyses were quite realistic, aside from the idealizations embodied in the IPIRG pipe loop itself. Hence, the IPIRG simulated seismic experimental data should be reasonably representative of the behavior of actual plant piping if it were to contain large flaws while under severe seismic loading. The data also provide unique information for validation of in-service flaw evaluation and leak-before-break (LBB) procedures. Additionally, the cracked-pipe super-element developed in the IPIRG program allows for sophisticated analyses to more realistically assess pipe system fracture behavior other than by using uncracked pipe peak elastic stresses.

ACKNOWLEDGMENTS

The IPIRG-2 Program was an international group research program coordinated by the U.S. Nuclear Regulatory Commission through the Electrical, Materials and Mechanical Engineering Branch of the Office of Nuclear Regulatory Research under Contract No. NRC-04-91-063 to Battelle. Mr. M. Mayfield was the USNRC program manager. Dr. A. Hopper was the Battelle program manager.

The members of the IPIRG-2 Program and their representatives to the IPIRG Technical Advisory Group (TAG) were:

Bulgaria	
- CUAEPP	Mr. Y. Yanev
Canada	
- AECB	Mr. B. Jarman and Mr. K. Pereira
- Ontario Hydro	Mr. M. Kozluk
Czech Republic	
- NRI	Dr. J. Zdárek, Dr. M. Brumovsky, Dr. P. Kadečka, Mr. J. Palyza
France	
- CEA	Ms. F. Gantenbein, Mr. E. Debec-Mathet
- EDF	Mr. C. Faidy, Mr. P. Le Delliou
- Framatome	Dr. Ph. Gilles
Hungary	
- HAEC	Mr. A. Fehérvári
Italy	
- ANPA-DISP	Dr. C. Maricchiolo
Japan	
- CREIPI	Dr. K Kashima, Mr. N. Miura
Lithuania	
- VATESI	Mr. P. Vaisnys
Republic of Korea	
- KINS	Dr. J. B. Lee, Dr. Y. H. Choi
- SKKU	Dr. Y. J. Kim
Republic of China	
- INER/AEC	Dr. Li-Fu Lin

Slovak Republic

- VUJE	Dr. L. Kupca
- NRA	Dr. J. Misak

Sweden

- SKI	Dr. G. Hedner
- SA	Dr. B. Brickstad

Switzerland

- KKL	Mr. R. Wanner
- HSK	Dr. D. H. Njo

United Kingdom

- Nuclear Electric, plc	Dr. T. Chivers

United States

- USNRC-RES	Mr. M. Mayfield
- USNRC-NRR	Mr. K. Wichman
- EPRI	Mr. S. Gosselin, Dr. Y. K. Tang

We would like to acknowledge the many contributions of the IPIRG-2 TAG members to the success of this program.

NOMENCLATURE

1. Symbols

A_i	Sine series coefficient
f_i	Sine series frequency in Hertz
C	Damping
[C]	Structural damping matrix
I	Mass moment of inertia
I(t)	Deterministic earthquake enveloping function
%I	Percent of loading due to pipe inertial loading
K	Stiffness
[K]	Structural stiffness matrix
M	Mass
[M]	Structural mass matrix
M_t	Total moment
M_{sp}	Moment due to a static push
R	Stress ratio - minimum stress divided by maximum stress
S_m	ASME code design stress intensity
S_y	ASME Section III yield strength
t	Time
{U}	Structure displacement
{$\dot{U}$}	Structure velocity
{$\ddot{U}$}	Structure acceleration
x, y, z	Orthogonal coordinate directions

$\{\ddot{X}\}$	Ground acceleration
ϕ_i	Random phase angle

2. Acronyms and Initialisms

ASCE	American Society of Civil Engineers
ASME	American Society of Mechanical Engineers
BWR	Boiling Water Reactor
B&W	Babcock and Wilcox
DEGB	Double-ended guillotine break
EPRI	Electric Power Research Institute
FOAKE	First of a kind engineering
NSSS	Nuclear steam supply system
IPIRG-1	First International Piping Integrity Research Group
IPIRG-2	Second International Piping Integrity Research Group
N	Normal operating loading
NRC	Nuclear Regulatory Commission
N+SSE	Normal operating plus safe shut-down earthquake loading
OBE	Operating basis earthquake
PSD	Power spectral density
PWR	Pressurized water reactor
SRP	Standard Review Plan
SSE	Safe shutdown earthquake
TVA	Tennessee Valley Authority

U.S.	United States
USNRC	United States Nuclear Regulatory Commission

PREVIOUS REPORTS IN SERIES

Previous Reports from the IPIRG-1 Program

"Evaluation and Refinement of Leak-Rate Estimation Models," NUREG/CR-5128, Revision 1, June 1994.

"Loading Rate Effects on Strength and Fracture Toughness of Pipe Steels Used in Task 1 of the IPIRG Program," Topical Report, NUREG/CR-6098, October 1993.

"Stability of Cracked Pipe Under Inertial Stresses," NUREG/CR-6233, Volume 1, August 1994.

Previous Reports from the NRC's Short Cracks in Piping and Piping Welds Program

"Short Cracks in Piping and Piping Welds," First Semiannual Report, NUREG/CR-4599, Vol. 1, No. 1, March 1991.

"Short Cracks in Piping and Piping Welds," Second Semiannual Report, NUREG/CR-4599, Vol. 1, No. 2, April 1992.

"Short Cracks in Piping and Piping Welds," Third Semiannual Report, NUREG/CR-4599, Vol. 2, No. 1, September 1992.

"Short Cracks in Piping and Piping Welds," Fourth Semiannual Report, NUREG/CR-4599, Vol. 2, No. 2, February 1993.

"Short Cracks in Piping and Piping Welds," Fifth Semiannual Report, NUREG/CR-4599, Vol. 3, No. 1, October 1993.

"Short Cracks in Piping and Piping Welds," Sixth Semiannual Report, NUREG/CR-4599, Vol. 3, No. 2, March 1994.

"Short Cracks in Piping and Piping Welds," Progress Report, NUREG/CR-4599, BMI-2173, Vol 4, No. 1, April 1995.

"Fracture Behavior of Short Circumferential Short-Surface-Cracked Pipe," NUREG/CR-6298, November 1995.

"Fracture Evaluations of Fusion Line Cracks in Nuclear Pipe Bimetallic Welds," NUREG/CR-6297, April 1995.

"Effect of Dynamic Strain Aging on the Strength and Toughness of Nuclear Ferritic Piping at LWR Temperatures," NUREG/CR-6226, October 1994.

"Effects of Toughness Anisotropy and Combined Loading on Fracture Behavior of Ferritic Nuclear Pipe," NUREG/CR-6299, April 1995.

"Refinement and Evaluation of Crack-Opening Analyses for Circumferential Through-Wall Cracks in Pipes," NUREG/CR-6300, April 1995.

"Probabilistic Pipe Fracture Evaluations for Leak-Rate Detection Applications," NUREG/CR-6004, April 1995.

"Stainless Steel Submerged Arc Weld Fusion Line Toughness," NUREG/CR-6251, April 1995.

"Validity Limits in J-Resistance Curve Determination: Volume 1: An Assessment of the J_M Parameter," NUREG/CR-6264, Volume 1, February 1995.

"Validity Limits in J-Resistance Curve Determinations: Volume 2: A Computational Approach to Ductile Crack Growth Under Large-Scale Yielding Condition," NUREG/CR-6264, Volume 2, February 1995.

Previous Reports from the NRC's Degraded Piping Program - Phase II

"Degraded Piping Program - Phase II," Semiannual Report, NUREG/CR-4082, Vol. 1, Oct. 1984.

"Degraded Piping Program - Phase II," Semiannual Report, NUREG/CR-4082, Vol. 2, June 1985.

"Degraded Piping Program - Phase II," Semiannual Report, NUREG/CR-4082, Vol. 3, March 1986.

"Degraded Piping Program - Phase II," Semiannual Report, NUREG/CR-4082, Vol. 4, July 1986.

"Degraded Piping Program - Phase II," Semiannual Report, NUREG/CR-4082, Vol. 5, Dec. 1986.

"Degraded Piping Program - Phase II," Semiannual Report, NUREG/CR-4082, Vol. 6, April 1988.

"Degraded Piping Program - Phase II," Semiannual Report, NUREG/CR-4082, Vol. 7, March 1989.

"Degraded Piping Program - Phase II," Semiannual Report, NUREG/CR-4082, Vol. 8, March 1989.

"NRC Leak-Before-Break (LBB.NRC) Analysis Method for Circumferentially Through-Wall Cracked Pipes Under Axial Plus Bending Loads," Topical Report, NUREG/CR-4572, March 1986.

"Elastic-Plastic Finite Element Analysis of Crack Growth in Large Compact Tension and Circumferentially Through-Wall-Cracked Pipe Specimen--Results of the First Battelle/NRC Analysis Round Robin," Topical Report, NUREG/CR-4573, September 1986.

"An Experimental and Analytical Assessment of Circumferential Through-Wall Cracked Pipes Under Pure Bending," Topical Report, NUREG/CR-4574, June 1986.

"Predictions of J-R Curves With Large Crack Growth From Small Specimen Data," Topical Report, NUREG/CR-4687, September 1986.

"An Assessment of Circumferentially Complex-Cracked Pipe Subjected to Bending," Topical Report, NUREG/CR-4687, September 1986.

"Analysis of Cracks in Stainless Steel TIG Welds," Topical Report, NUREG/CR-4806, November 1986.

"Approximate Methods for Fracture Analyses of Through-Wall Cracked Pipes," Topical Report, NUREG/CR-4853, January 1987.

"Assessment of Design Basis for Load-Carrying Capacity of Weld-Overlay Repair," Topical Report, NUREG/CR-4877, February 1987.

"Analysis of Experiments on Stainless Steel Flux Welds," Topical Report, NUREG/CR-4878, February 1987.

"Experimental and Analytical Assessment of Circumferentially Surface-Cracked Pipes Under Bending," Topical Report, NUREG/CR-4872, April 1987.

Previous Related Documents from NRC's Degraded Piping Program - Phase I Reports

"The Development of a Plan for the Assessment of Degraded Nuclear Piping by Experimentation and Tearing Instability Fracture Mechanics Analysis," NUREG/CR-3142, Vols. 1 and 2, June 1983.

Other Related Program Reports

"Validation of Analysis Methods for Assessing Flawed Piping Subjected to Dynamic Loading," NUREG/CR-6234, August 1994.

1.0 INTRODUCTION

1.1 Background

Nuclear pipe fracture research programs that have been conducted in the international community in the last 10 to 12 years have primarily focused on cracks in straight pipe and welds subjected to rather simple loading, i.e., quasi-static load-controlled and displacement-controlled loading or single-frequency dynamic loading. One of the effects that has not been experimentally investigated is the effect that cyclic, variable-amplitude, multi-frequency loading has on the behavior of cracked pipe, i.e., seismic loading. In the past, there have been a number of research programs that have examined the effect of simulated seismic loading on the behavior of uncracked pipe, but limited data exist on the effect of complex load histories on cracked pipe. Simulated seismic pipe system experiments conducted in IPIRG-2 provide experimental data to help fill this void.

Three seismically loaded experiments were conducted in IPIRG-2. Two of the experiments had surface cracks and one had a through-wall crack. In most details, these experiments were identical to the pipe system experiments conducted in IPIRG-1. They were, however, loaded by a "seismically inspired" forcing function (i.e., consistent with an actual seismic event, but adjusted to fit the constraints of the IPIRG test system) instead of the single-frequency, increasing-amplitude sinusoidal forcing function that was used previously. In order to conduct these experiments, the seismic loading forcing function had to be designed. This report summarizes the details and rationale of the design procedure.

Figure 1.1 shows the IPIRG pipe system (Refs. 1.1 and 1.2). The system is configured as an expansion loop with over 30 m (100 feet) of 406 mm (16 inch) diameter Schedule 100 pipe. The pipe loop is supported and constrained at several locations using various specialized pieces of hardware. These supports were designed to produce specific well-defined boundary conditions that could be easily modeled in numerical calculations. There was no intent to simulate supports used in actual nuclear plants. Rather, the emphasis was to gather data to assess fracture mechanics capabilities, without the complications of large unknowns in the basic stress analysis. The pipe loop is rigidly supported at two fixed ends, it is vertically supported on hydrostatic bearings at two locations, and it is constrained laterally at three locations with spherical bearings. A large computer-controlled hydraulic actuator is used to excite the pipe in one direction at a single location.

1.2 Report Format

The report documents the design process for the IPIRG-2 simulated seismic forcing function. Specific topics addressed include:

- The design philosophy and approach,
- The design details for the basic forcing function, and
- Scaling of the basic function.

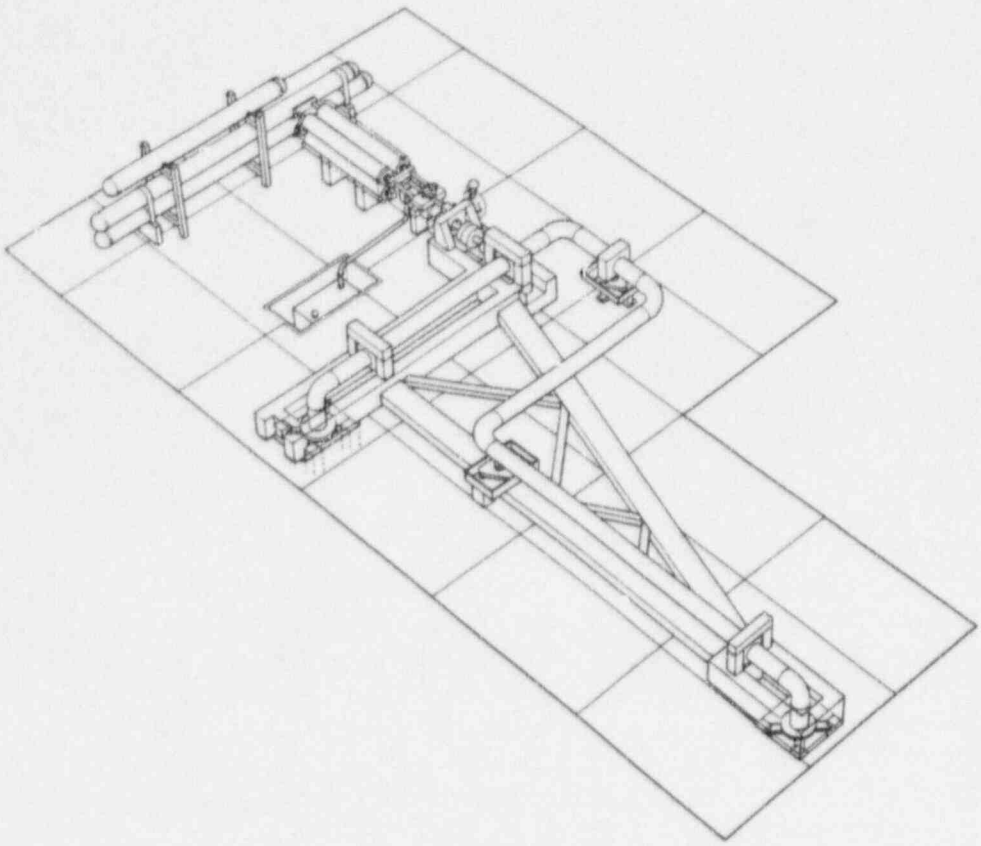

Figure 1.1 The IPIRG pipe system

Many choices had to be made during the design process which, in some cases were completely arbitrary. This report provides a record of the thought processes that influenced the design choices so that the complete context of the results of the seismic cracked-pipe experiments is known.

1.3 References

1.1 Olson, R. J., Darlaston, B. J., Mayfield, M. E., and Schmidt, R. A., "The IPIRG Dynamic Pipe Loop Test Facility," Nuclear Engineering and Design, Vol. 144, pp 77-90, 1993.

1.2 Scott, P., Olson, R., and Wilkowski, G., "The IPIRG-1 Pipe System Fracture Tests: Experimental Results," in Fatigue, Flaw Evaluation and Leak-Before-Break Assessments, ASME PVP Vol. 280, pp 135-151, June 1994.

2.0 DESIGN OF THE BASIC SEISMIC FORCING FUNCTION

2.1 Objective and Philosophy of the Design

The global objective of the simulated seismic experiments was to determine what effect, if any, variable-amplitude, multi-frequency loading has on cracked pipe in a pipe system. The principal parameters of interest were maximum moment and propensity for a double-ended guillotine break (DEGB) after maximum moment was achieved.

To achieve the objective, two possible scenarios were considered for testing the surface-cracked pipes:

(1) **Test two different materials with one forcing function**. In IPIRG-1, it was shown in the pipe system tests that the cyclic loading appeared to be detrimental to the material's fracture resistance for base metals, and the loading rate corresponding to a seismic event can increase or decrease a material's fracture resistance. Carbon steels susceptible to dynamic strain aging may have a lower fracture resistance at seismic loading rates. It was anticipated that simulated seismic loading may have a greater or lesser effect on the fracture resistance than the single-frequency loading used in the IPIRG-1 program. Experiments conducted under this scenario would use a carbon steel base metal, which is susceptible to dynamic strain aging and cyclic effects, and a stainless steel base metal, which is susceptible to cyclic effects, to provide a direct basis of comparison with companion quasi-static and single-frequency dynamic load cases.

(2) **Test one material with two spectrum-consistent forcing functions**. An infinite number of displacement-time histories can be developed from the same response spectrum, and some of the displacement-time histories may be more challenging to the integrity of a cracked pipe than others. If there are significant differences, a "severe" displacement-time history and a relatively benign displacement-time history can be developed from the same response spectrum and used in two IPIRG-2 tests. The data from these two experiments could be used to assess the inaccuracies or margins in design response spectrum analyses compared to real behavior or nonlinear time-history analyses. The material for these tests could be either stainless steel base metal or carbon steel base metal.

The plan for testing the one through-wall-cracked pipe was to be consistent with whichever option was selected for the surface cracks: scale the forcing function if Scenario 1 were used, or develop a separate through-wall-cracked pipe forcing function if Scenario 2 were selected. Both of the testing scenarios have technical appeal and both are consistent with the technical objective of the simulated seismic experiments.

After much deliberation, it was decided that Scenario 1 would be followed, i.e., test two materials with one forcing function. The principal arguments for using Scenario 1 were that the data would be much easier to interpret and the experiments would be easier to conduct. The Scenario 1 experiments are easier to conduct because less pretest analyses are required. The interpretation of the Scenario 1 experiments is easier because both materials experience the same loading histories. In addition, the Scenario 1 experiments are philosophically identical to the IPIRG-1 pipe system experiments. In

Scenario 2, on the other hand, separate iterative analyses would have been required to design the forcing functions. The forcing functions would have had to have been scaled differently to be certain that surface-crack penetration would occur. This would have complicated Scenario 2 comparisons with quasi-static and single-frequency experiments.

Thus, the IPIRG-2 seismic forcing function design effort focussed on finding a single seismic time history that would induce surface-crack penetration for a fixed flaw size in carbon steel and stainless steel base metal pipes, and that could be suitably scaled so that a short through-wall crack in carbon steel base metal could be grown.

2.2 Design Approach

The ideas governing the design of the seismic forcing function were embodied in the following three premises:

1. The objective of the design process was only to define an actuator displacement time-history, and not to necessarily explore the full probabilistic nature of true seismic events.

2. Accepted seismic design procedures were to be used.

3. The criteria for selecting a particular forcing function were principally based on the engineering requirements for the test system, i.e., servo-hydraulic constraints.

This design approach provided a framework for selecting possible technical approaches, limiting the scope of the design effort, and a rationale for assessing the merits of competing design alternatives.

The specific steps taken to implement the design approach were as follows:

1. The NRC Regulatory Guide 1.60 ground acceleration response spectrum provided the basic description of the seismic input.

2. An artificial time-history of ground acceleration was generated that is spectrum-consistent with Step 1.

3. A simple model of a pressurized water reactor (PWR) plant was used as a transfer function between the time-history ground acceleration and an assumed location for the pipe system.

4. The relative motion between two "floors" in the PWR model represented the displacements to be applied to the pipe system.

5. The time-history of actuator motion for the IPIRG pipe loop was achieved by finding a displacement time history that would give the same moment-time response at the crack location as the multi-point excitation defined in Step 4.

6. Scaling of the input ground acceleration was fixed by a desire to have the surface-crack penetration be due to ductile tearing and not fatigue, and a need to maintain an adequate margin on servo-hydraulic capacities.

7. A finite element model of the pipe system, including a nonlinear representation of the cracks, was used to predict the response of the pipe system to the simulated seismic loading. The predicted response was the basis for Step 6.

With these basic steps, a reasonably realistic seismic forcing function was developed. The forcing function included all of the essential elements of a true seismic event at a plant in a relatively simple fashion, without unnecessary complications.

2.3 Design Details

The previous section outlined the design philosophy and steps for generating the loading for the IPIRG-2 simulated seismic loading experiments. As indicated previously, the objective of the design process was to define a time-history for the actuator for the IPIRG pipe system facility. This section presents the details of the design process.

2.3.1 Seismic Input

The earthquake that the IPIRG pipe system was assumed to be exposed to is characterized by the horizontal and vertical design response spectra in NRC Regulatory Guide 1.60 (Ref. 2.1). The Regulatory Guide 1.60 spectra, shown in Figures 2.1 and 2.2, are scaled to a maximum of 1.0 g horizontal acceleration and accompanying displacement of 914 mm (36 inches). For analysis purposes, the spectra are linearly scaled to the maximum horizontal acceleration of the given earthquake and damping is linearly interpolated from the figures. These spectra are based on statistical analyses of 49 actual horizontal components of earthquake ground motion and are typical for a site underlain by rock or soil and not relatively close to the epicenter of the earthquake.

2.3.2 Earthquake Time-History

Time-history analysis is generally considered necessary to qualify or design systems and components that exhibit highly nonlinear behavior. The cracked section in the IPIRG-2 pipe system experiments is an example of such a "component". Because there are no recorded earthquake ground motions that exhibit the uniform frequency distributions shown in Figures 2.1 and 2.2, it is necessary to generate a spectrum-consistent time-history of motion whose response spectrum matches the design spectrum at a given damping value.

There are a number of methods, References 2.2 to 2.9, for developing a time-history from a response spectrum. Some rely upon modifying existing earthquake records, while others synthesize the response from power spectral density functions, Gaussian shot noise, or superposition of continuous waves. For the present study, the time-history of ground motion was synthesized using the last approach. In particular, the computer program SIMQKE (Refs. 2.10 and 2.11) was used.

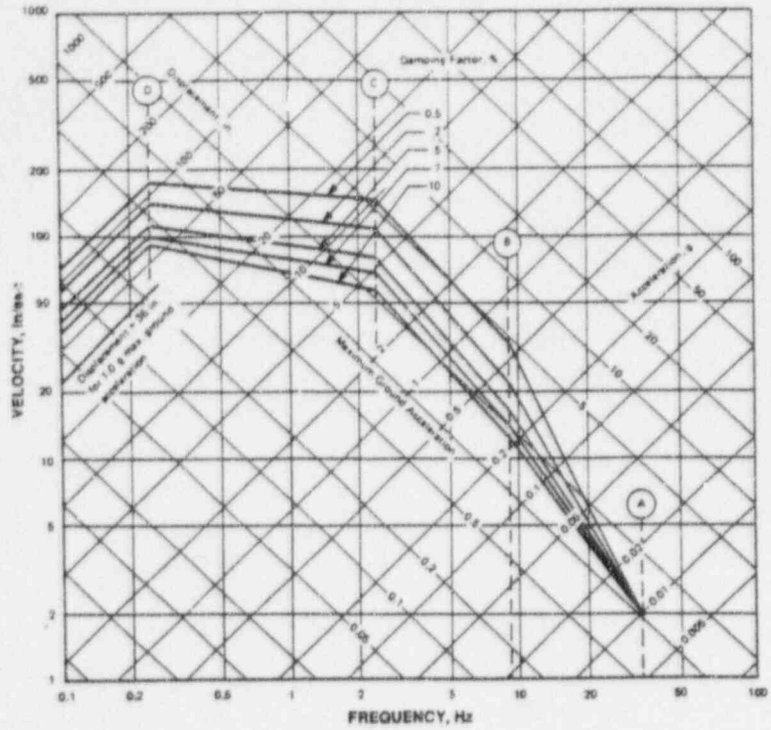

Figure 2.1 NRC Regulatory Guide 1.60 horizontal design response spectra scaled to 1 g horizontal ground acceleration

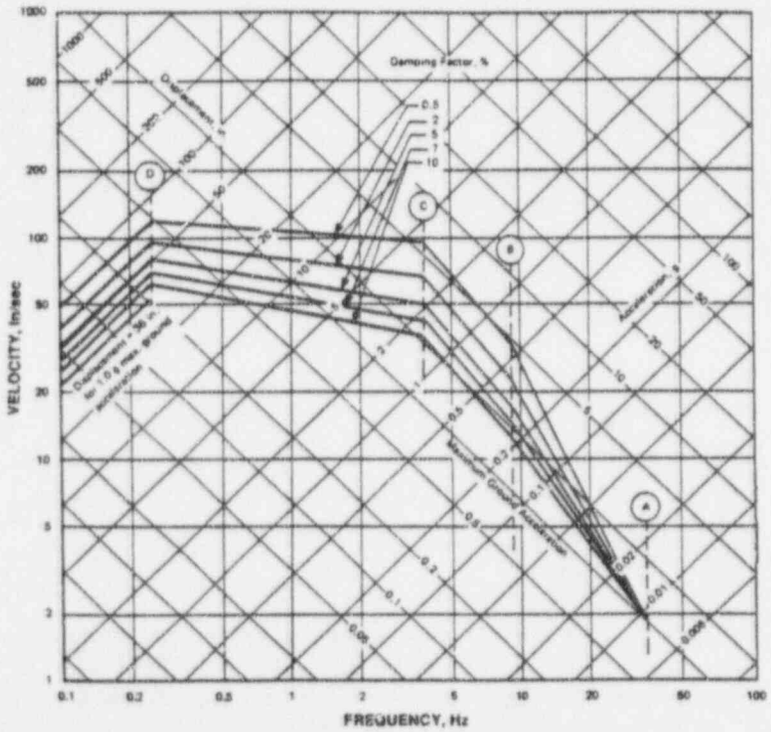

Figure 2.2 NRC Regulatory Guide 1.60 vertical design response spectra scaled to 1 g horizontal ground acceleration

The SIMQKE procedure for synthesizing an earthquake time-history uses a superposition of a large number of sine waves with random phase angles to describe ground motion acceleration:

$$\ddot{X}(t) = I(t)\sum_{i=1}^{n} A_i \sin(2\pi f_i + \phi_i) \qquad (2\text{-}1)$$

The amplitudes A_i are iteratively adjusted to match the prescribed input response spectrum through the use of a smooth power spectral density function generated by SIMQKE that is based on the input response spectrum, the damping, and strong motion duration. The function I(t) is a deterministic enveloping function that simulates the transient character of real earthquakes (build up, stationary portion, and motion decay).

SIMQKE will match input spectra very closely if enough iterations are permitted. There are, however, other prescriptions besides matching an input response spectrum that generally are considered when a simulated seismic time-history is being developed. Specifically, the requirements of the U.S. NRC's Standard Review Plan (SRP) 3.7.1 (Ref. 2.12) and ASME Section III - Division 1, Appendix N (Ref. 2.13) are often followed.

SRP 3.7.1 puts constraints on the total duration of the time history (10 to 25 seconds) and the duration of the stationary strong-motion phase (6 to 15 seconds). In addition, to be considered acceptable for analysis using a single time history, the time history must (1) envelope the design response spectra, (2) frequencies in Equation 2.1 must have a prescribed maximum spacing, and (3) there is a minimum power spectral density requirement. SRP 3.7.1 also specifies that three mutually orthogonal axes of excitation must be considered and damping must be in accordance with Regulatory Guide 1.61 (Ref. 2.14). Use of the spectra in Regulatory Guide 1.60 is acceptable.

ASME Section III - Division 1 Appendix N, which is nonmandatory, recommends many of the same things found in SRP 3.7.1. For instance, Regulatory Guide 1.60 is recommended as the basis for developing simulated seismic time histories, the stationary strong motion duration should be at least 6 seconds, three orthogonal axes of excitation should be considered, etc. In contrast to SRP 3.7.1, Appendix N does contain recommendations for time phasing of excitations in the three orthogonal directions. According to Appendix N, the time phasing is acceptable if the correlation coefficient is less than 0.16 and the coherence function ranges between 0.0 and 0.3 with an average value of approximately 0.2. (The correlation coefficient is a statistical measure of the association between two variables between -1 and +1. A correlation coefficient of 0 implies that the two variables are uncorrelated. The coherence function, which has a value between 0 and 1, and is a function of frequency, measures the extent to which one function can be predicted from another function by an optimum linear least squares relationship. If the two functions are completely unrelated, the coherence will be zero.)

Synthesized x, y, and z acceleration time histories based on Regulatory Guide 1.60 and meeting the prescriptions of SRP 3.7.1 are shown in Figures 2.3 through 2.5. Compliance with the spectrum enveloping requirement for the x direction at various damping ratios is illustrated in Figures 2.6

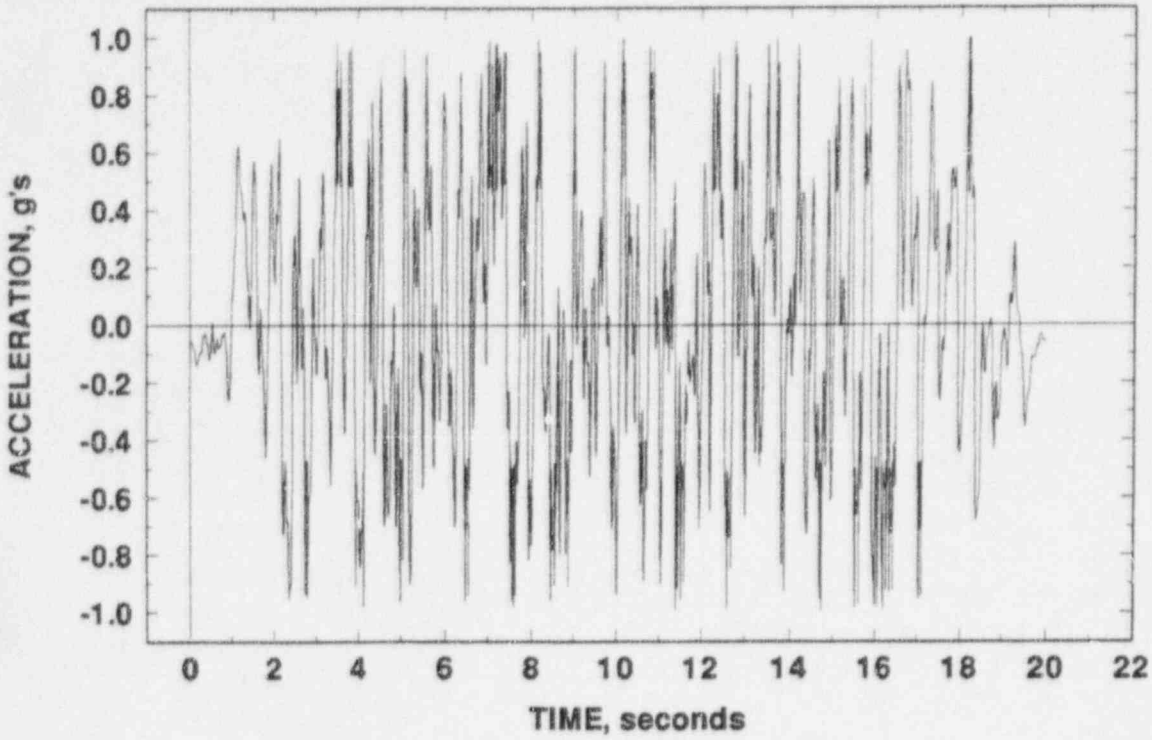

Figure 2.3 Synthesized seismic x-direction (horizontal) ground motion response at 1.0 g

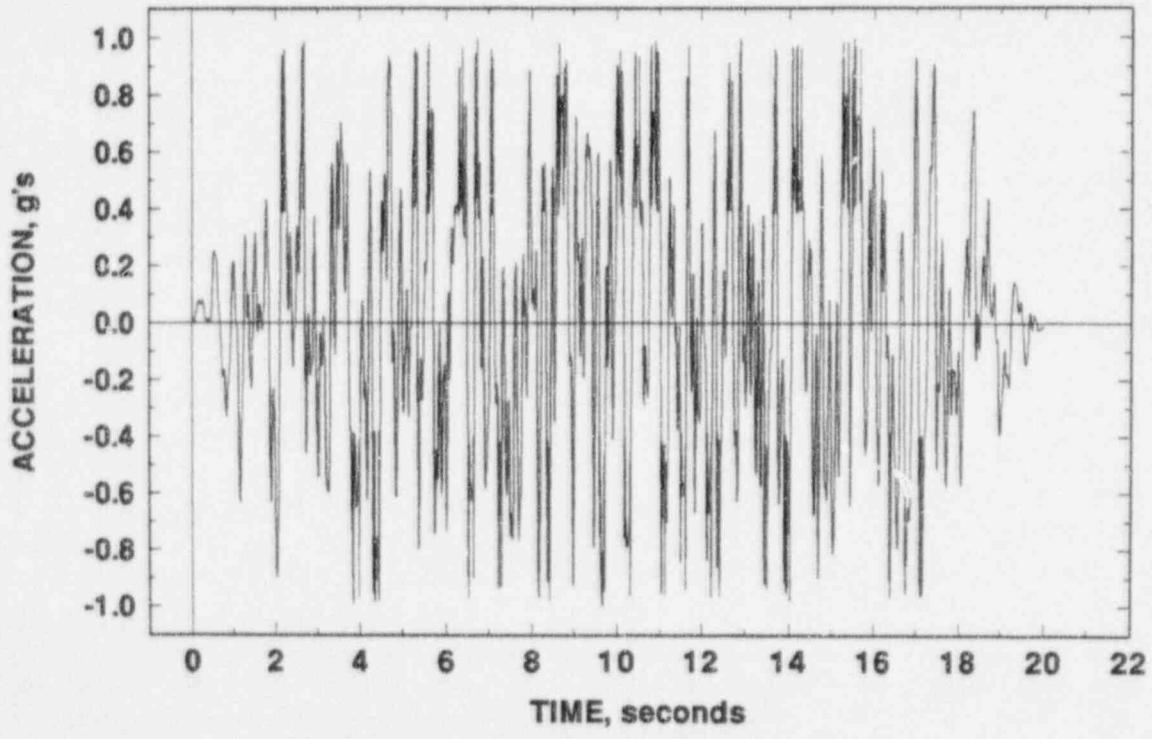

Figure 2.4 Synthesized seismic y-direction (horizontal) ground motion response at 1.0 g

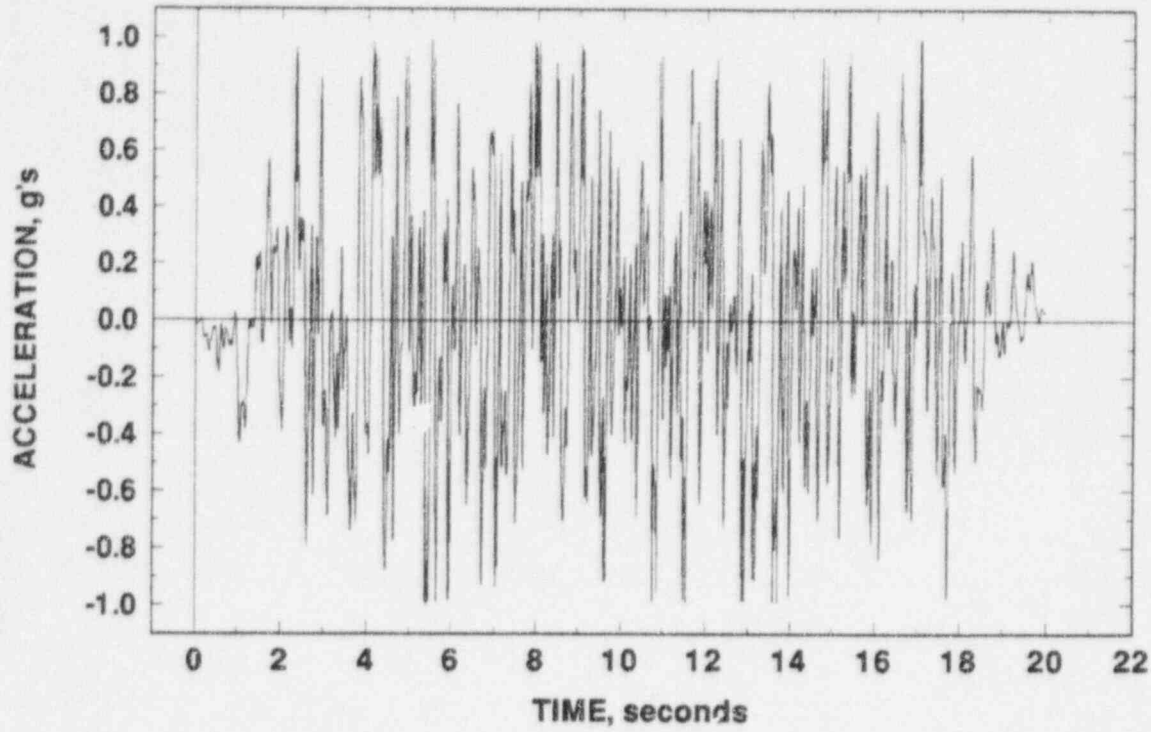

Figure 2.5 Synthesized seismic z-direction (vertical) ground motion response at 1.0 g

through 2.10, while conformance with the SRP 3.7.1 PSD minimum is shown in Figure 2.11. Similar sets of spectrum enveloping and PSD minimum plots for the y and z directions are shown in Figures 2.12 through 2.22. There is no PSD requirement for the z direction.

The time histories have a 20 second total duration and a stationary phase duration of 10 seconds. Both of these fit the requirements of SRP 3.7.1 and Appendix N. The correlation coefficients for the three excitations ($r_{xy}=0.04$, $r_{xz}=0.07$, $r_{yz}=0.06$) are within the Appendix N requirement. The coherence requirement of Appendix N, which is nonmandatory, however, is not met by the time histories, because the coherence is 0.0 for all three combinations of excitations. This in an inherent limitation in SIMQKE and is related to the way that SIMQKE generates time histories.

The synthesized time histories of acceleration shown in Figures 2.3 to 2.5 meet all of the SRP 3.7.1 requirements for analysis using a single time history and they meet nearly all of the nonmandatory requirements of ASME Section III - Division 1 Appendix N. In addition, the time histories developed are, for the most part, consistent with the ASCE standards (Ref. 2.15).

2.3.3 Building Response

The time-history of ground acceleration is the fundamental "driving force" for motion of the pipe system. However, the ground acceleration does not directly excite the pipe. Rather, the ground motion excites the plant or building that the pipe is in, and this in turn excites the pipe. The building or plant is coupled to the ground by a foundation and has a distribution of mass and stiffness. Because of this, the building acts like a filter for much of the ground motion accelerations. To make

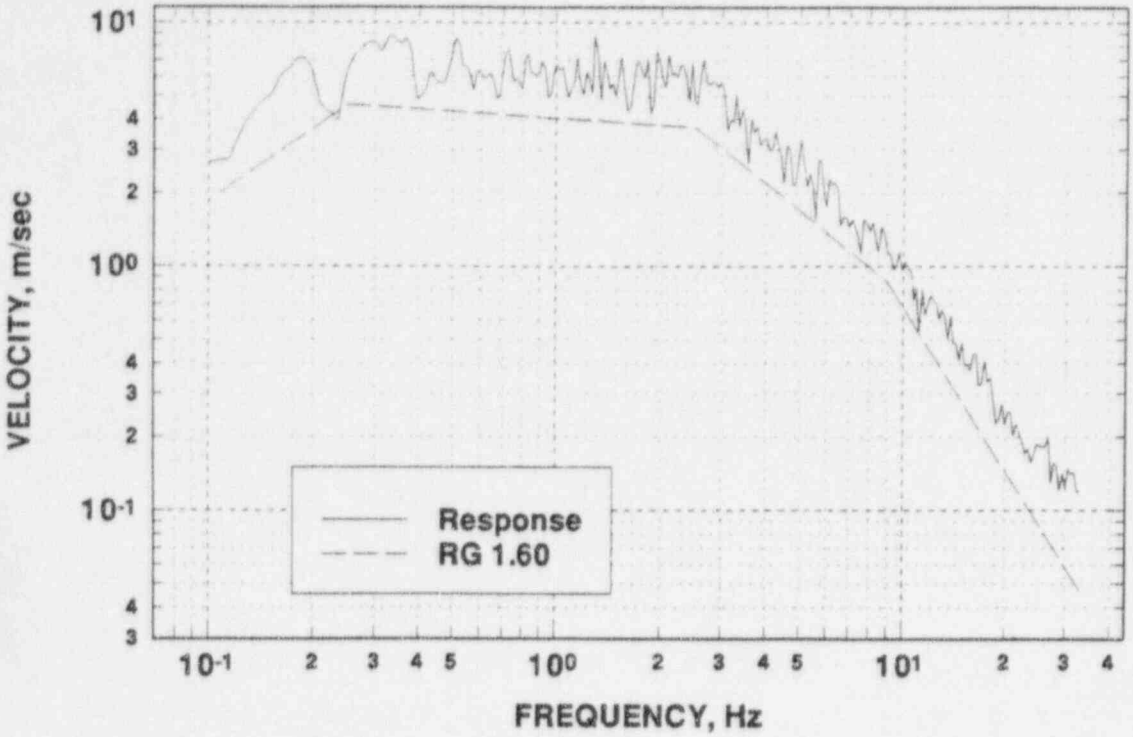

Figure 2.6 X-direction (horizontal) spectra at 0.5-percent critical damping at 1.0 g

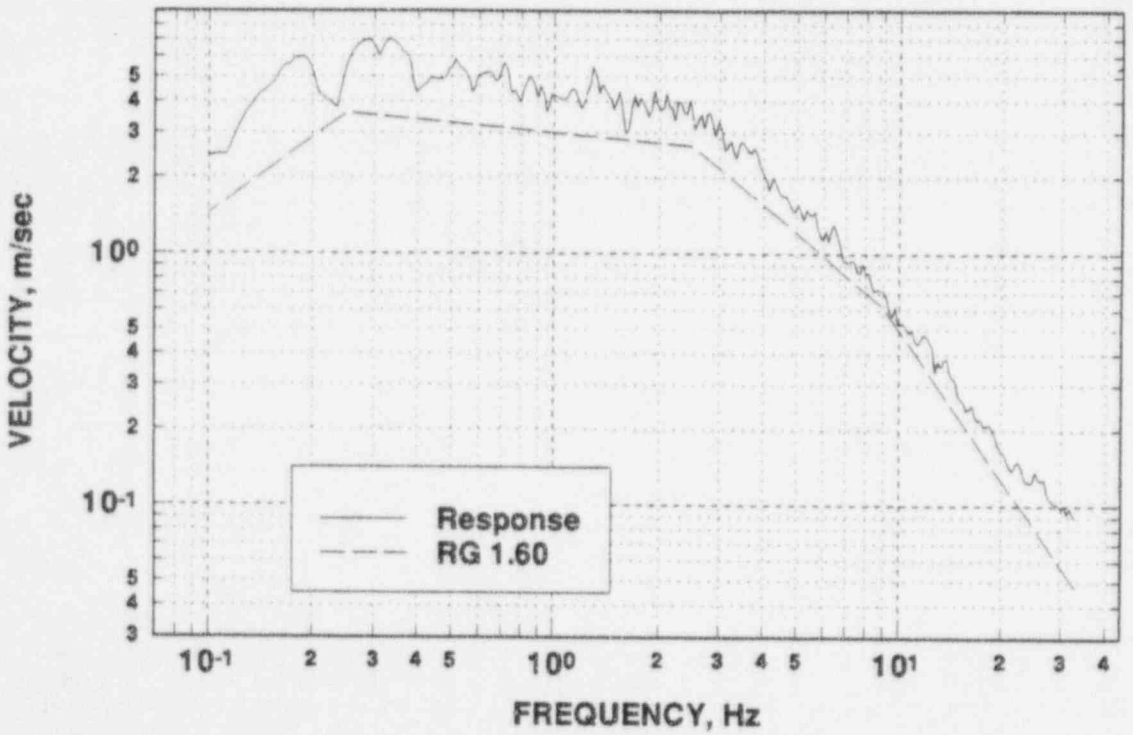

Figure 2.7 X-direction (horizontal) spectra at 2-percent critical damping at 1.0 g

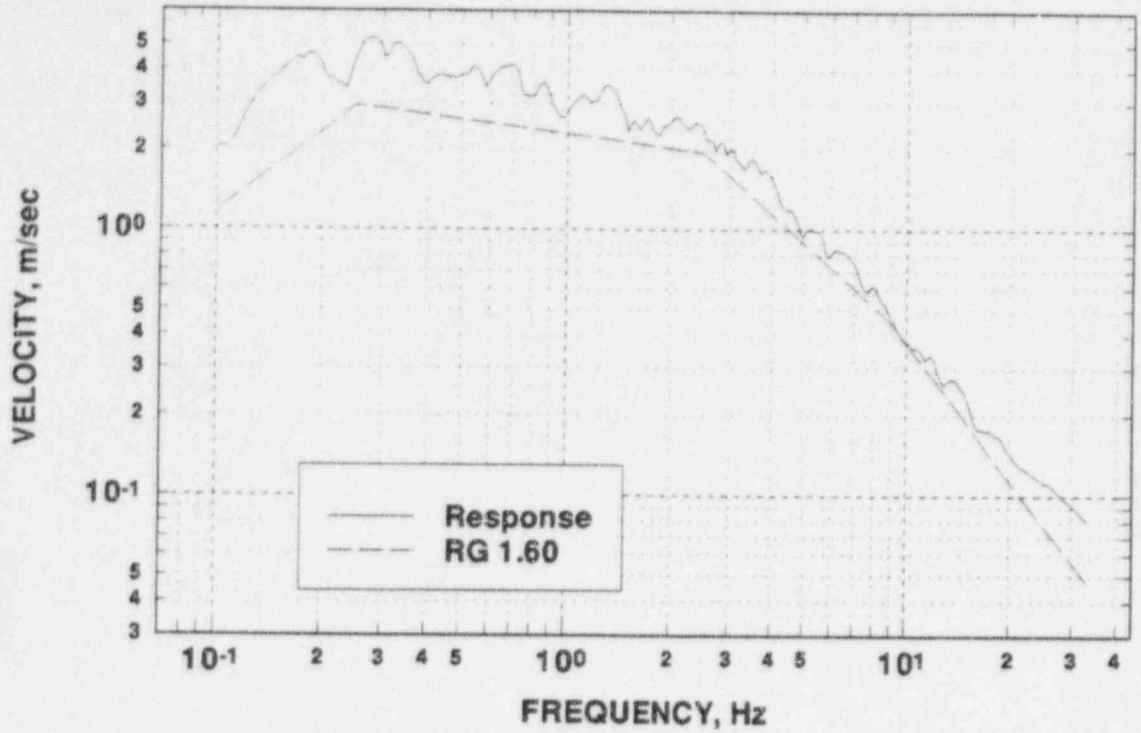

Figure 2.8 X-direction (horizontal) spectra at 5-percent critical damping at 1.0 g

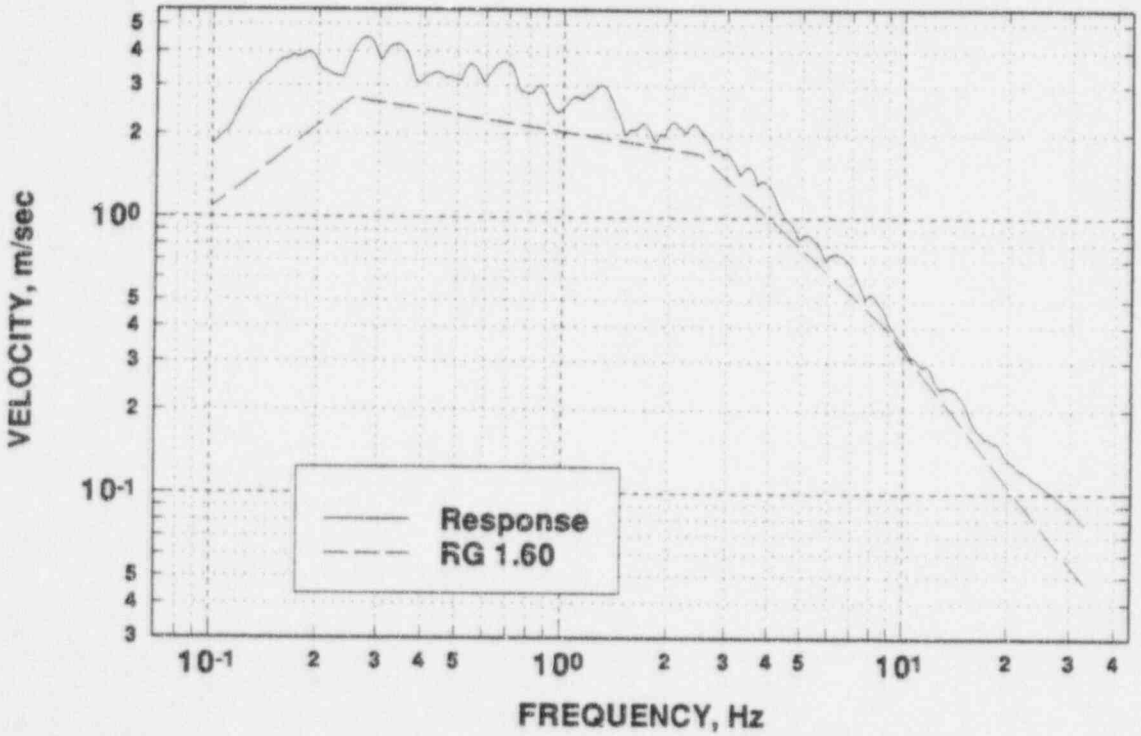

Figure 2.9 X-direction (horizontal) spectra at 7-percent critical damping at 1.0 g

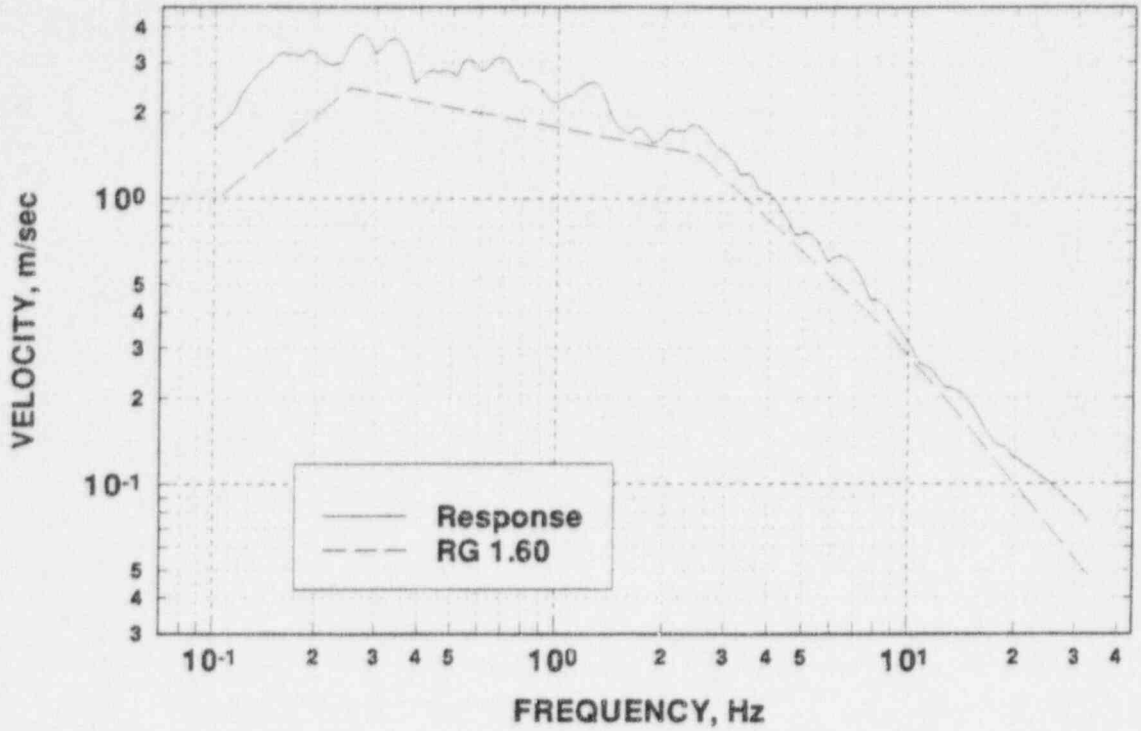

Figure 2.10 X-direction (horizontal) spectra at 10-percent critical damping at 1.0 g

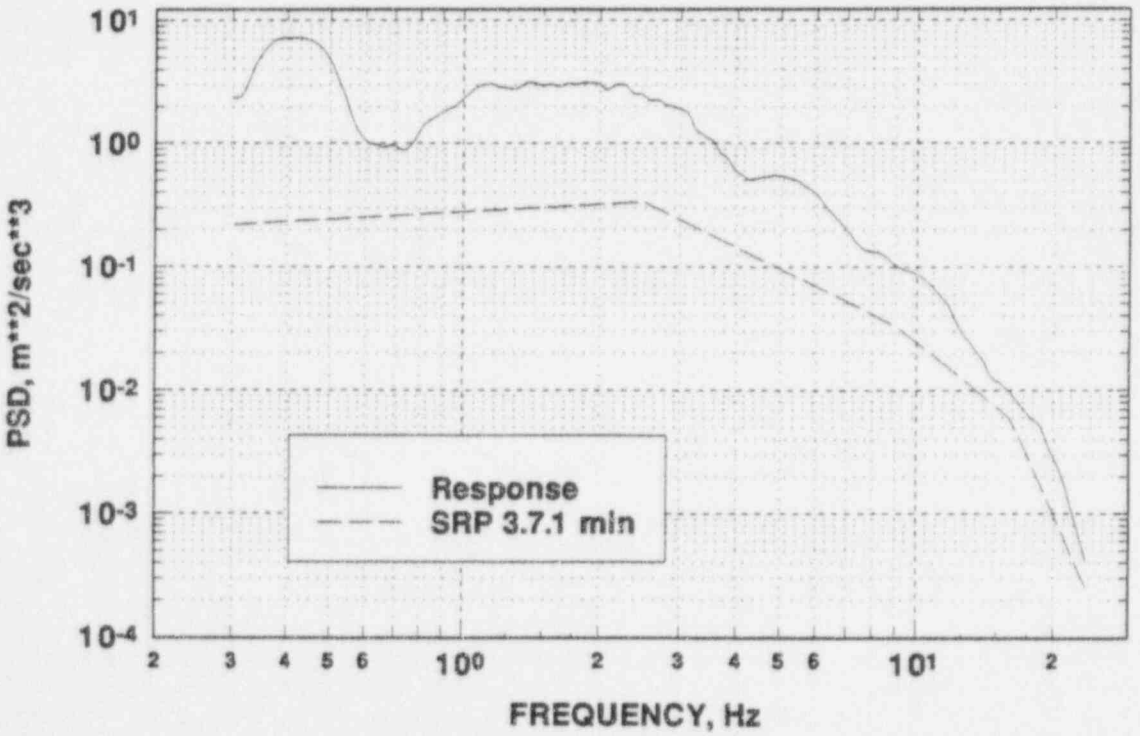

Figure 2.11 X-direction (horizontal) power spectra density at 1.0 g

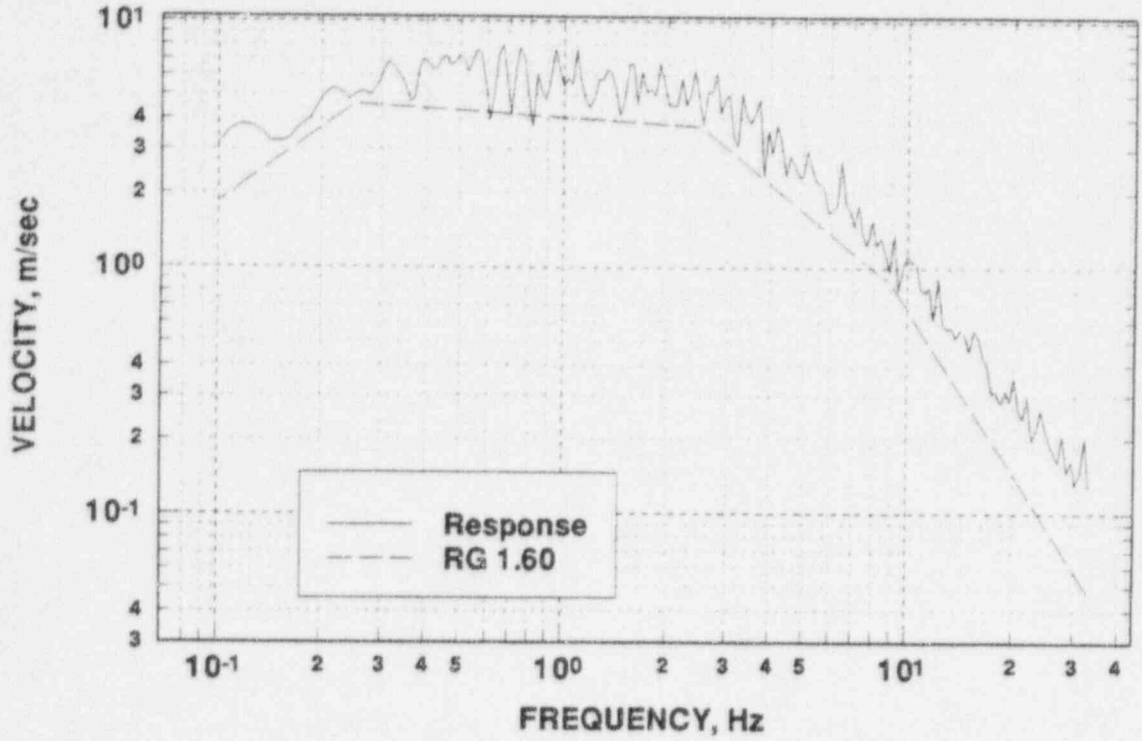

Figure 2.12 Y-direction (horizontal) spectra at 0.5-percent critical damping at 1.0 g

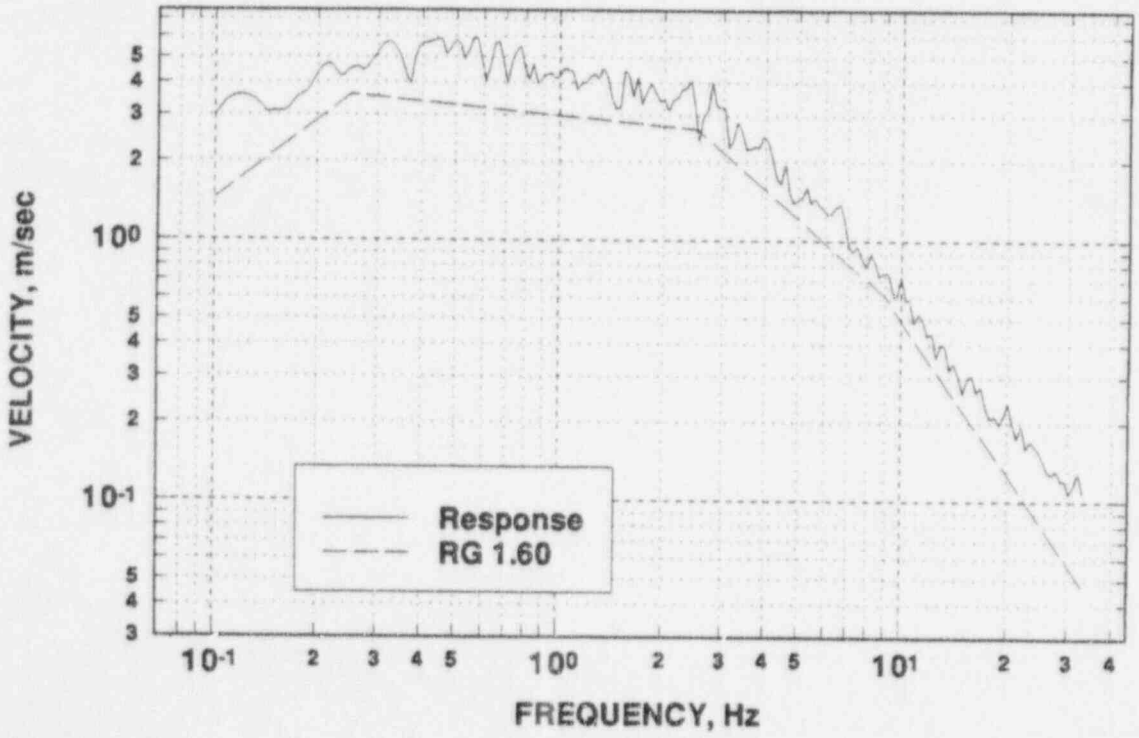

Figure 2.13 Y-direction (horizontal) spectra at 2-percent critical damping at 1.0 g

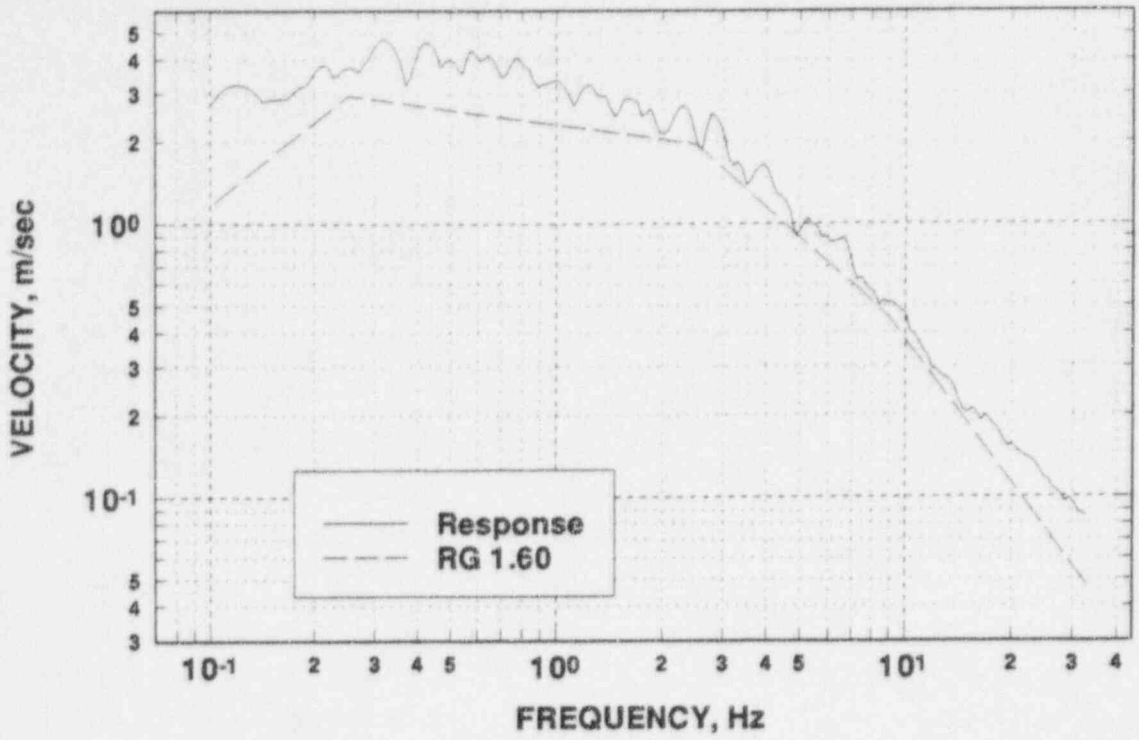

Figure 2.14 Y-direction (horizontal) spectra at 10-percent critical damping at 1.0 g

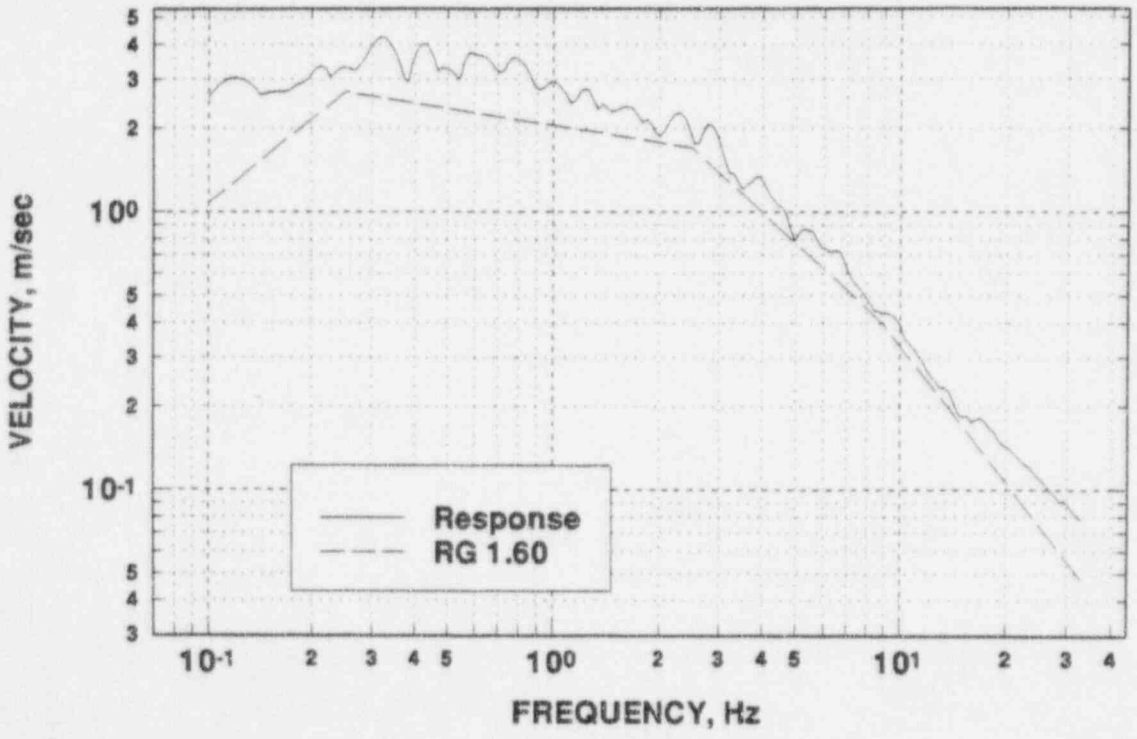

Figure 2.15 Y-direction (horizontal) spectra at 5-percent critical damping at 1.0 g

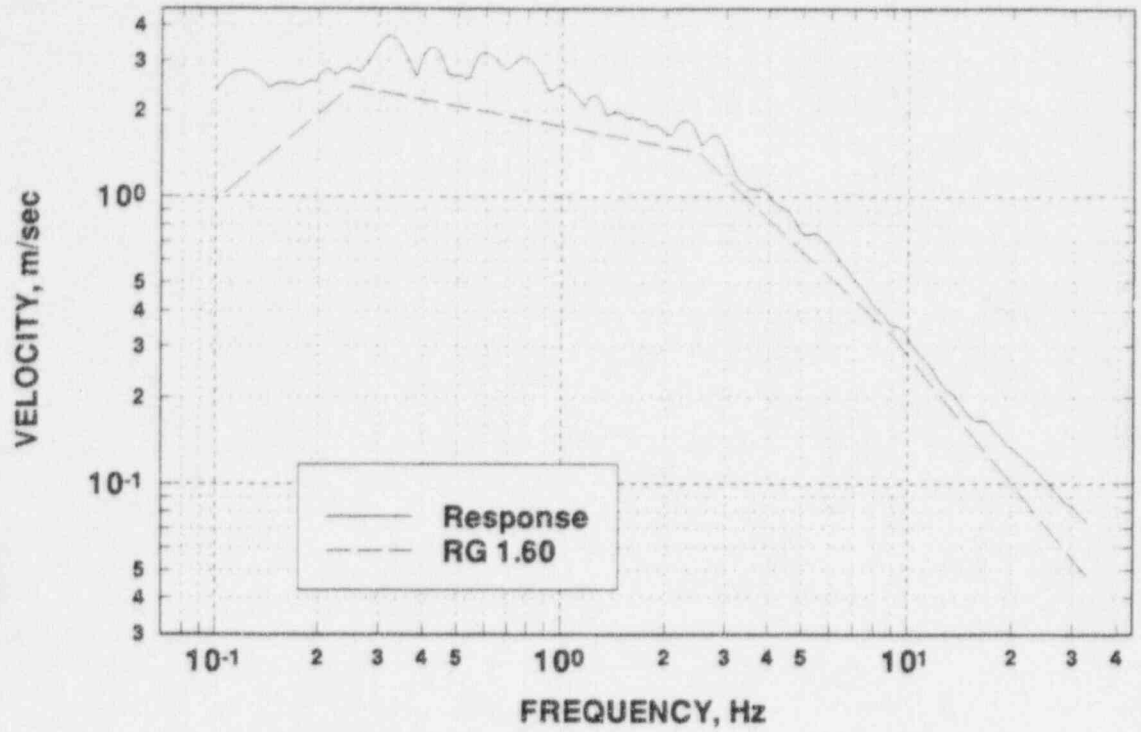

Figure 2.16 Y-direction (horizontal) spectra at 10-percent critical damping at 1.0 g

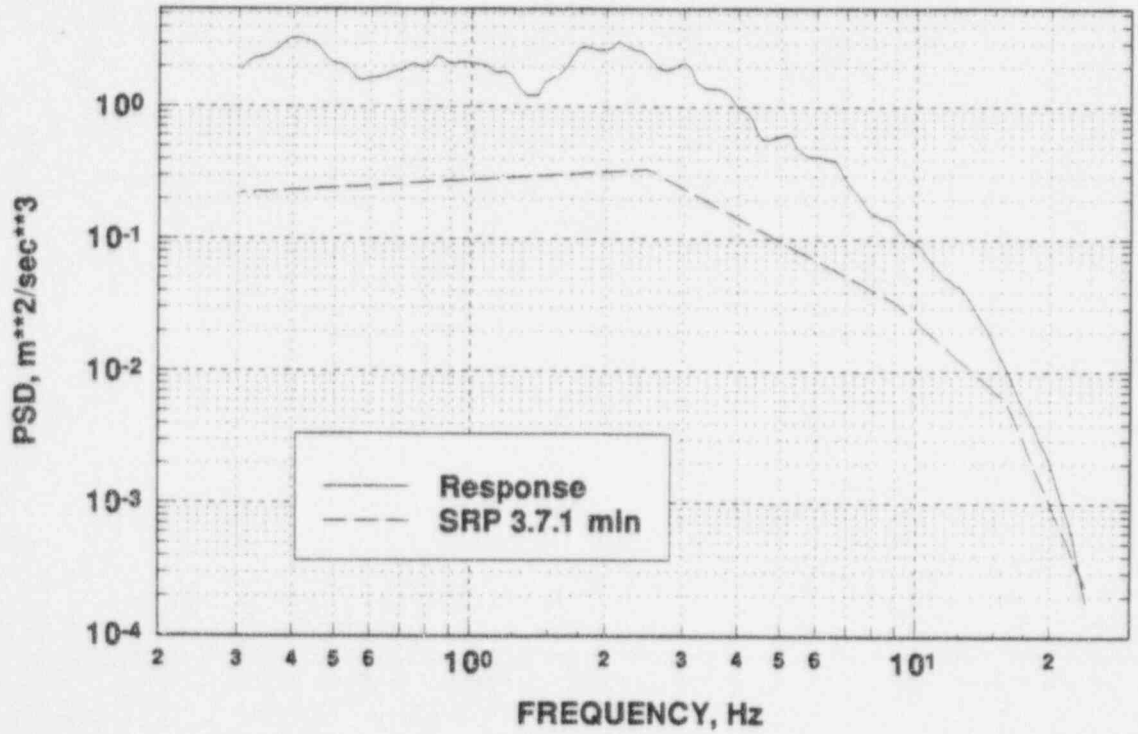

Figure 2.17 Y-direction (horizontal) power spectral density at 2-percent at 1.0 g

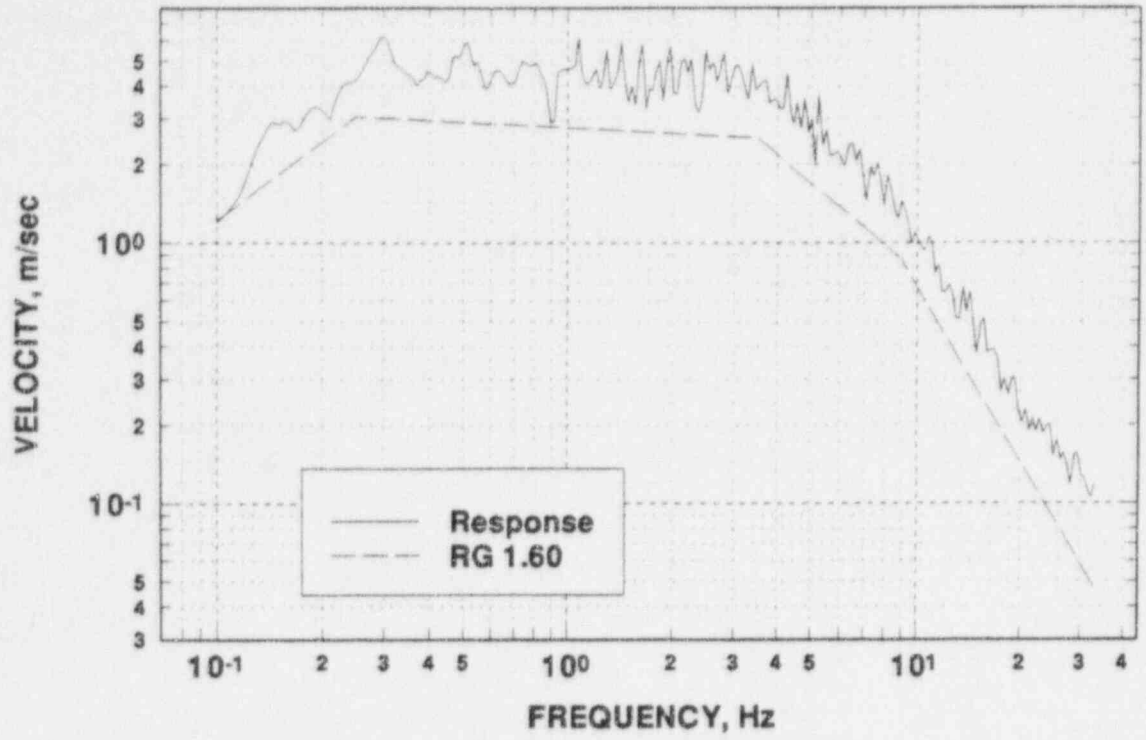

Figure 2.18 Z-direction (vertical) spectra at 0.5-percent critical damping at 1.0 g

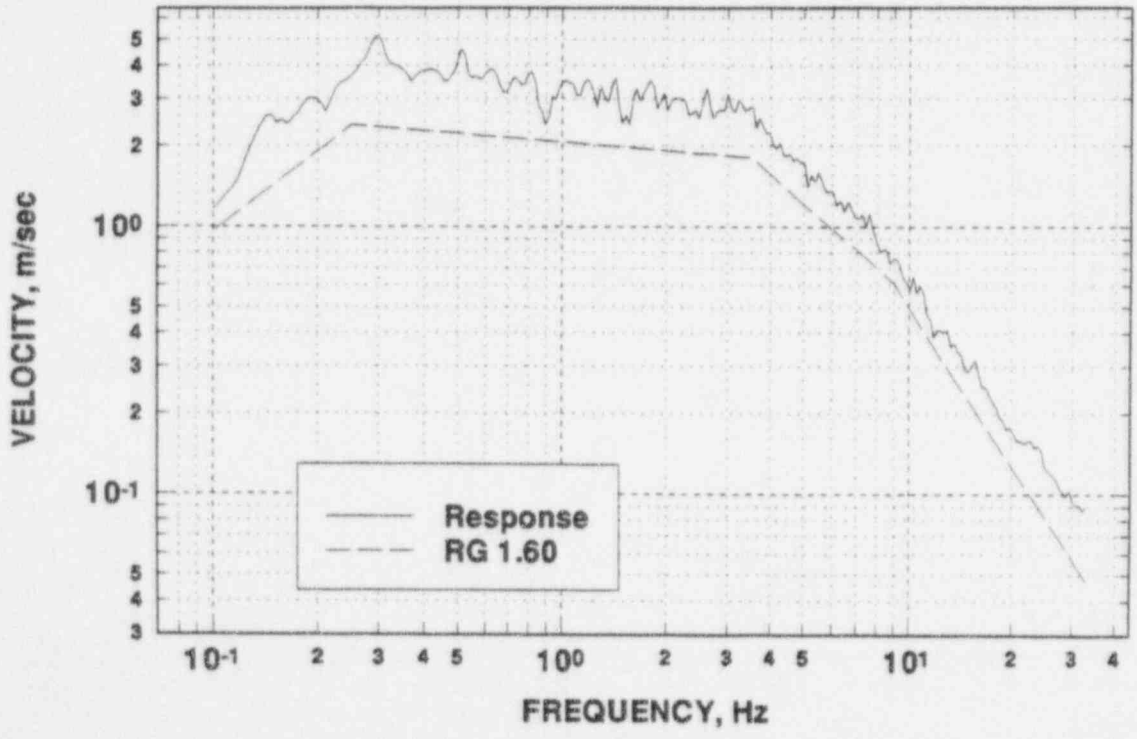

Figure 2.19 Z-direction (vertical) spectra at 2-percent critical damping at 1.0 g

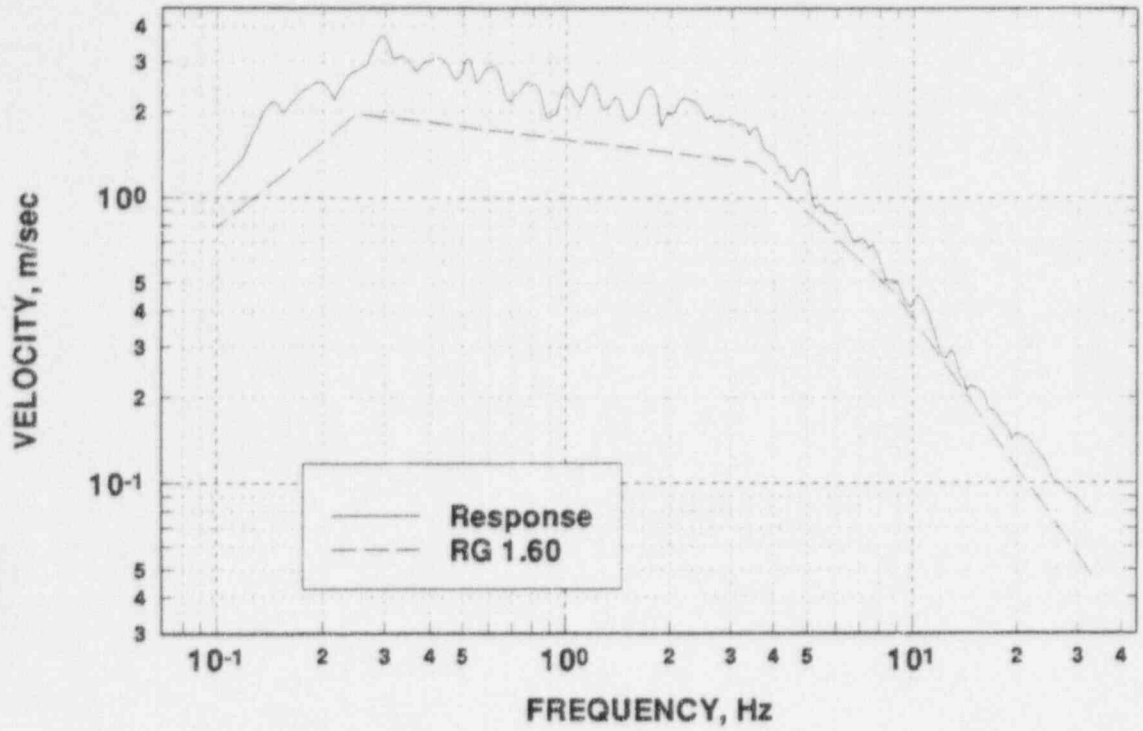

Figure 2.20 Z-direction (vertical) spectra at 5-percent critical damping at 1.0 g

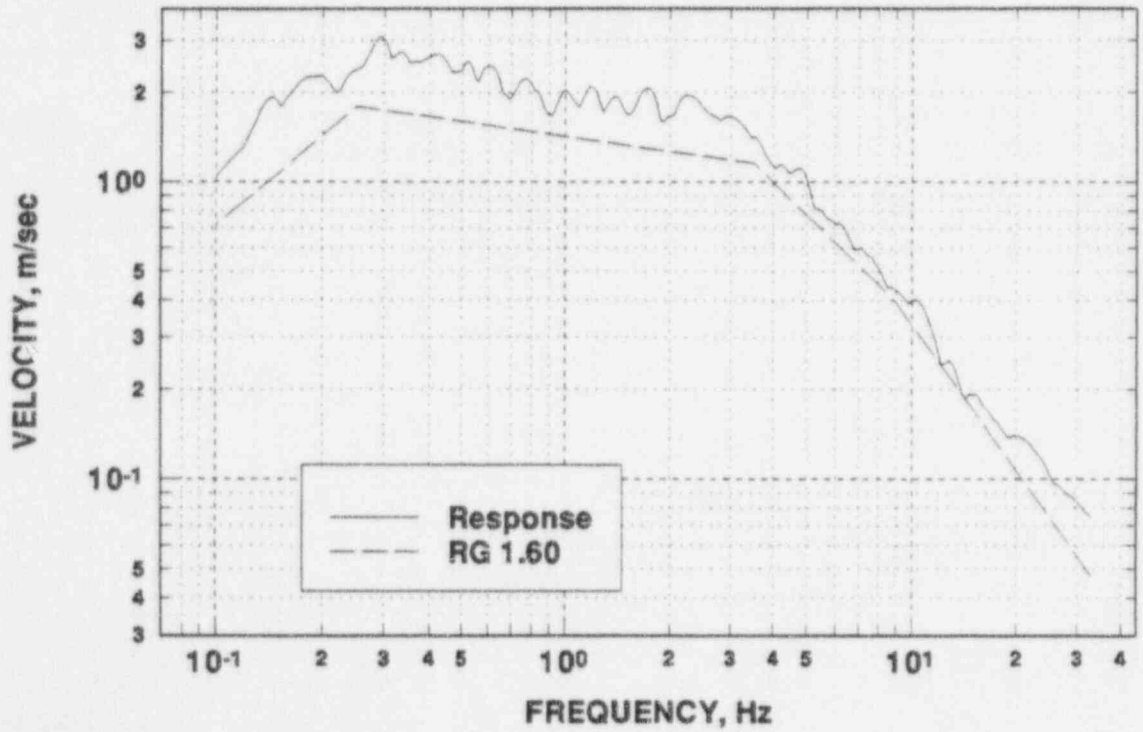

Figure 2.21 Z-direction (vertical) spectra at 7-percent critical damping at 1.0 g

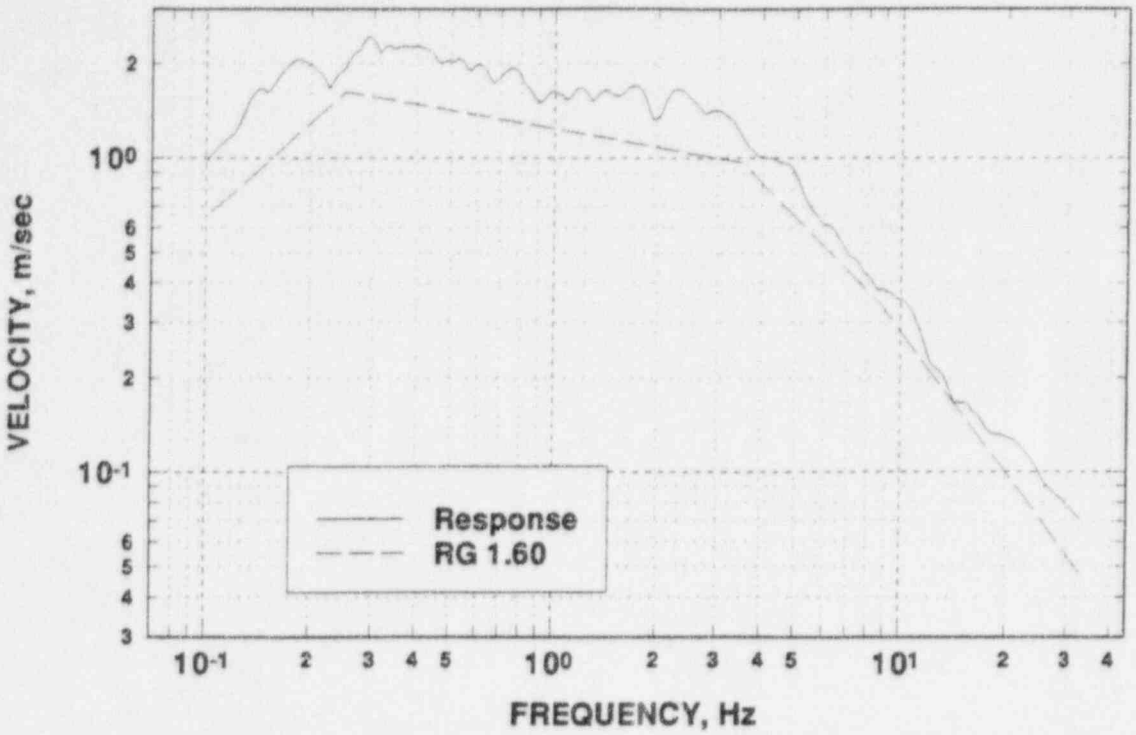

Figure 2.22 Z-direction (vertical) spectra at 10-percent critical damping at 1.0 g

the seismic motions applied to the IPIRG pipe system realistic, a building response model was developed.

The model used to couple the pipe to the ground acceleration is the 9 degree-of-freedom mass, spring, and damper system shown in Figure 2.23. Details of the model are given in Table 2.1. This is a rather simple model of a PWR plant (Ref. 2.16) placed on a relatively soft soil foundation (Refs. 2.17 and 2.18), but it embodies the essential transfer function characteristics needed to make the pipe excitation reasonably credible. The basic plant model was developed by Stone and Webster for some soil-structure interaction studies, while the soil properties were used in analyses to study the coupling between soil motion and plant equipment. The model includes the base mat (Mass 1), the containment (Mass 2), and the reactor internal components (Mass 3). The model assumes rigid behavior of the plant in the z (vertical) direction. The structure-foundation interaction is modeled as a lumped spring and dashpot circular base (Refs. 2.19 and 2.20).

To assess the suitability of the simple PWR model, the natural frequencies of the model were calculated. Table 2.2 lists the frequencies, while Figures 2.24 through 2.28 show the mode shapes for the model. The frequencies are consistent with typical results from nuclear plants as shown in Figure 2.29 (Ref. 2.21). Although the natural frequencies are toward the low side of the data shown in Figure 2.29, they are not unreasonable. This suggests that the model will capture the essential behavior of a real facility.

Table 2.1 Stiffness and mass properties for the PWR model

Property	Value	Units
K_{mass-2}	$4.524*10^9$ $(2.583*10^7)$	N/m (lb/in)
K_{mass-3}	$4.378*10^9$ $(2.500*10^7)$	N/m (lb/in)
K_h	$9.321*10^9$ $(5.322*10^7)$	N/m (lb/in)
K_v	$1.036*10^{10}$ $(5.914*10^7)$	N/m (lb/in)
K_r	$3.143*10^{12}$ $(2.782*10^{13})$	N-m/rad (in-lb/rad)
M_1	$3.503*10^7$ $(2.000*10^5)$	kg (lb-sec^2/in)
I_1	$2.712*10^{10}$ $(2.400*10^{11})$	kg-m^2 (lb-sec^2-in)
M_2	$6.932*10^6$ $(3.958*10^4)$	kg (lb-sec^2/in)
M_3	$4.524*10^6$ $(2.583*10^4)$	kg (lb-sec^2/in)
C_h	468,200 $(2.673*10^9)$	kN-sec/n (lb-sec/in)
C_r	767,700 $(4.384*10^6)$	kN-sec/n (lb-sec/in)
C_q	$4.143*10^{11}$ $(3.667*10^{15})$	kN-n-sec/rad (in-lb-sec/rad)

Table 2.2 Natural frequencies of the PWR model

Mode	Frequency (Hz)	Description
1, 2	1.38	Rocking about the base, internal components and containment moving in phase
3, 4	2.34	Pendulous motion, internal components and containment moving in phase
5	2.38	Vertical motion
6, 7	4.68	Base almost stationary, internal components and containment out of phase
8, 9	5.94	Base moving laterally and out of phase with internal components and containment

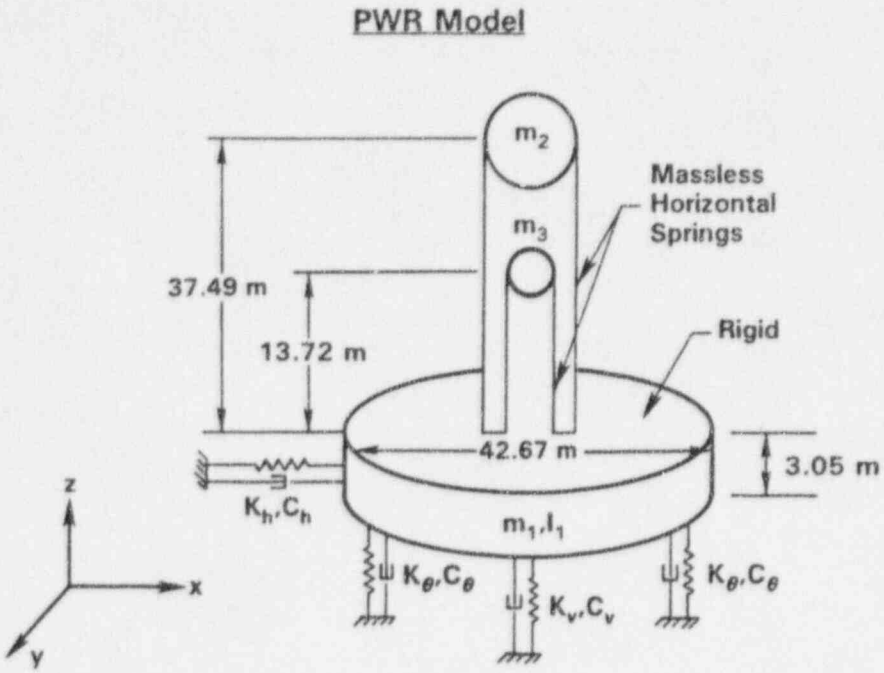

Figure 2.23 PWR system model

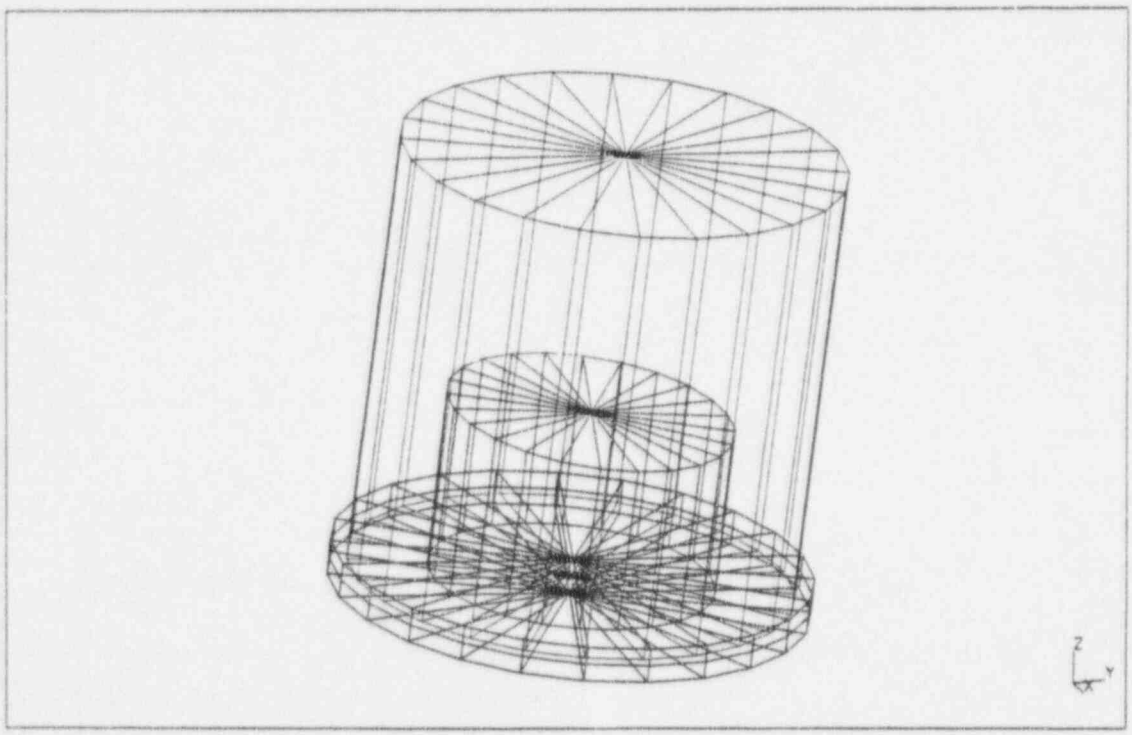

Figure 2.24 PWR model Mode 1 (Mode 2 orthogonal) - rocking about the base, internal components and containment moving in phase, 1.38 Hz

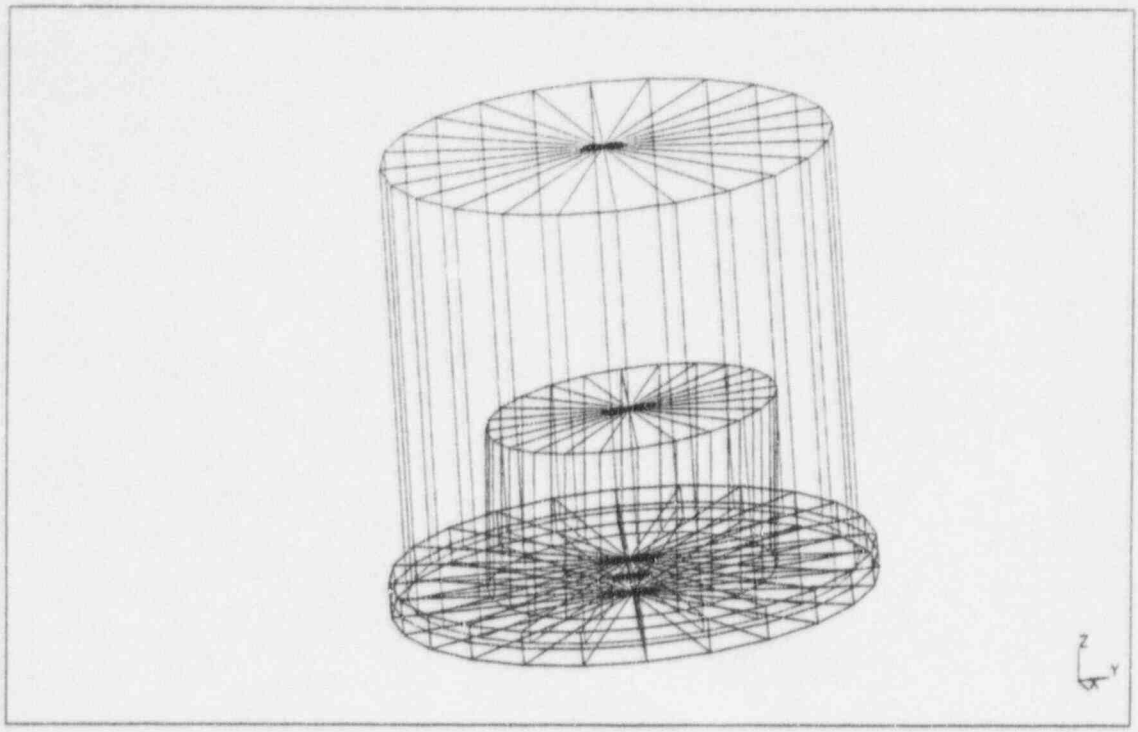

Figure 2.25 PWR model Mode 3 (Mode 4 orthogonal) - pendulous motion, internal components and containment moving in phase, 2.34 Hz

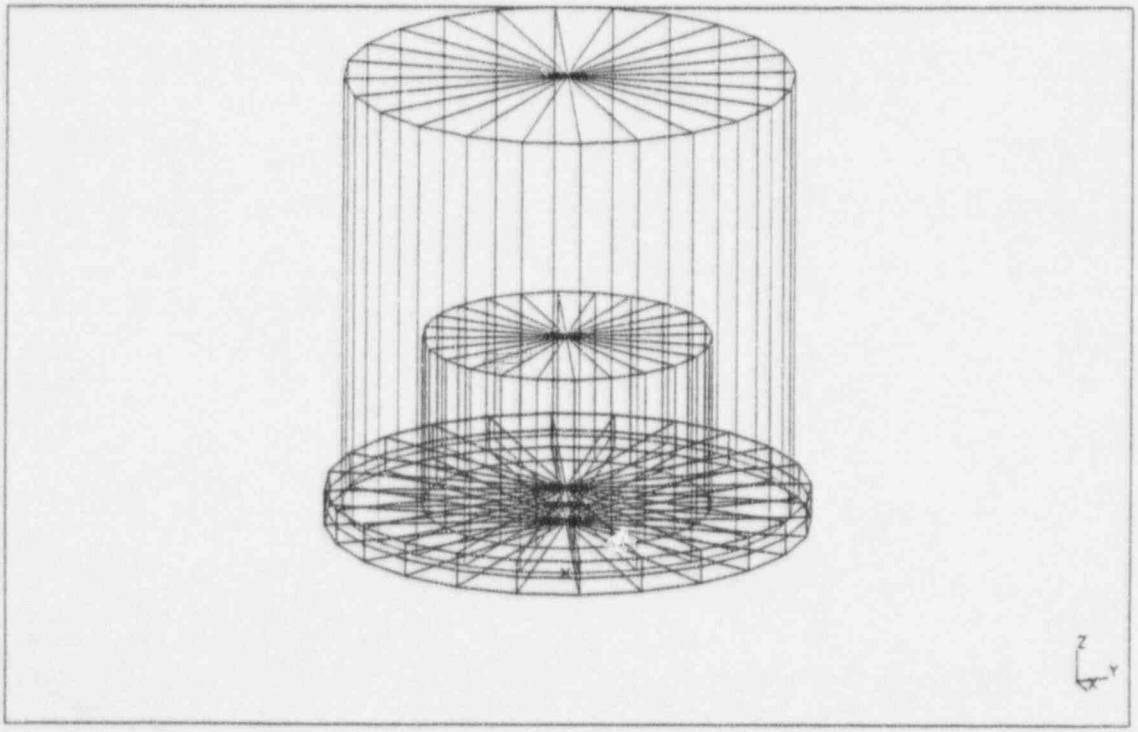

Figure 2.26 PWR model Mode 5 - vertical motion, 2.38 Hz

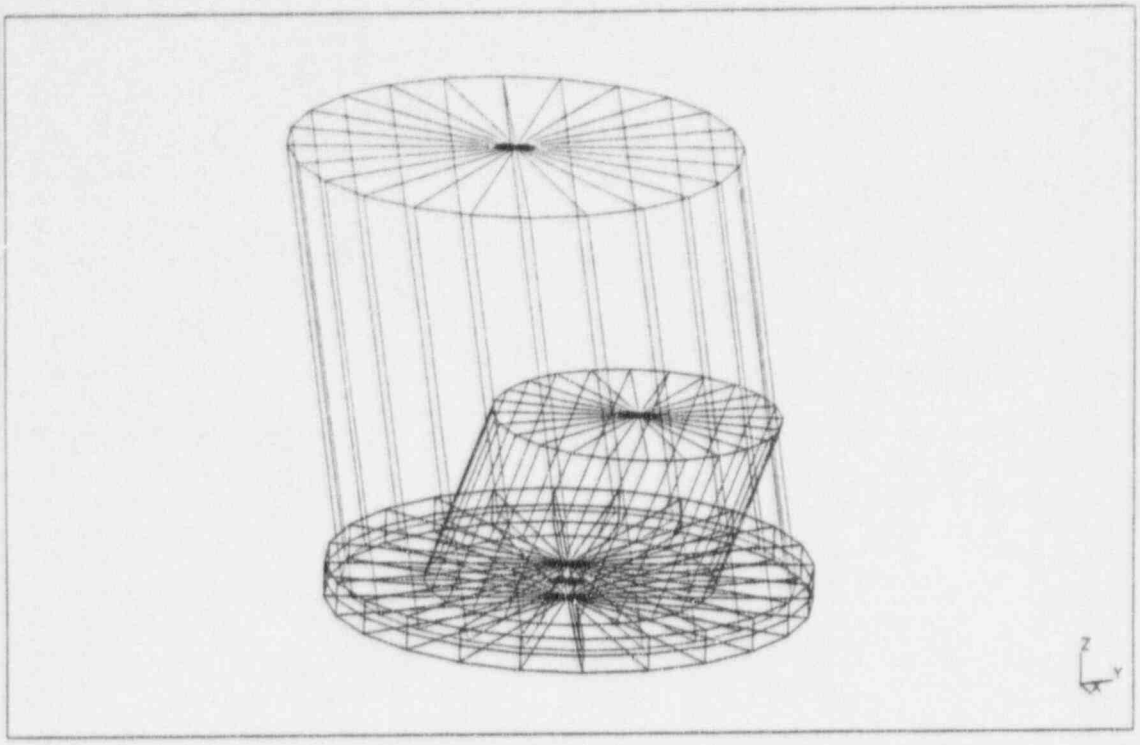

Figure 2.27 PWR model Mode 6 (Mode 7 orthogonal) - base almost stationary, internal components and containment out of phase, 4.68 Hz

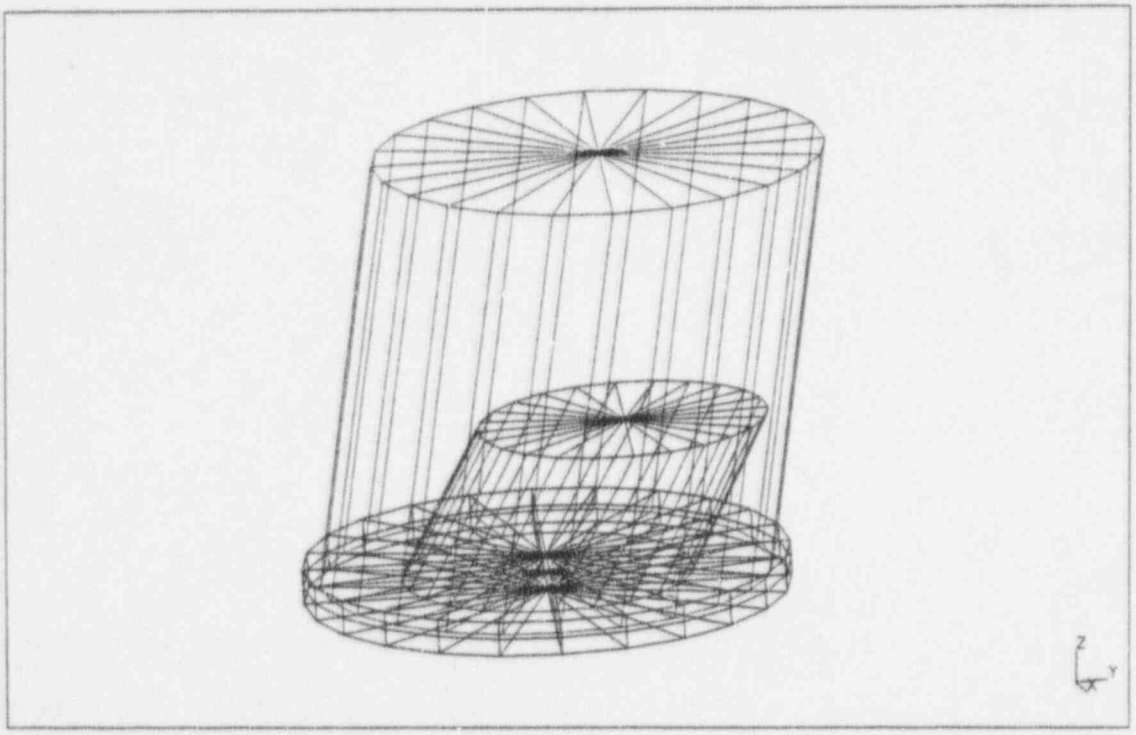

Figure 2.28 PWR model Mode 8 (Mode 9 orthogonal) - base moving laterally and out of phase with internal components and containment, 5.94 Hz

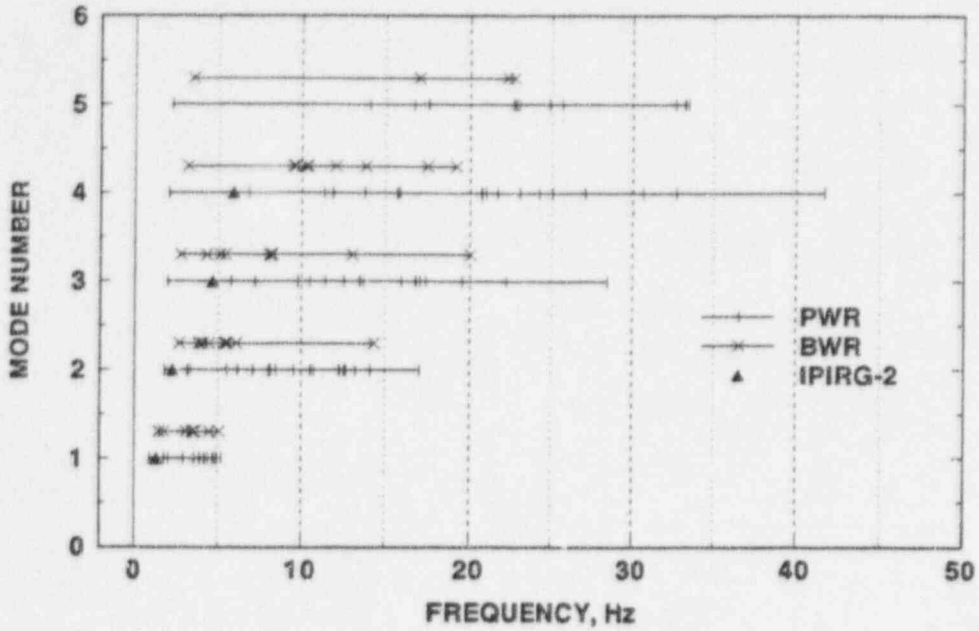

Figure 2.29 Reactor building natural frequency comparison*

Given the mass and stiffness characteristics of the PWR model, the equations of motion can be written in matrix form as:

$$[M]\{\ddot{U}\} + [C]\{\dot{U}\} + [K]\{U\} = -[M]\{\ddot{X}(t)\} \qquad (2\text{-}2)$$

where [M], [C], and [K] are the mass, damping, and stiffness matrices, respectively, {U} is the vector of displacements relative to the base, and $\{\ddot{X}(t)\}$ is the vector of ground accelerations as a function of time applied in three directions to the base. Although the equations of motion for the building are as shown in Equation 2-2, the actual analysis is effected as shown in Figure 2.30.

The motion analysis of the building model was performed using the ANSYS® (Ref. 2.21) finite element computer program. Using Revision 4.4, the equations of motion were integrated at 0.005 second time steps using 5-percent Rayleigh (mass and stiffness) damping with the Newmark (Ref. 2.22) time integrator. The damping was selected to be consistent with Regulatory Guide 1.61 (Ref. 2.14) recommendations for prestressed concrete structures at SSE level excitations.

Figures 2.31 through 2.37 show the response of the building at the three lumped mass locations. The smallest horizontal response (x or y) is at the base mat, while the largest is at the containment. The large response at the containment is due to its height.

---

* Polk, H., "Summary of Frequencies for Reactor and Auxiliary Buildings," letter to L. C. Shao, Chief, Structural Engineering Branch, U.S. Nuclear Regulatory Commission, March 1, 1975.

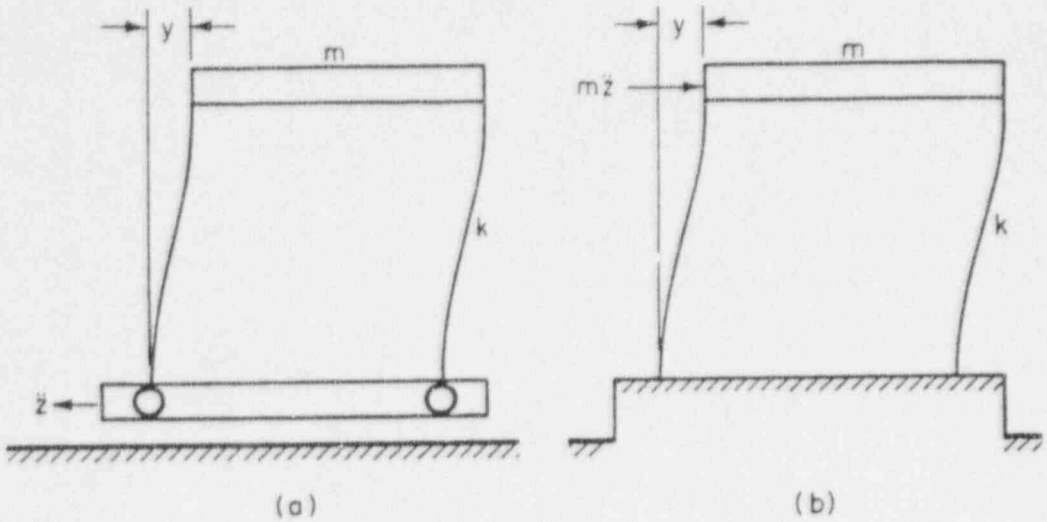

Displacement y is the same in both cases.

Figure 2.30 Building motion dynamic response analysis

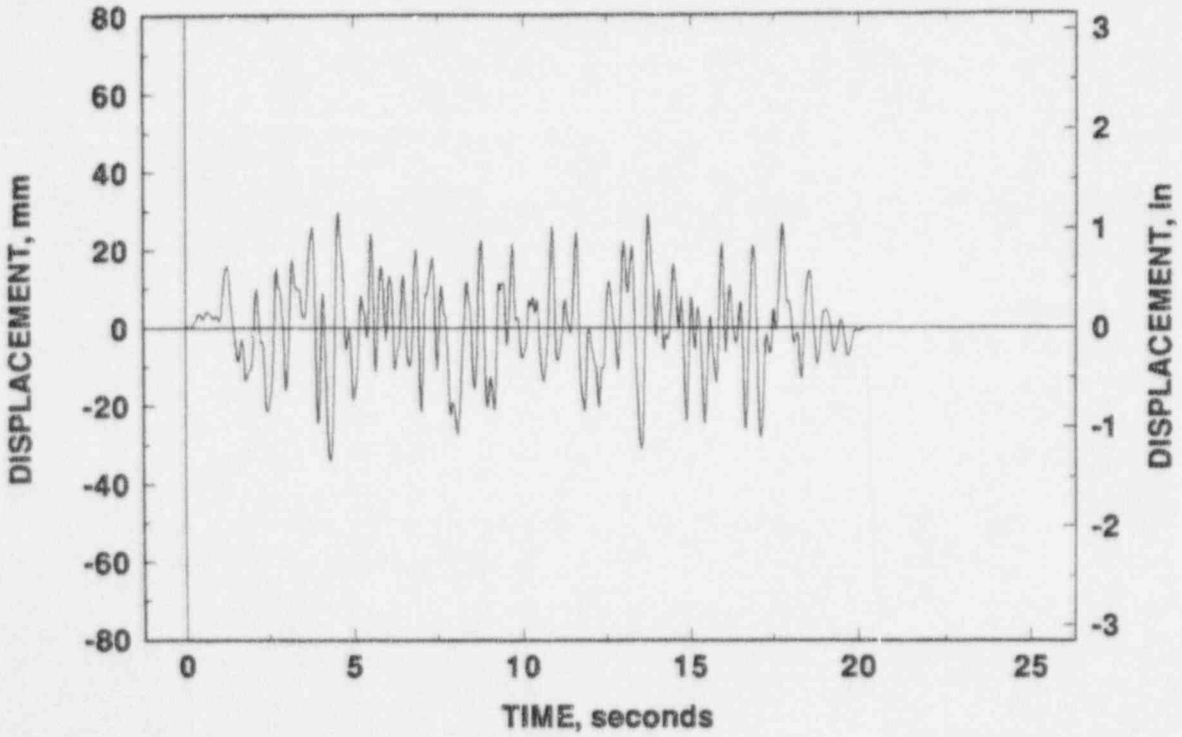

Figure 2.31 PWR model Z-direction (vertical) response due to a 1.0 g earthquake

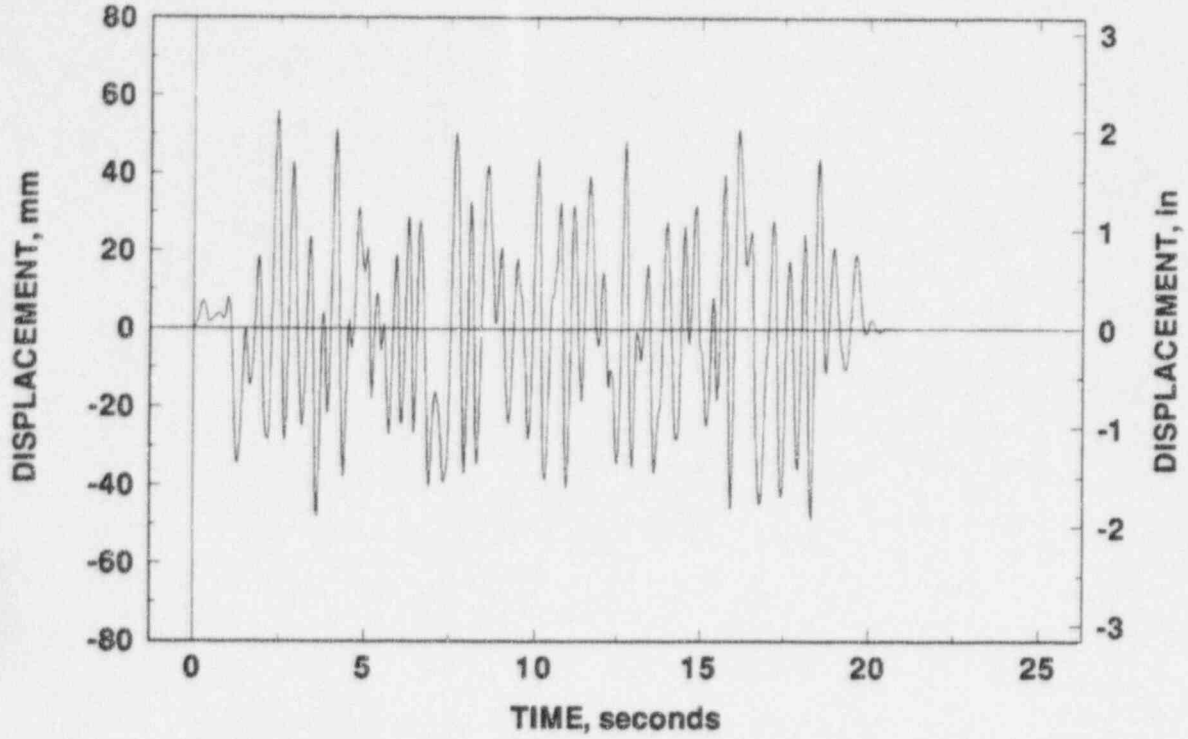

Figure 2.32 PWR model base mat (m_1) X-direction response due to a 1.0 g earthquake

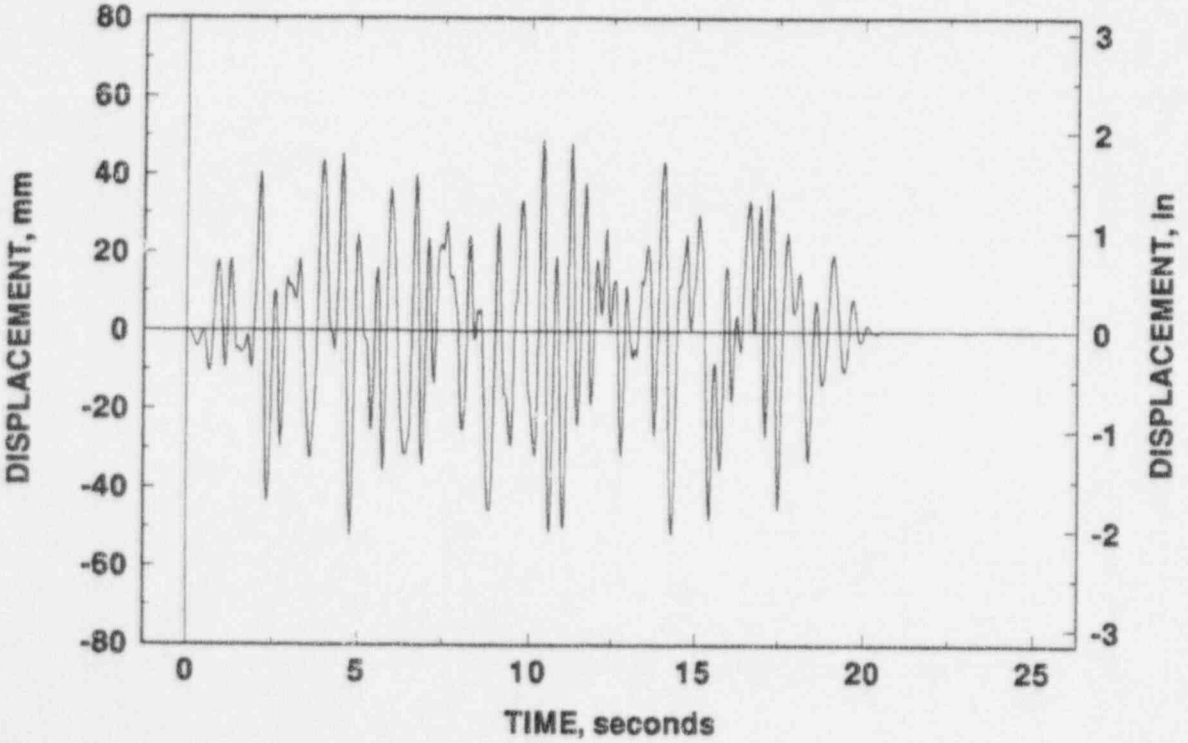

Figure 2.33 PWR model base mat (m_1) Y-direction response due to a 1.0 g earthquake

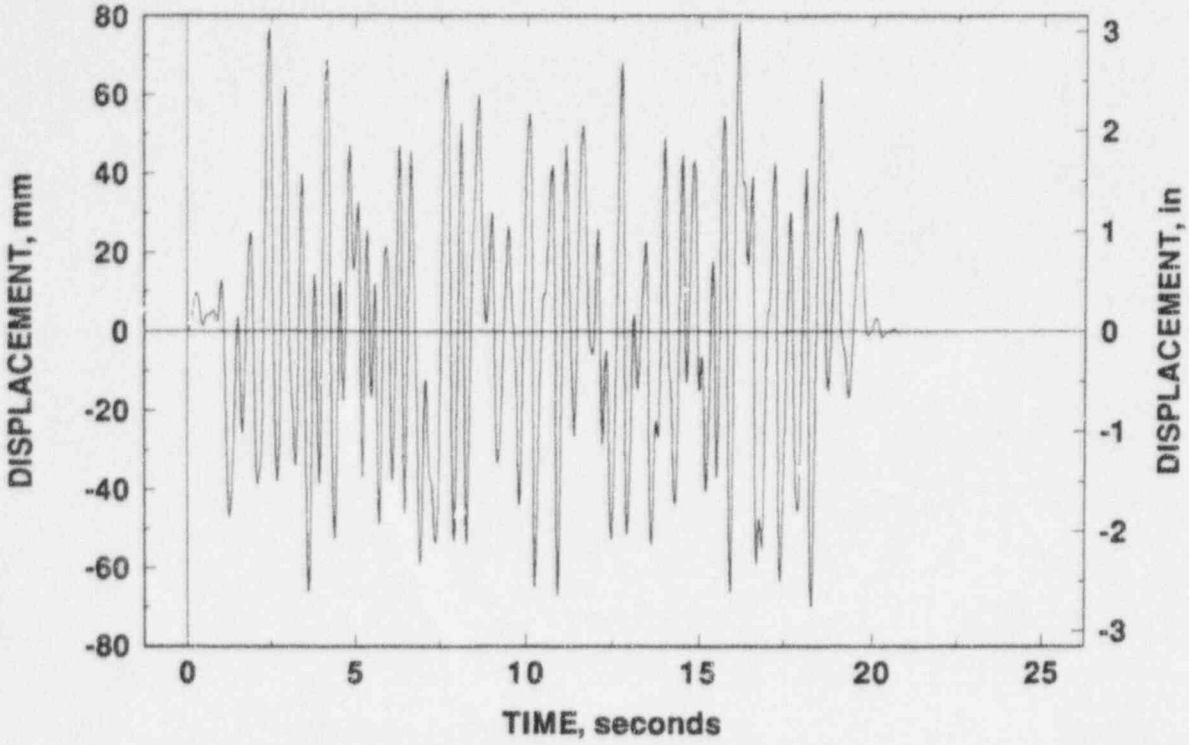

Figure 2.34 PWR model containment (m_2) X-direction response due to a 1.0 g earthquake

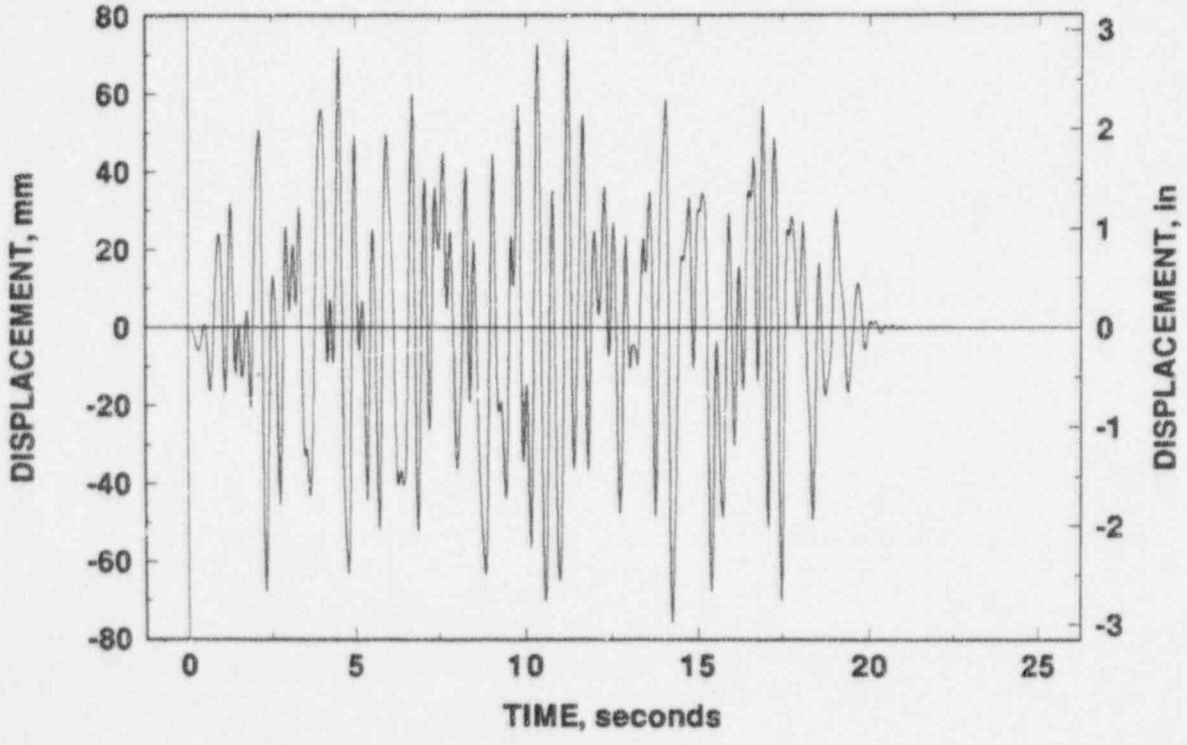

Figure 2.35 PWR model containment (m_2) Y-direction response due to a 1.0 g earthquake

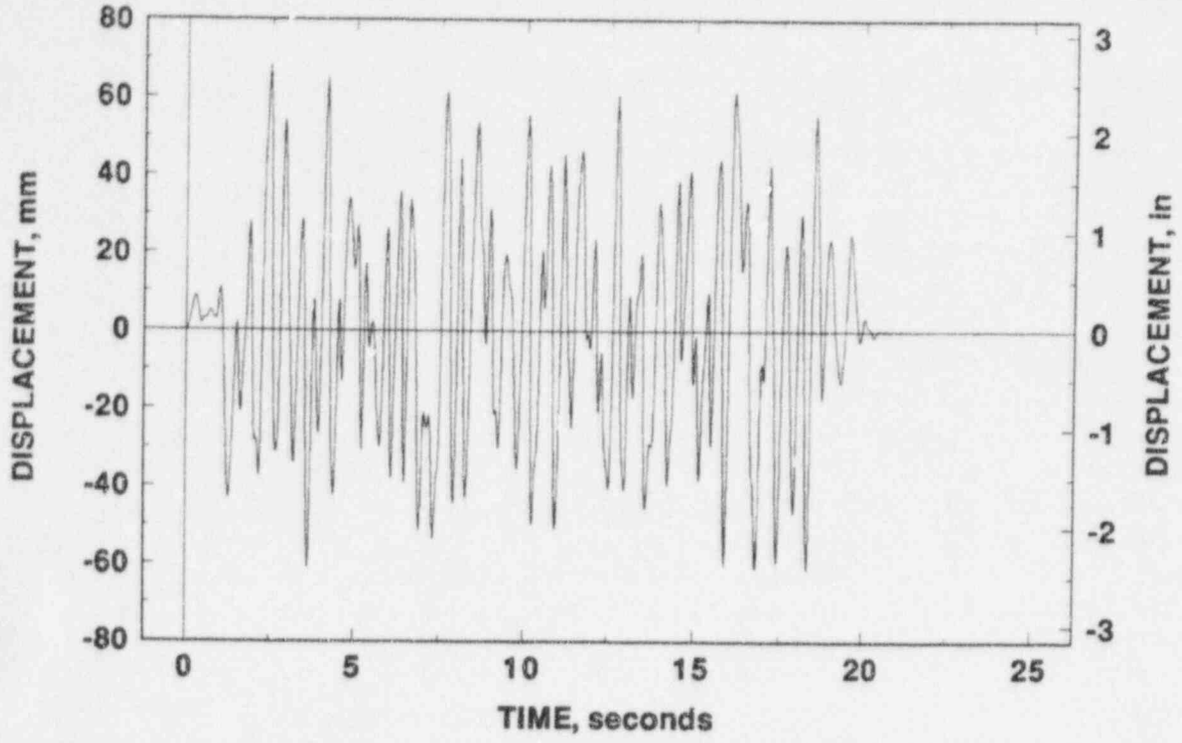

Figure 2.36 PWR model reactor internals (m_3) X-direction response due to a 1.0 g earthquake

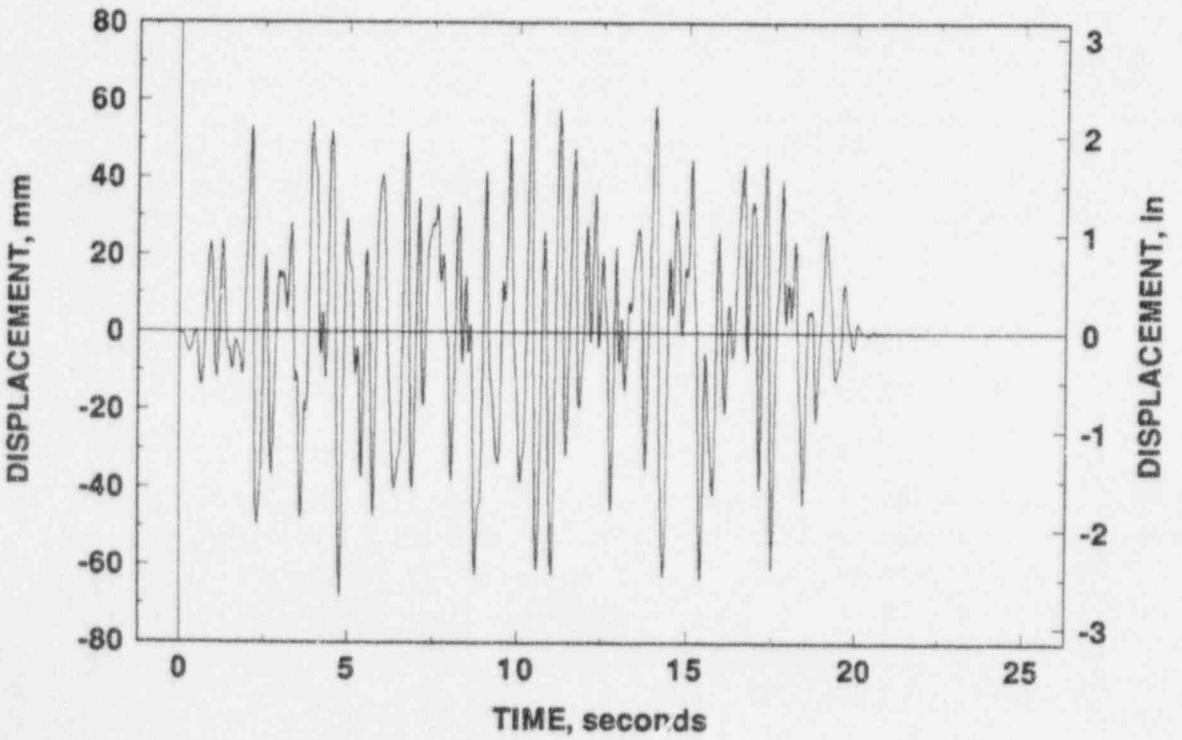

Figure 2.37 PWR model reactor internals (m_3) Y-direction response due to a 1.0 g earthquake

2.3.4 Pipe Motion

The time-history of displacement for a piece of pipe in a nuclear plant is a function of where the pipe is located in the plant. To establish the specific loading on a pipe, therefore, the building response as a function of time and the kinematic relationships implied by the location of the pipe in the building must be combined. For the IPIRG pipe system, there are three "attachment" points; the two fixed ends and the actuator location. The selection of the assumed locations of these points within the PWR plant model, in this case, is completely arbitrary. Given an assumed locations for these points, however, the time-history of motion for the "attachment" points can easily be determined.

For the purposes of this study, it was assumed that the actuator location on the IPIRG pipe system was located at Mass 3 of the PWR model (see Figure 2.23). The two fixed ends of the IPIRG pipe system were assumed to be at an elevation 8.07 m (318 inches) below the actuator location and at a horizontal distance of 18.54 m (730 inches) from the actuator location. The rationale for selection of the assumed distance of the fixed ends from the actuator location is that this distance is similar to the distance from the point where the main steam line exits the reactor to where it passes through the containment wall on the Clinton nuclear power plant, see Figure 2.38.

Performing the required kinematic operations that relate motion at the nodes of the PWR model to the assumed locations of the IPIRG pipe system fixed ends, the time history of motion at the fixed-ends can be calculated. Figures 2.39 through 2.42 show the motions to be applied to the IPIRG pipe system. Because the PWR model assumes rigid behavior in the z (vertical) direction, z displacements at the assumed actuator and fixed end locations are identical.

Relative to the motion at the assumed actuator location, Figures 2.39 and 2.40, the motion at the fixed ends, Figures 2.41 and 2.42, is smaller and appears to be slightly "filtered". Due principally to the lower elevation in the plant and the fact that it moves with the containment, the fixed end location does not respond as readily to some of the higher frequencies in the ground acceleration.

The IPIRG pipe system is constrained to excitation in a single direction. Therefore, to complete the prescription for the pipe motion, this fact has to be incorporated in the definition of the pipe motion that will be used to conduct the experiments. Two completely arbitrary assumptions were made:

- Only horizontal motion was considered
- The direction of excitation was taken as the direction where the motion of Mass 3 has its maximum magnitude.

Figures 2.43 and 2.44 show two-dimensional trajectories of the actuator location and the fixed ends locations along with a line that defines constrained single direction of motion. Using the vector components of the two-dimensional motion in the given direction, the final motion at the actuator location and fixed ends is as shown in Figures 2.45 and 2.46. The relative motion between the two locations is shown in Figure 2.47.

The pipe motion shown in Figures 2.45 and 2.46 defines the seismic anchor motion for the pipe system analyses. The companion inertial load at 1.0 g, based on consistent assumptions of horizontal

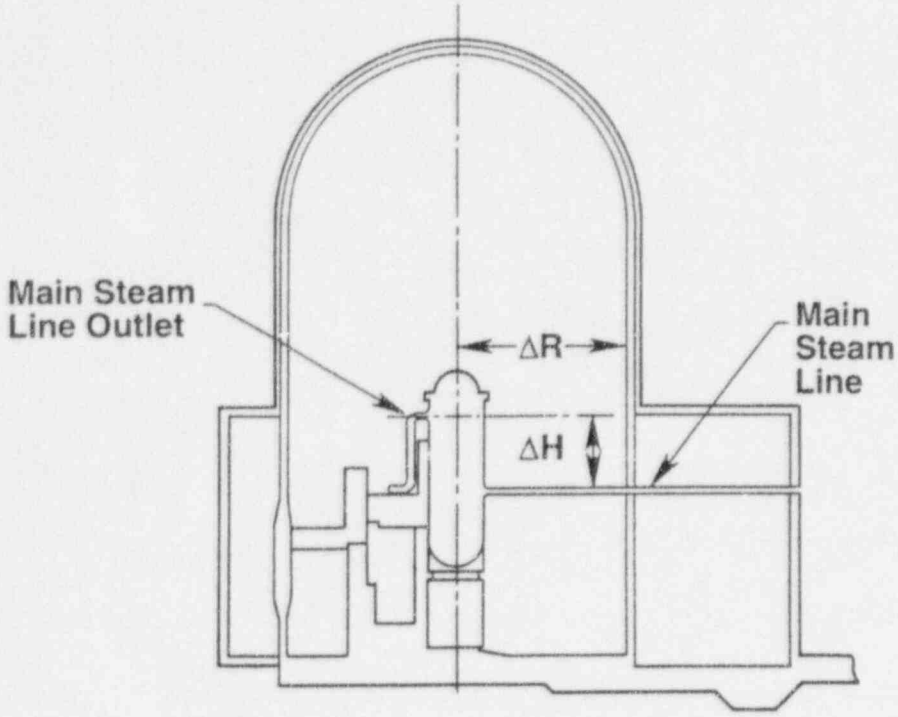

Figure 2.38 Illustration of the assumed distance of the fixed pipe ends from the actuator location for the IPIRG pipe system relative to schematic of Clinton nuclear power plant

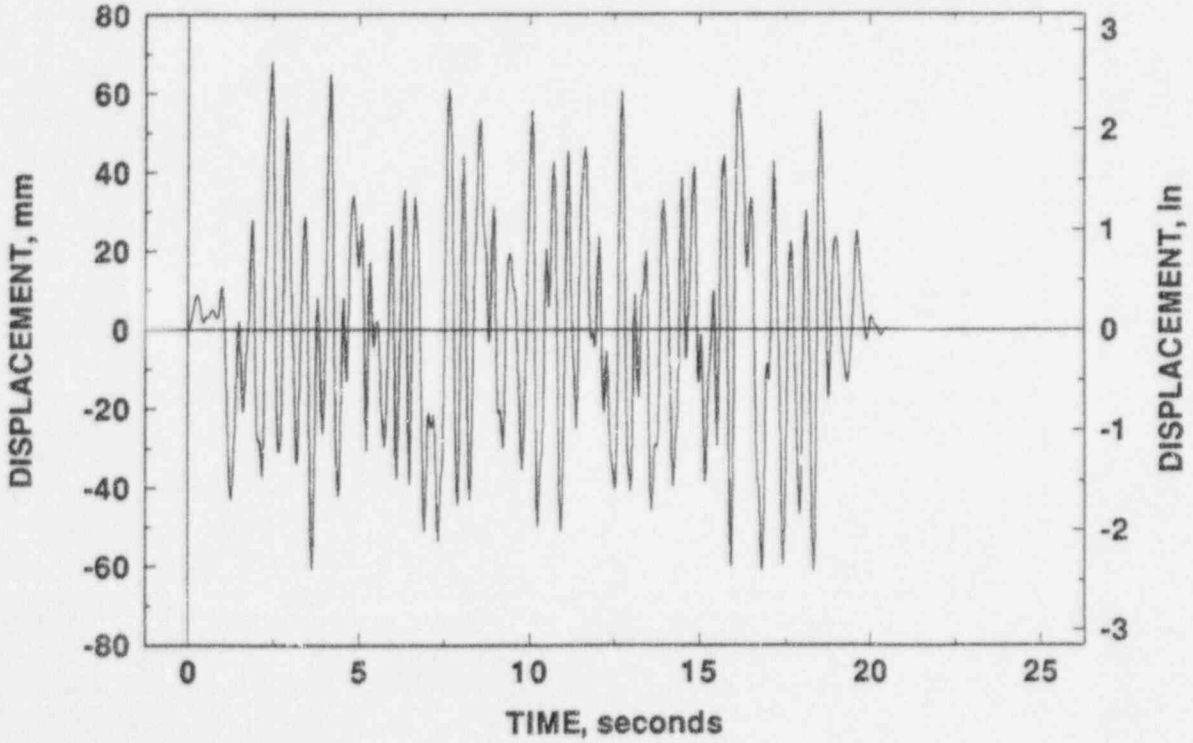

Figure 2.39 Simulated seismic dynamic response at the IPIRG pipe system actuator location in the X direction due to a 1.0 g earthquake

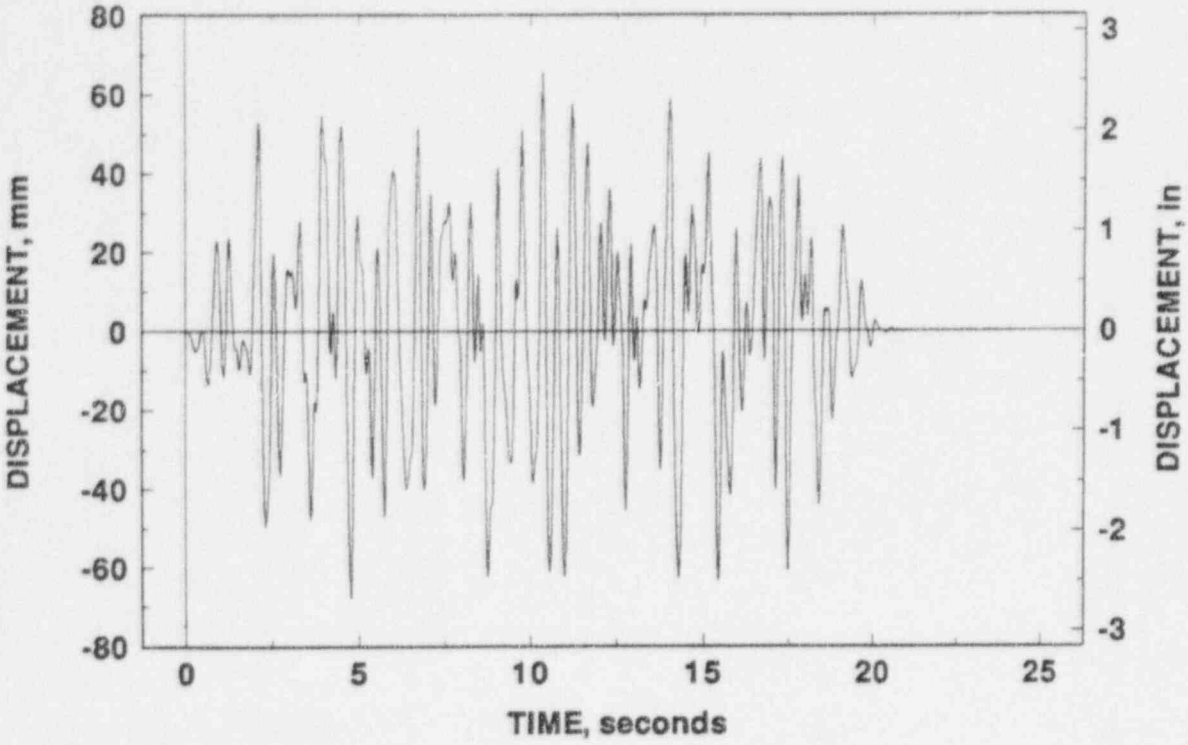

Figure 2.40 Simulated seismic dynamic response at the IPIRG pipe system actuator location in the Y direction due to a 1.0 g earthquake

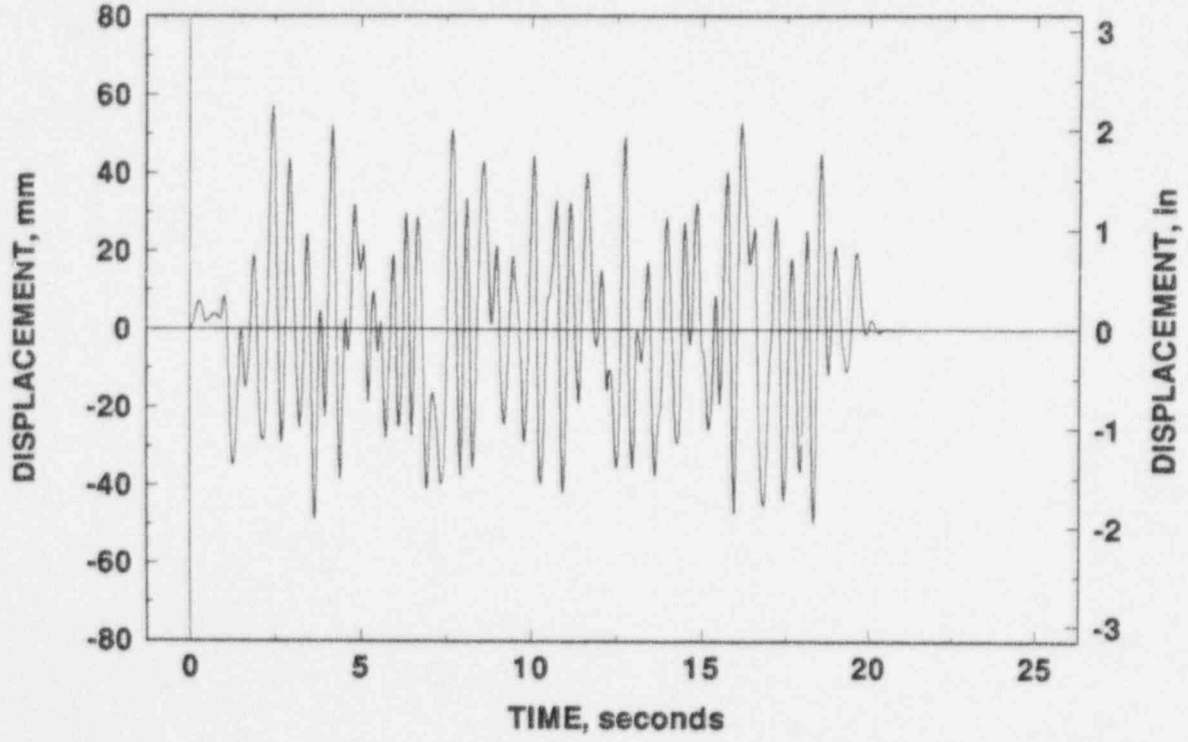

Figure 2.41 Simulated seismic dynamic response at the IPIRG pipe system fixed ends in the X direction due to a 1.0 g earthquake

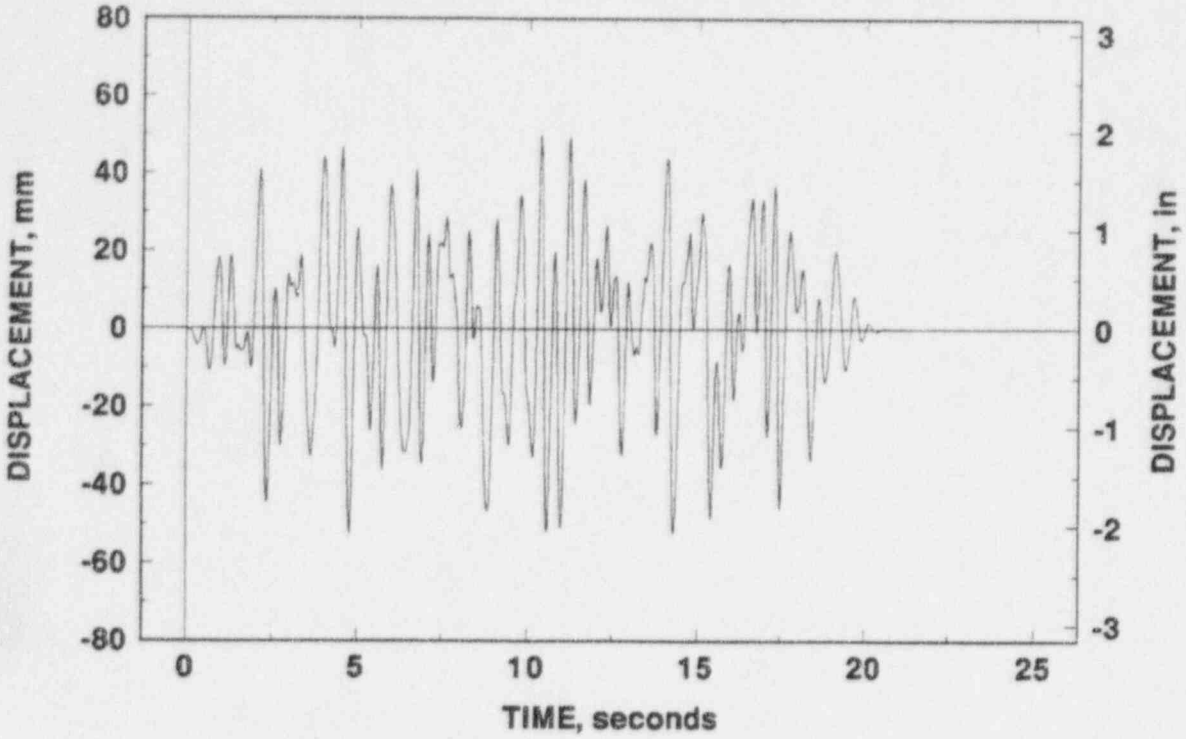

Figure 2.42 Simulated seismic dynamic response at the IPIRG pipe system fixed ends in the Y direction due to a 1.0 g earthquake

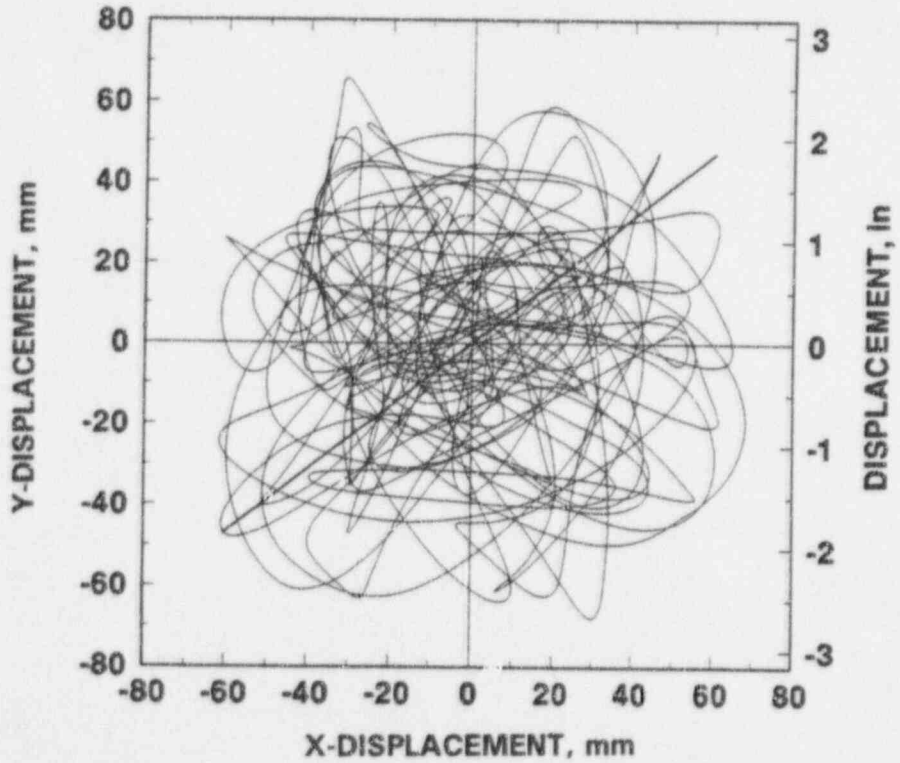

Figure 2.43 Horizontal motion at the assumed actuator location and assumed single direction of excitation for the IPIRG pipe system

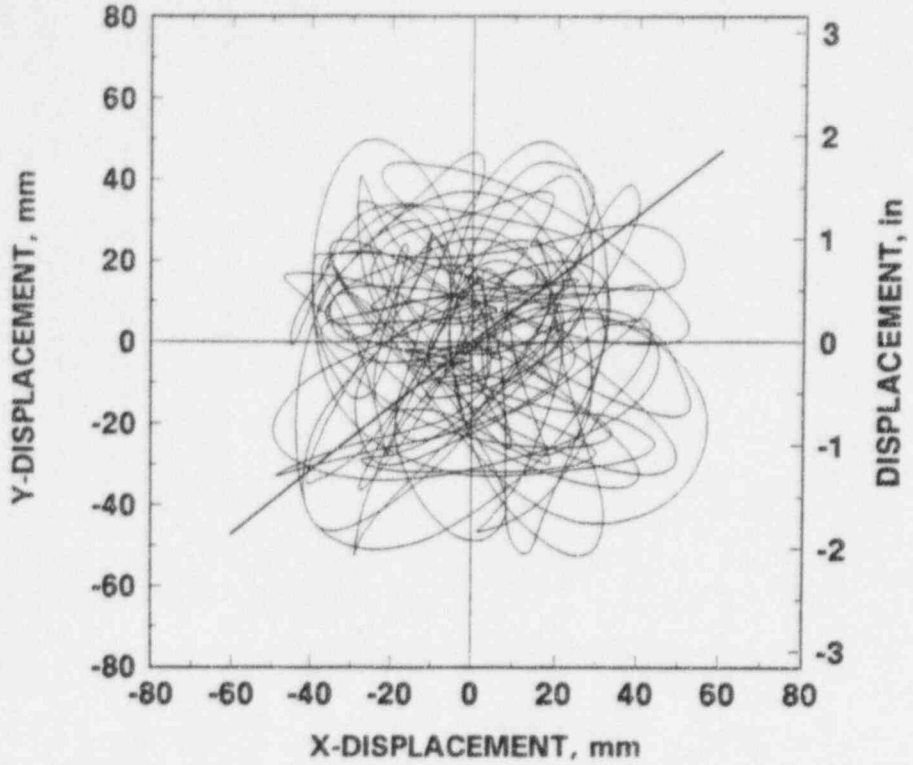

Figure 2.44 Horizontal motion at the assumed fixed ends location and assumed single direction of excitation for the IPIRG pipe system

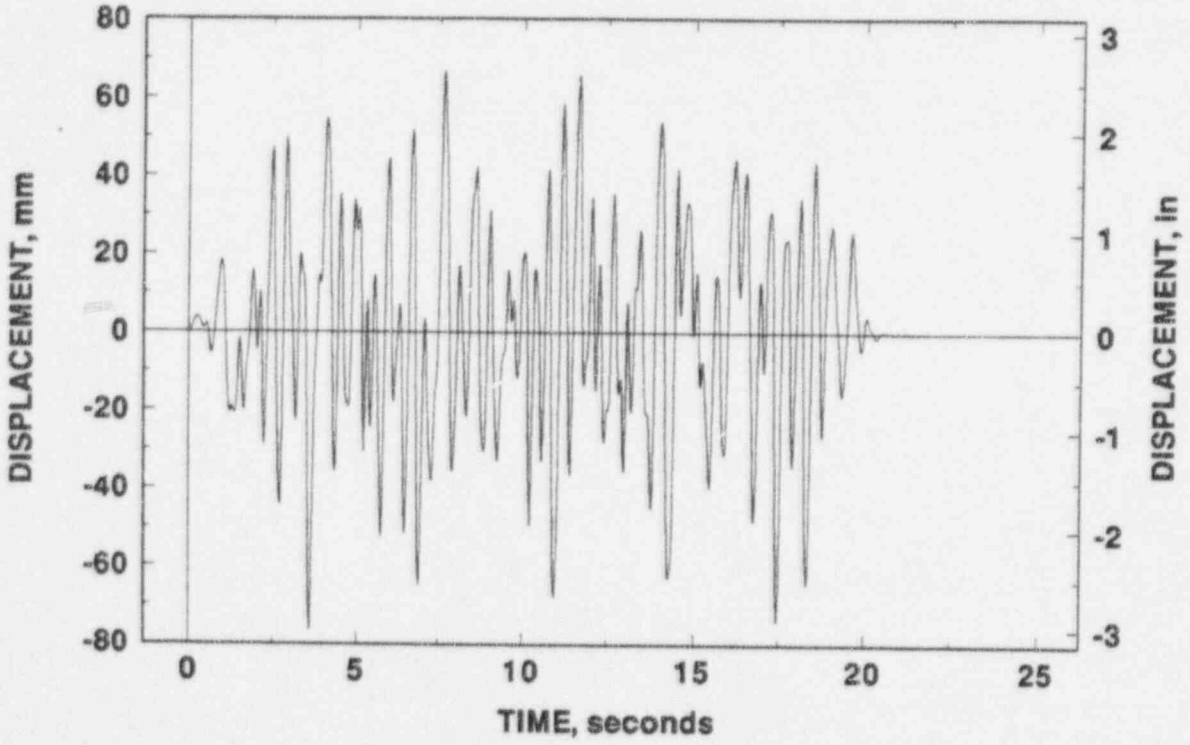

Figure 2.45 Time history of seismic anchor motion at 1.0 g, IPIRG pipe system actuator location

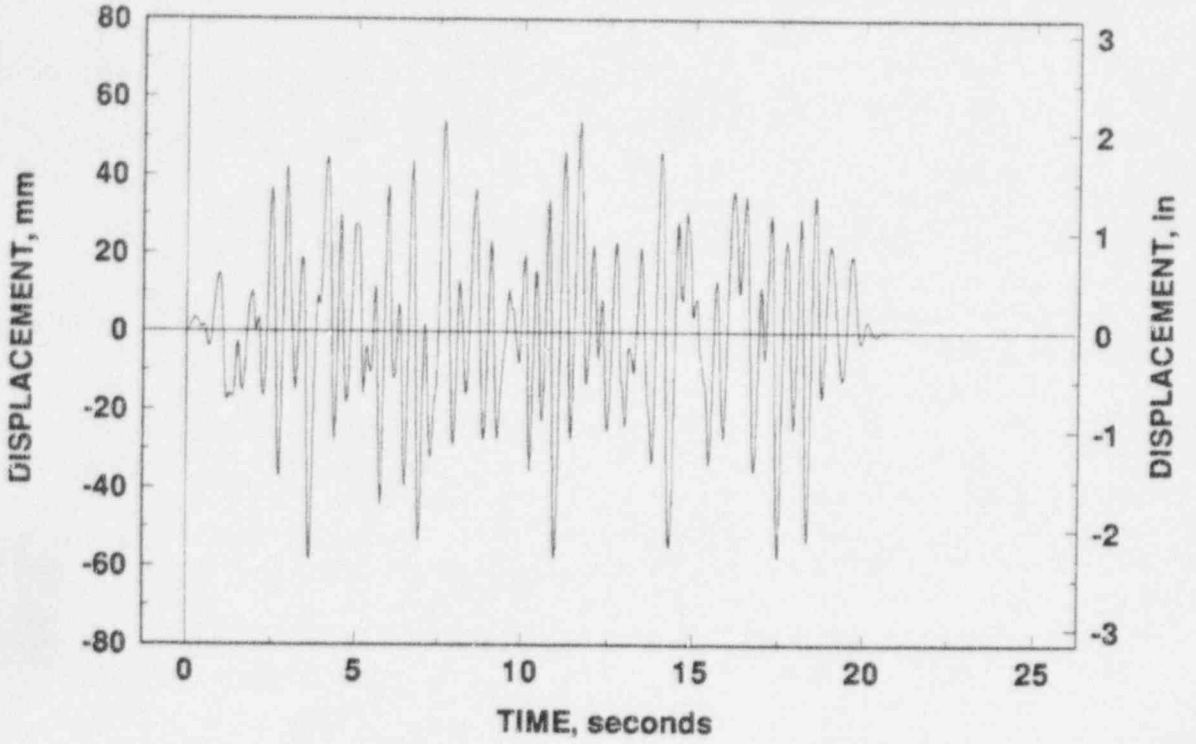

Figure 2.46 Time history of seismic anchor motion at 1.0 g, IPIRG pipe system fixed ends

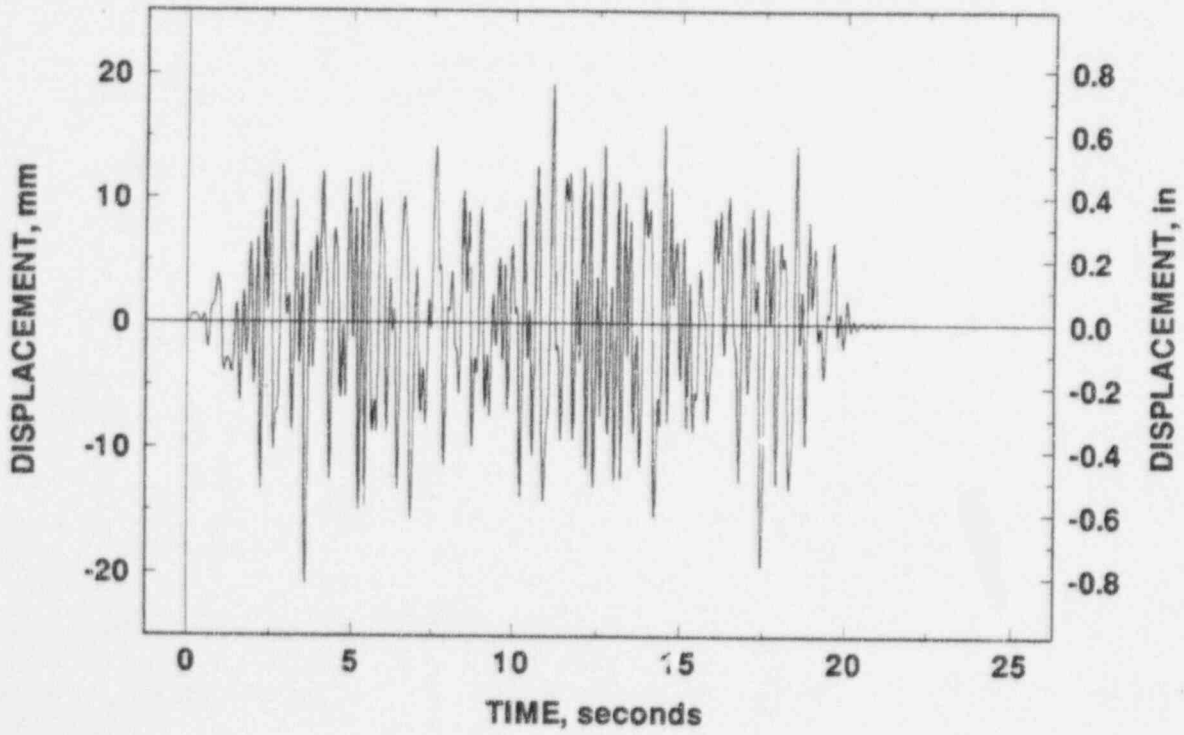

Figure 2.47 Time history of relative seismic anchor motion at 1.0 g for the IPIRG pipe system

motion in a single direction, is shown in Figure 2.48. The complete pipe excitation is the sum of the seismic anchor motion and the inertial load.

2.3.5 Single-Point Excitation

The IPIRG pipe system, shown in Figure 2.49, has only a single point of excitation. The basic IPIRG seismic forcing function, in contrast, includes motion at all three support points and inertial load due to acceleration of the building. By some means, the multi-point excitation had to be reduced to single-point excitation.

Although there were a number of ideas for how a multi-point excitation could be converted to single-point excitation, no documented formal procedure could be found to suggest how this could be done. So, all reasonable ideas were tried until one that worked was found. Basically, the objective was to find an actuator displacement time history that would give nearly the same moment-time response at the cracked-section location as excitation that included the seismic anchor motion defined in Figures 2.45 and 2.46, and the inertial load defined in Figure 2.48. To limit the resources required to do the required analyses, "super-element" finite element models were used in which all the portions of the finite element pipe system model on either side of the crack location were lumped into a few selected degrees of freedom connected by crack springs. In this case, the crack springs were assumed to remain linear.

Figure 2.50 shows the moment as a function of time for the seismic anchor motion plus inertial load at a 0.25 g scaled excitation using an uncracked linear pipe system model. Figure 2.51 shows the same data along with results from an analysis with only seismic anchor motion excitation. Point-by-point comparison of the two solutions indicates that the total and seismic anchor motion solutions differ by at most 5 percent. Thus, for all practical purposes, the inertial loading can be ignored, i.e., pipe loop response can be characterized simply by the seismic anchor motion loading.

As mentioned previously, several ideas were considered reasonable ways to convert multi-point excitation to single-point excitation. The three most promising candidates were:

- Using the relative displacement between the fixed ends and actuator location as the excitation
- Using some sort of reciprocal idea - if an actuator displacement yields a cracked section location moment-time history, perhaps a cracked-section location moment-time history would yield the required displacement-time function
- The displacement at the fixed ends (Figure 2.46) or at the actuator location (Figure 2.45) could perhaps be scaled.

Figures 2.52 through 2.54 show the results of comparisons between the seismic anchor motion case (multi-point excitation) and analyses using the methods listed above. The first two methods do not compare very favorably. The last method gives a single-point excitation moment-time history that is remarkably close to the multi-point excitation case.

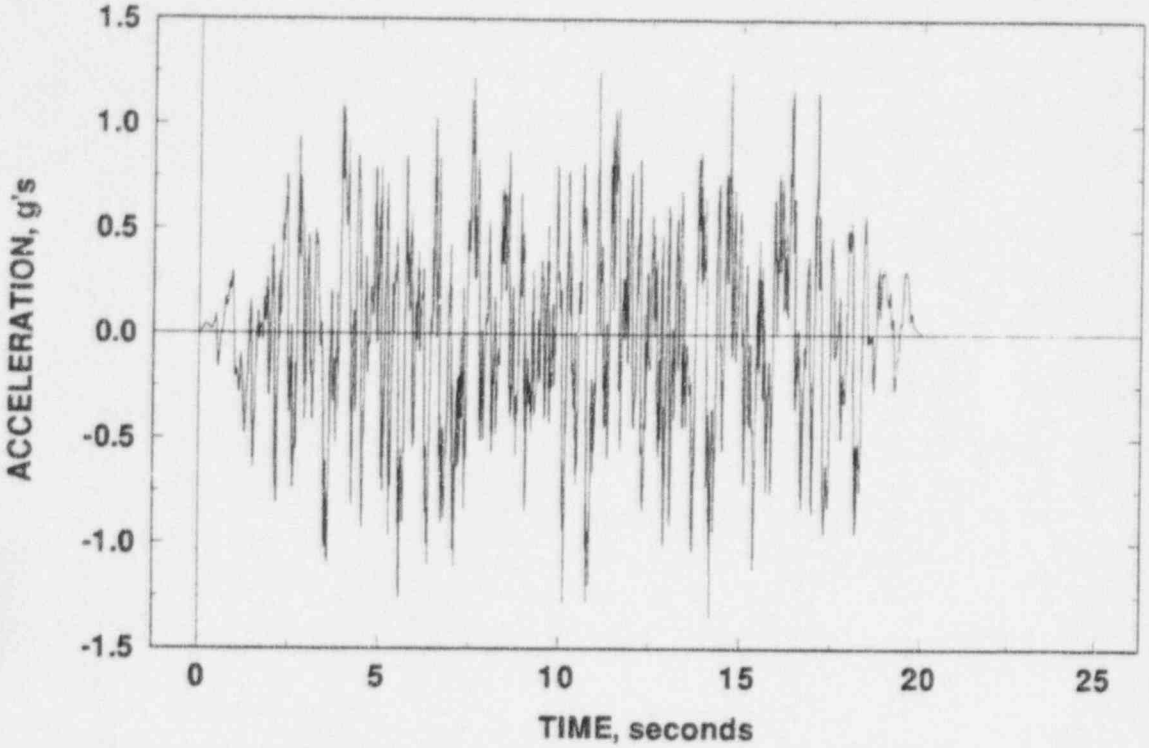

Figure 2.48 Time history of seismic inertial load at 1.0 g for the IPIRG pipe system

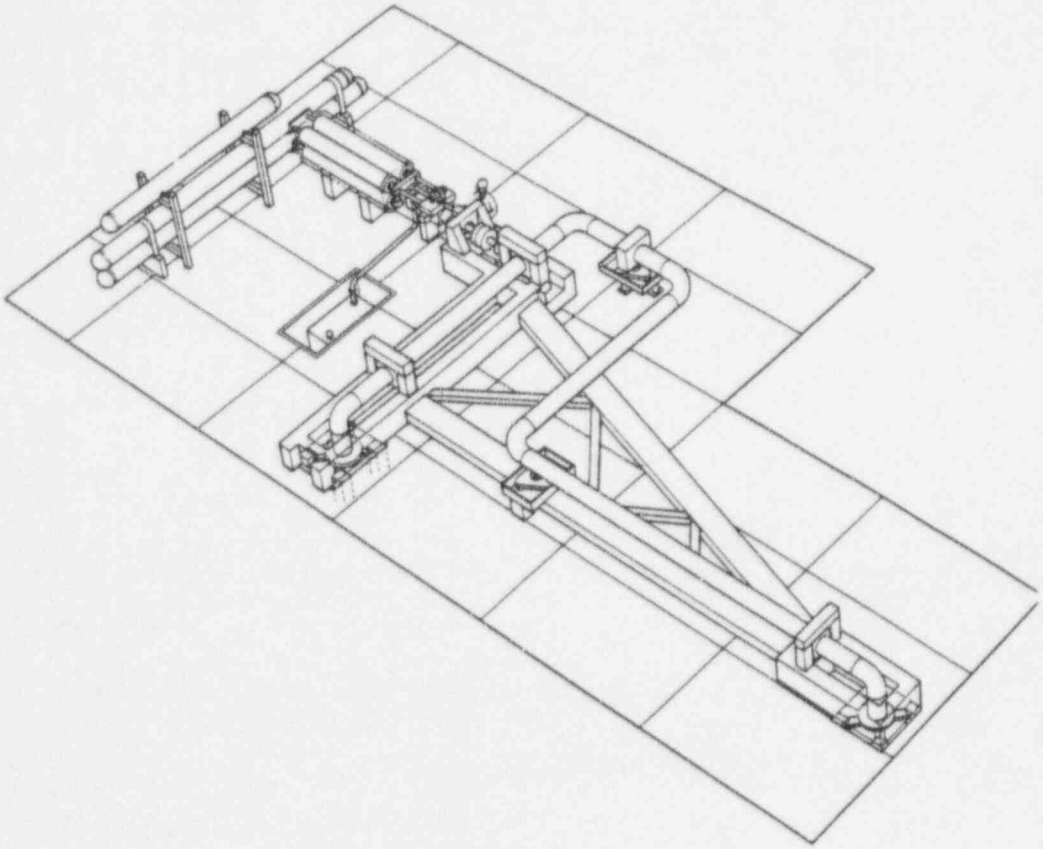

Figure 2.49 The IPIRG pipe system

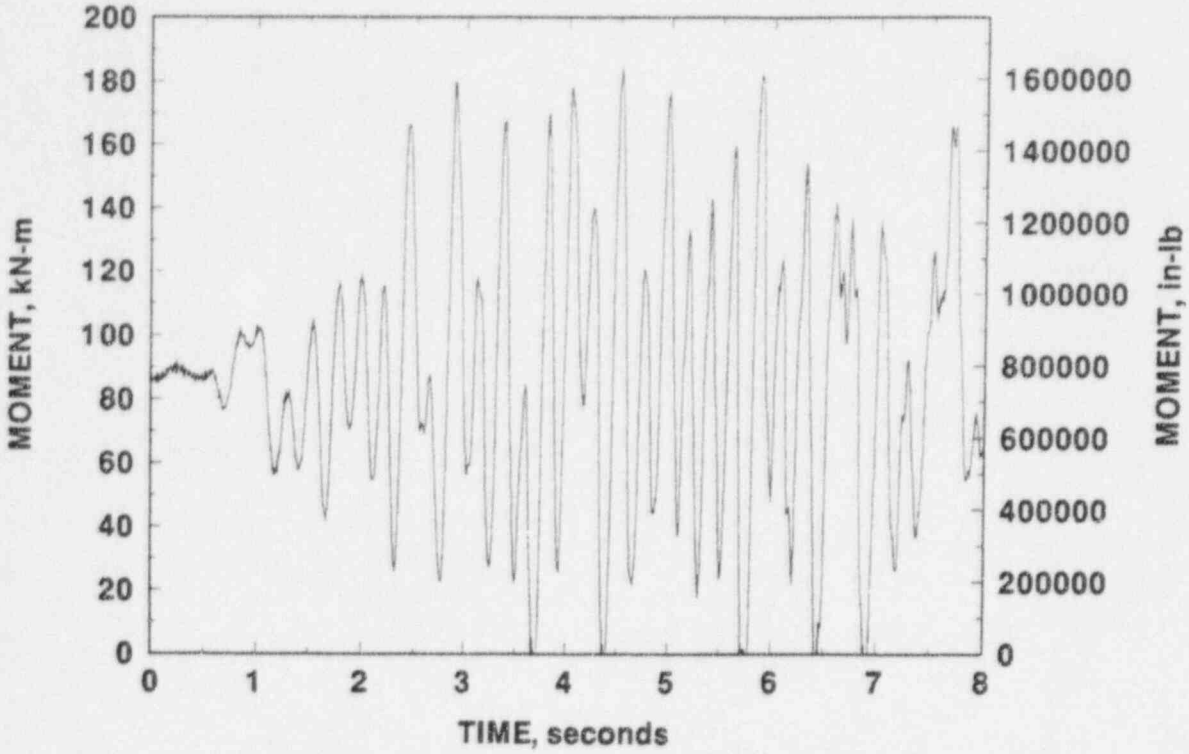

Figure 2.50 Cracked section location response from a linear analysis due to seismic anchor motion and inertial loading at 0.25 g

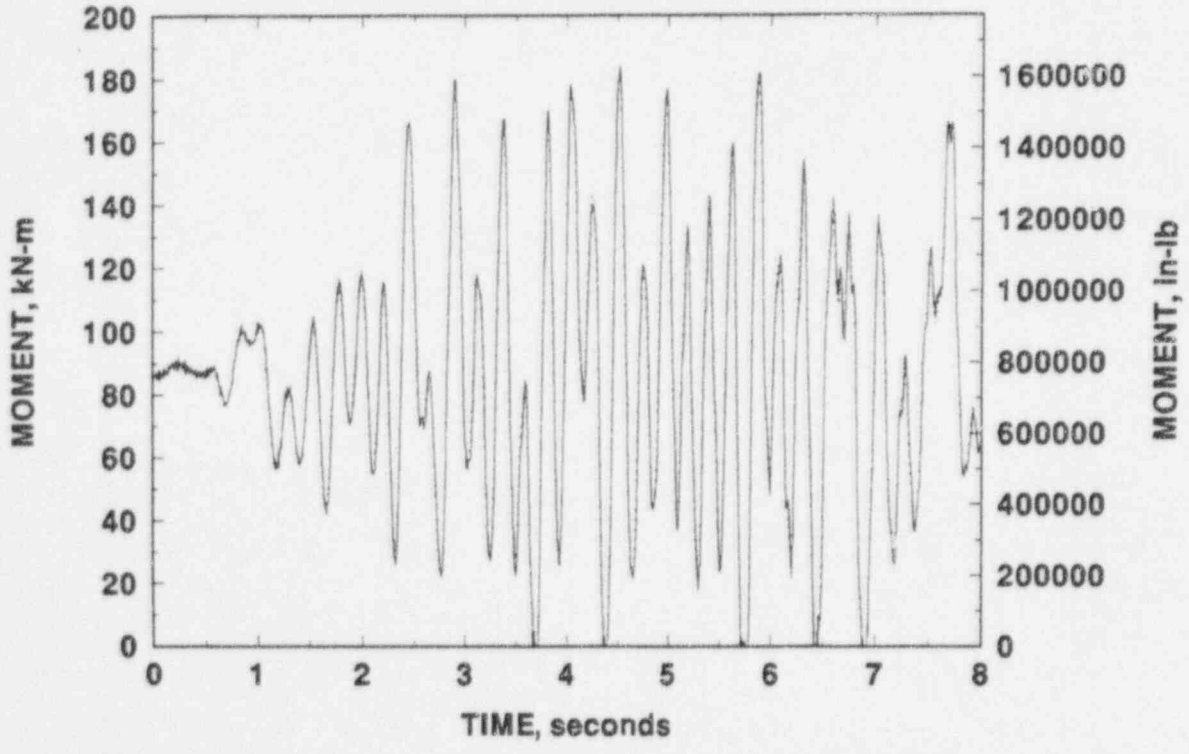

Figure 2.51 Cracked section location response from a linear analysis due to seismic anchor motion at 0.25 g

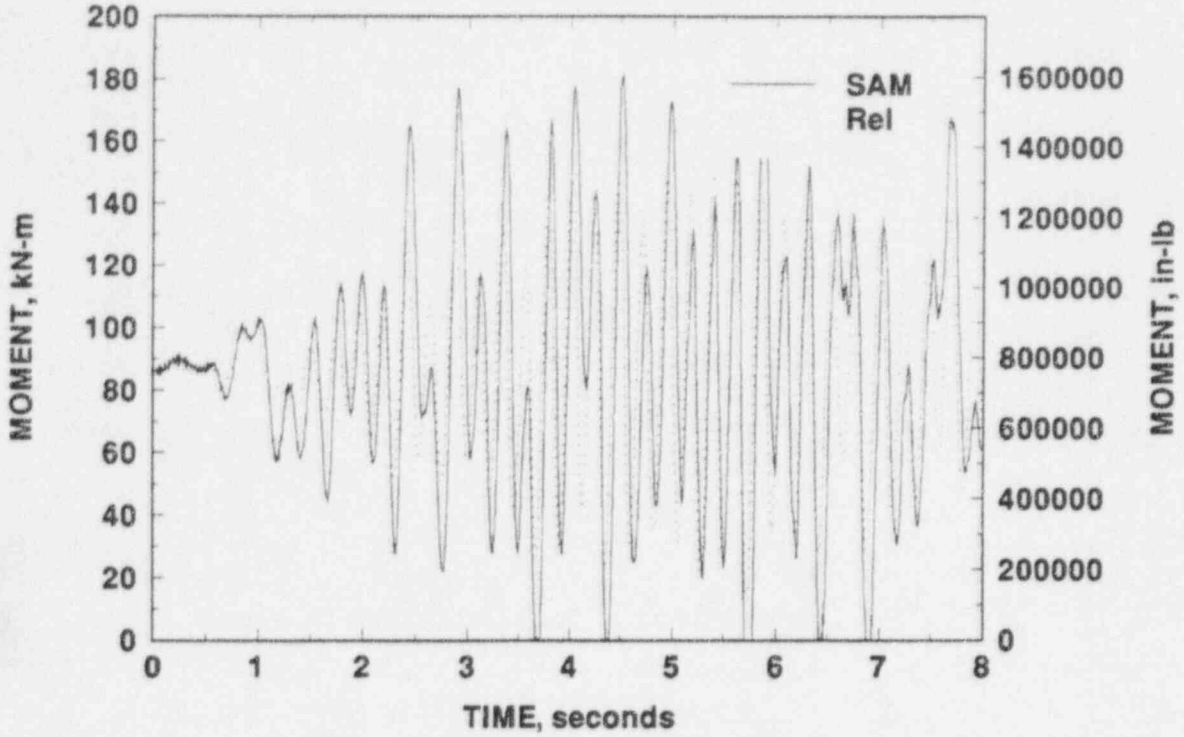

Figure 2.52 Comparison of multi-point excitation (seismic anchor motion - SAM) with single-point excitation using relative anchor motion

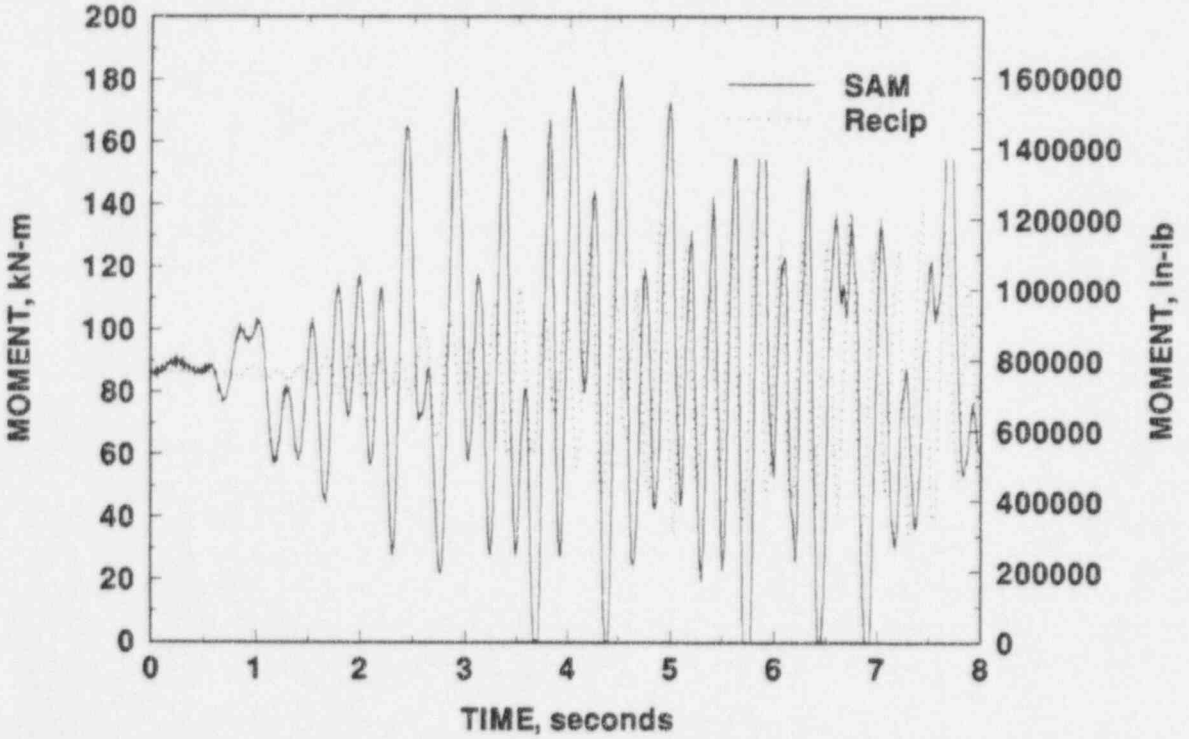

Figure 2.53 Comparison of multi-point excitation (seismic anchor motion - SAM) with single-point excitation using a reciprocal idea

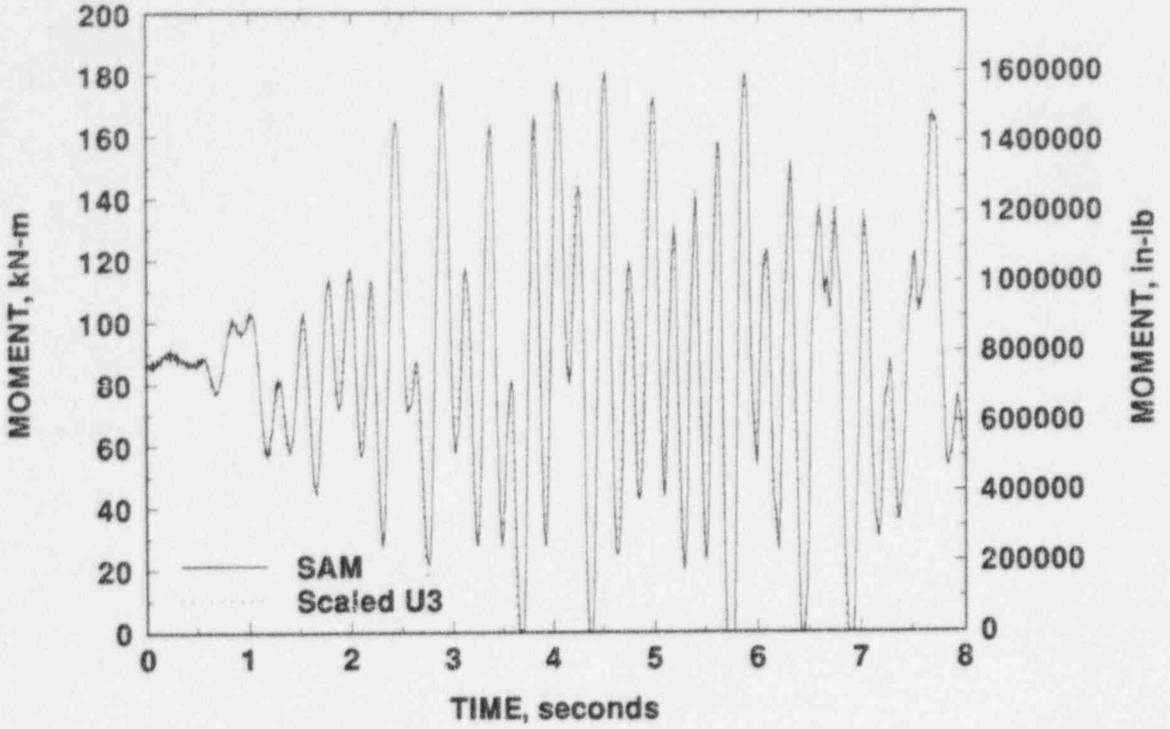

Figure 2.54 Comparison of multi-point excitation (seismic anchor motion - SAM) with single-point excitation using scaled actuator displacement (time history = 1.012 displacement of m_3)

By simply scaling the actuator location seismic anchor motion displacement time-history up by a factor of 1.012, the moment-time history at the cracked section location very closely duplicates the moment-time history when seismic anchor motion and inertial loads are applied. This is an unexpectedly simple result, which almost certainly is not general. The peculiar nature of the excitation assumptions and selection of the assumed locations for the attachment of the IPIRG pipe to the PWR model make the conversion from multi-point excitation to single point excitation trivial.

2.4 Summary

The basic seismic forcing function for the IPIRG simulated seismic experiments was designed using industry-accepted seismic design procedures. Starting from Regulatory Guide 1.60 ground acceleration spectra, artificial time histories of ground acceleration were created using the SIMQKE computer program. The ground motion was then applied to a simple PWR plant model. The basic motion to be applied by the actuator to the IPIRG pipe system was then defined using the time-history response of the PWR model and a few simplifying assumptions about how the IPIRG pipe might be connected to the PWR model.

The result of this design process is the function shown in Figure 2.55. The analyses conducted to design the forcing function were linear, so applying suitable constraints, the basic function can be scaled to meet the specific objectives of the IPIRG-2 seismic experiments.

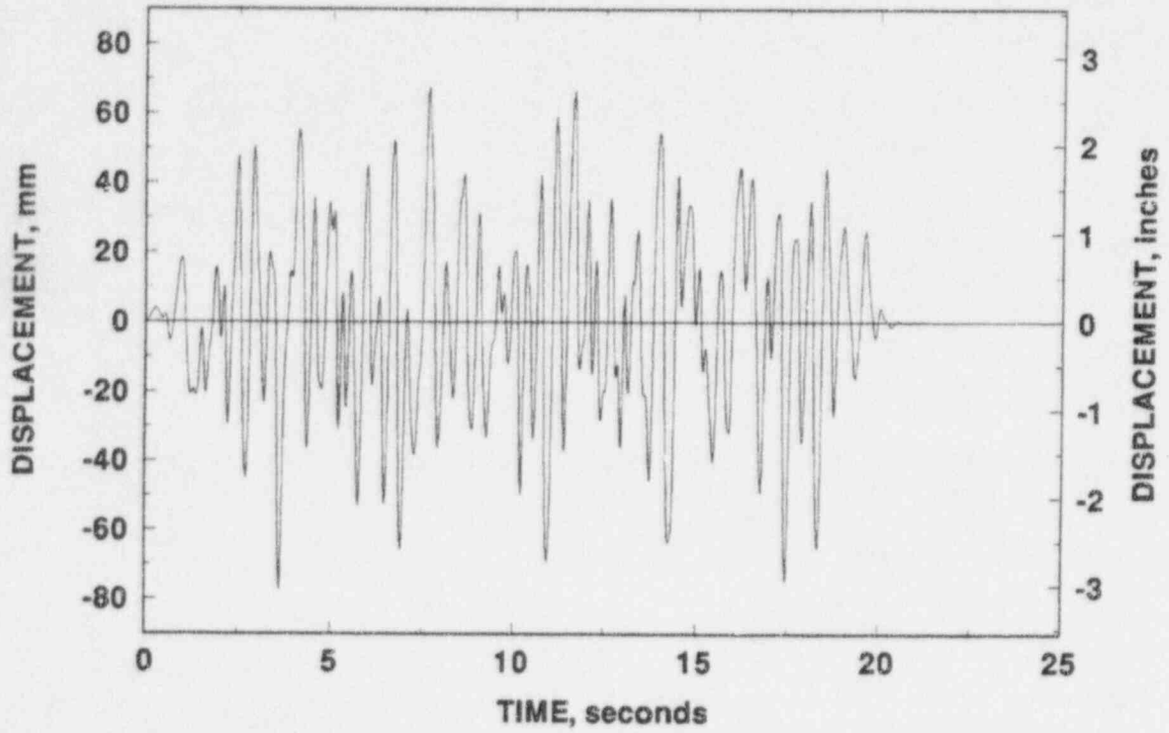

Figure 2.55 Basic IPIRG Seismic forcing function actuator displacement time history scaled to 1.0 g

2.5 References

2.1 "Design Response Spectra for Seismic Design of Nuclear Power Plants," Regulatory Guide 1.60, Revision 1, December 1973.

2.2 Tsai, N. C., "Spectrum Compatible Motions for Design Purpose," Journal of the Engineering Mechanics Division, Vol. 98, No. 2, ASCE, pp 345-356, 1972.

2.3 Housner, G. W., and Jennings, P. C., "Generation of Artificial Earthquakes," Journal of the Engineering Mechanics Division, Vol. 90, No. 1, ASCE, pp. 113-150, 1964.

2.4 Amin, M. and Ang, A. H. S., A Nonstationary Stochastic Model of Earthquake Motions, University of Illinois Civil Engineering Studies, Urbana, IL, 1966.

2.5 Rizzo, P. C., Shaw, D. E., and Jarecki, S. J., "Development of Real/Synthetic Time-Histories to Match Smooth Design Spectra," 2nd SMiRT Conference Proceedings, Berlin, Germany, Paper K 1/5, September 1973.

2.6 Hou, S. N., Earthquake Simulation Models and Their Application, Ph.D. Thesis, Massachusetts Institute of Technology, Cambridge, Massachusetts, 1968.

2.7 Hou, S. N., Earthquake Simulation Models and Their Application, M.I.T. Department of Civil Engineering Research Report R68-17, May 1968.

2.8 Jenkins, J. M., "General Considerations in the Analysis of Spectra," Technometrics, Vol. 3, pp 133-166, 1961.

2.9 Levy, S., and Wilkinson, J. P. D., "Generation of Artificial Time-Histories Rich in All Frequencies, From Given Response Spectra," 3rd SMiRT Conference Proceedings, London, United Kingdom, Paper K 1/7, September 1975.

2.10 SIMQKE - A Program for Artificial Motion Generation, Users' Manual and Documentation, available through National Information Service for Earthquake Engineering (NISEE), Earthquake Engineering Research Center, Berkeley, California, November 1976.

2.11 Gasparini, D., and Vanmarcke, E. H., "Simulated Earthquake Motions Compatible with Prescribed Response Spectra," M.I.T. Department of Civil Engineering Report R76-4, Order No. 527, January 1976.

2.12 "Seismic Design Parameters," Standard Review Plan 3.7.1, Revision 2, August 1989.

2.13 American Society of Mechanical Engineers, Boiler and Pressure Vessel Code, Section III - Division 1, Appendix N: Dynamic Analysis Methods, pp 638, 1989.

2.14 "Damping Values for Seismic Analysis of Nuclear Power Plants," Regulatory Guide 1.61, October 1973.

2.15 American Society of Civil Engineers, ASCE Standard - Seismic Analysis of Safety-Related Nuclear Structures and Commentary on Standard for Seismic Analysis of Safety Related Nuclear Structures, ASCE 4-86, pp 6-9, 1987.

2.16 Chiapetta, R., Effect of Soil-Structure Interaction on the Response of Reactor Structures to Seismic Ground Motion, US AEC Report ORO-3822-4, IITRI J6157, IIT Research Institute, Chicago, Illinois, pp 30-38, April 1970.

2.17 Chiapetta, R., Effect of Soil-Structure Interaction on the Response of Reactor Structures to Seismic Ground Motion, US AEC Report ORO-3822-4, IITRI J6157, IIT Research Institute, Chicago, Illinois, pp 27, April 1970.

2.18 Agbabian Associates, Soil/Structure Interaction Guidelines, DOE/SF/01011-130, pp. 4-4 to 4-6, September 1981.

2.19 Richart, F. E., Hall, J. R., and Woods, R. D., Vibration of Soils and Foundations, Prentice-Hall, Englewood Cliffs, New Jersey, pp 191-243, 1970.

2.20 American Society of Civil Engineers, ASCE Standard - Seismic Analysis of Safety-Related Nuclear Structures and Commentary on Standard for Seismic Analysis of Safety Related Nuclear Structures, ASCE 4-86, pp 30, 1987.

2.21 ANSYS Engineering Analysis System User's Manual, Revision 4.4A, ANSYS, Inc., Houston, Pennsylvania, 15342, May 1989.

2.22 Newmark, N. M., "A Method of Computation for Structural Dynamics," Journal of the Engineering Mechanics Division, ASCE, Vol 8, pp 67-94, 1959.

3.0 SCALING THE SIMULATED SEISMIC FORCING FUNCTION

3.1 Introduction

The basic seismic forcing function was developed on the basis of a 1.0 g earthquake. To satisfy the requirements for the IPIRG-2 simulated seismic experiments, the basic 1.0 g earthquake needed to be scaled. The test philosophy used for the IPIRG-2 simulated seismic experiments was to apply three increasing levels of loading:

(1) "SSE" level - an excitation that would be considered representative of a safe shut-down earthquake (SSE) to demonstrate that design basis for current plants is adequate. Significant crack propagation should not occur under this loading.

(2) "Test" level - best estimate of scaled basic forcing function that would result in surface-crack penetration some time during the time history

(3) "Decision Tree" - a loading to be applied if the "test" loading does not result in surface-crack penetration or if the crack is small. Application of this load is contingent upon the critical instrumentation being functional after the "test" loading and the ability to be able to visually inspect the system by remote video (i.e., steam does not obscure the test section).

To define the various load levels, nonlinear-spring, cracked-pipe, finite element analyses were used (Refs. 3.1 and 3.2). In these analyses, the cracked section is modeled as a nonlinear moment-rotation spring. Analyses are performed in the time domain and growth of surface or through-wall cracks, the occurrence of surface-crack penetration and transition of a surface crack to a through-wall crack can be analytically predicted.

3.2 Stress Analysis Basics

The pipe system stress analyses used during the design of the seismic forcing function were identical to the calculations performed for the pretest design of the IPIRG-1 experiments, i.e., the measured 0.5-percent damping of the IPIRG pipe system was used, the surface-crack J-estimation scheme SC.TNP in the NRCPIPES code Version 1.0 (Ref. 3.3) was used to define the expected moment-rotation behavior of surface cracks, the through-wall crack J-estimation scheme LBB.ENG2 in the NRCPIPE code Version 1.4F (Ref. 3.4) was used to model through-wall-cracked pipe moment-rotation behavior, and the nonlinear equations of motion were integrated in time using ANSYS® (Ref. 3.5). The basic pipe system was modeled with standard straight and curved beam-type pipe elements.

Using the calculated response of the pipe to the seismic excitation, the seismic input was iteratively scaled to find an acceleration level that would cause a certain moment to be attained or that would cause the surface cracks to penetrate the pipe wall. Companion evaluations were performed to ensure that the servo-hydraulic capacity of the IPIRG pipe system test facility was not exceeded. Checks

were also performed to evaluate the fraction of the loading due to pipe inertia and to establish the stress ratio for the loading.

3.3 Scaling to Establish SSE Loading

The selection of a scaling factor for the "SSE" level loading was not necessarily straight forward because the definition of an SSE is quite variable and is plant specific. Obviously, in the spirit of generating a credible seismic forcing function, a reasonable scaling factor must be used. Fortunately, some data are available that provide some guidance for selection of a reasonable scaling factor.

Figure 3.1 shows a histogram of N+SSE stresses (normal operating stress+safe shut-down earthquake stress = pressure+dead weight+thermal expansion+safe shut-down earthquake load) (Ref. 3.6). These data were taken from a number of different pipes in five different operating U.S. nuclear plants and were normalized with respect to ASME Section II Part D S_y and S_m values (Ref 3.7). The data clearly indicate that actual N+SSE level stresses at straight pipe girth weld locations may be significantly below ASME Service Level B, C, or D limits. (Note: Elbow or other fitting stress values would be higher and may have approached the ASME limits.)

Table 3.1 summarizes various possible N+SSE stress levels applicable to the materials of interest for the IPIRG-2 simulated seismic experiments. Substituting the N+SSE stresses from Table 3.1 into Equation 9 of Article NB-3652 in the ASME Boiler and Pressure Vessel Code and assuming straight 406 mm (16 inch) Schedule 100 pipe and a test pressure of 15.5 MPa (2,250 psi), the corresponding moments are as shown in Table 3.2. For the IPIRG-2 pipe system specimens and test pressure, the pressure stress alone exceeds the actual minimum N+SSE stress level from the data base.

The selection of an N+SSE moment for the IPIRG-2 simulated seismic experiments is complicated by the scatter in the data shown in Table 3.2. The range of possible moments for N+SSE conditions is from 25.0 kN-m (221,000 in-lb) to 536.9 kN-m (4,752,000 in-lb), and the moments for A106 are 1.1 to 2.2 times the corresponding TP304 moments for similar conditions. As a compromise, a moment of 158.2 kN-m (1,400,000 in-lb) was selected as the IPIRG-2 N+SEE moment. The resulting scaled basic earthquake acceleration required to get a maximum moment of 158.2 kN-m (1,400,000 in-lb) is 0.2 g.

To judge whether or not a 0.2 g earthquake is a reasonable selection for the IPIRG-2 SSE level excitation, some comparisons were made to actual and/or proposed nuclear plant data. The first way to judge the suitability of a 0.2 g earthquake is to compare this level to the design basis SSE acceleration for some plants. Table 3.3 summarizes a comparison of acceleration levels. The conclusion is that 0.2 g is not unreasonable. A second way to judge the suitability of a 0.2 g earthquake is to compare the "floor response spectra" of the actuator motion with floor response spectra of some plants. Figures 3.2 and 3.3 show the 0.2 g IPIRG-2 SSE "floor response spectra", while Figures 3.4 to 3.7 show response spectra from some existing or proposed nuclear plants. Again, the conclusion is that the IPIRG-2 simulated seismic response is not unreasonable.

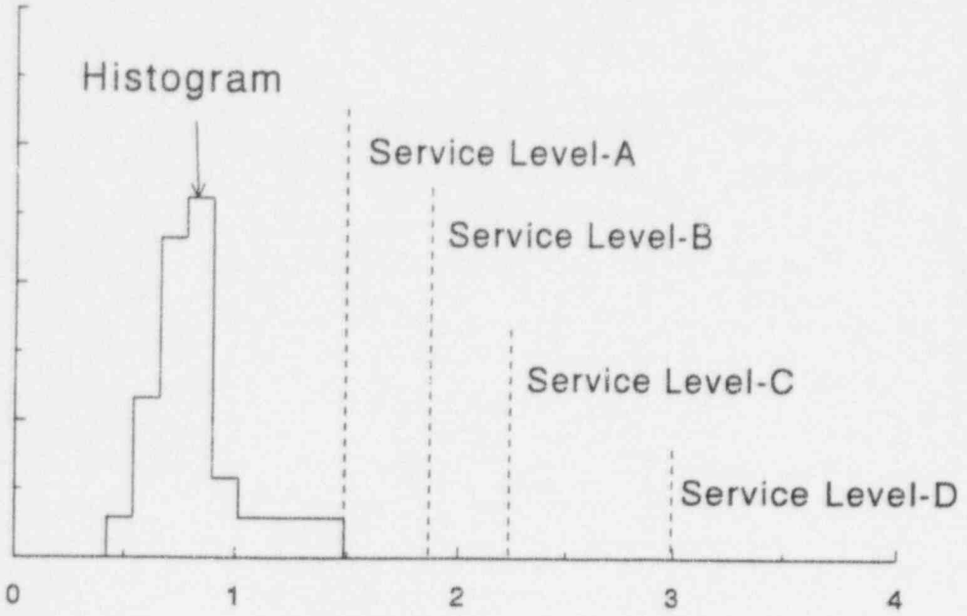

(a) ASME code S_m-based assessment

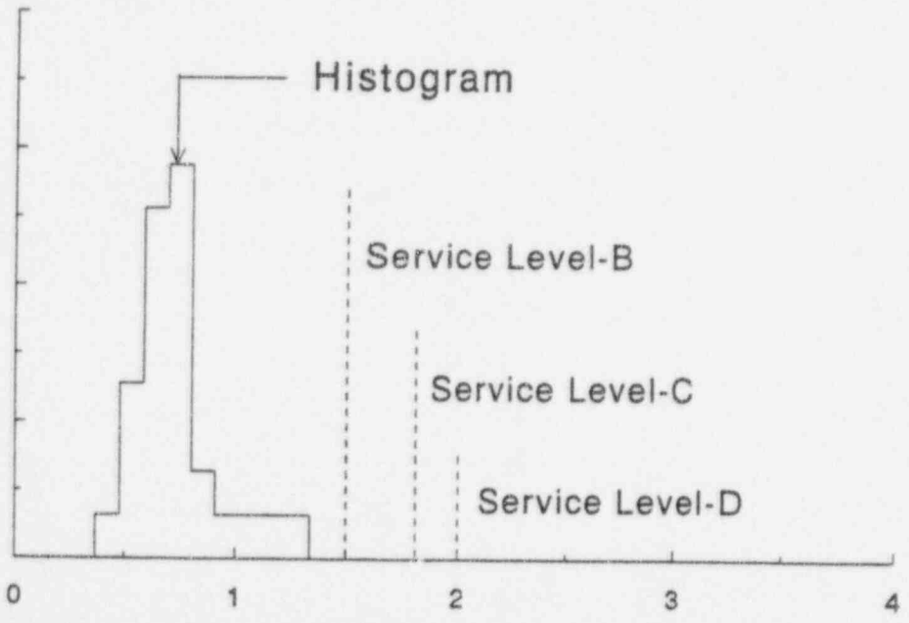

(b) ASME code S_y-based assessment

Figure 3.1 Normal operating + safe shut-down earthquake (N+SSE) design stresses for piping in several actual operating U.S. nuclear plants (Ref. 3.5)

Table 3.1 Normal operating + safe shut-down earthquake (N+SSE) stresses for A106 Grade B carbon steel and TP304 stainless steel pipes based on N+SSE stresses from piping in several actual operating U.S. nuclear plants

Stress	A106 Grade B, MPa (psi)	TP304, MPa (psi)
S_y (Ref 3.7)	186.9 (27,100)	129.6 (18,800)
S_m (Ref 3.7)	124.8 (18,100)	116.9 (16,950)
Maximum from histogram using S_y	252.3 (36,585)	175.0 (25,380)
Maximum from histogram using S_m	187.2 (27,150)	175.3 (25,425)
Mean from histogram using S_y	137.9 (20,000)	95.7 (13,875)
Mean from histogram using S_m	103.6 (15,025)	72.2 (14,070)
Minimum from histogram using S_y	69.1 (10,025)	48.0 (6,955)
Minimum from histogram using S_m	52.2 (7,565)	48.9 (7,085)

Table 3.2 Maximum moments at normal operating + safe shut-down earthquake (N+SSE) stress conditions for the IPIRG simulated seismic test specimens

Condition	A106 Grade B, kN-m (in-lb)	TP304, kN-m (in-lb)
Maximum from histogram using S_y	536.9 (4,752,000)	321.0 (2,841,000)
Maximum from histogram using S_m	355.1 (3,143,000)	321.8 (2,848,000)
Mean from histogram using S_y	217.3 (1,923,000)	99.2 (878,000)
Mean from histogram using S_m	121.3 (1,074,000)	102.9 (911,000)
Minimum from histogram using S_y	25.0 (221,000)	NA*
Minimum from histogram using S_m	NA*	NA*

* Pressure stress alone exceeds total N+SSE stress

Table 3.3 Comparison of the IPIRG-2 SSE level and typical nuclear plant SSE's

Plant	SSE
IPIRG-2 pipe system	0.20 g
B&W-205 3600 MW PWR	0.30 g
Westinghouse standardized four-loop, single unit 3425 MW NSSS	0.40 g
Zion PWR	0.17 g
Clinton BWR	0.26 g
Westinghouse AP600	0.30 g

Table 3.4 Selected results of basic IPIRG-2 seismic forcing function scaling analyses

Acceleration	A106 Grade B	TP304
1.25 g	surface-crack penetration at 7.6 seconds	97-percent of the moment needed for surface-crack penetration
1.38 g	surface-crack penetration at 2.9 seconds	99-percent of the moment needed for surface-crack penetration
1.50 g	surface-crack penetration at 2.4 seconds	surface-crack penetration at 2.9 seconds

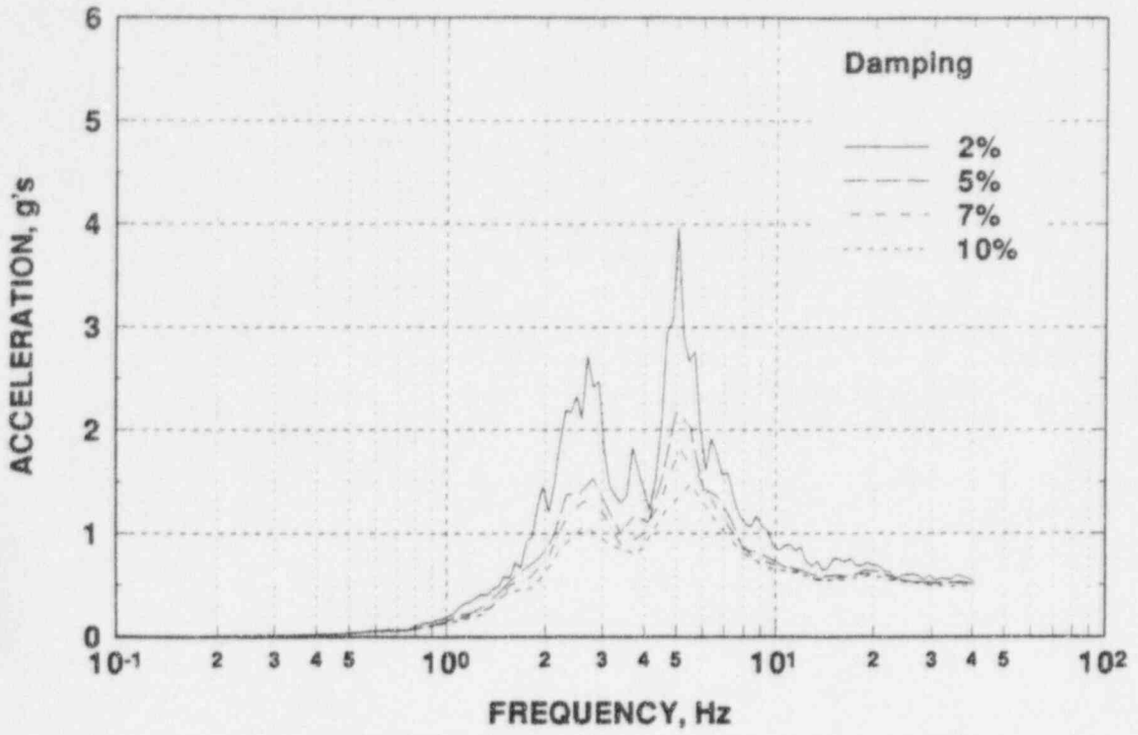

Figure 3.2 IPIRG-2 SSE (0.2 g) actuator response spectra

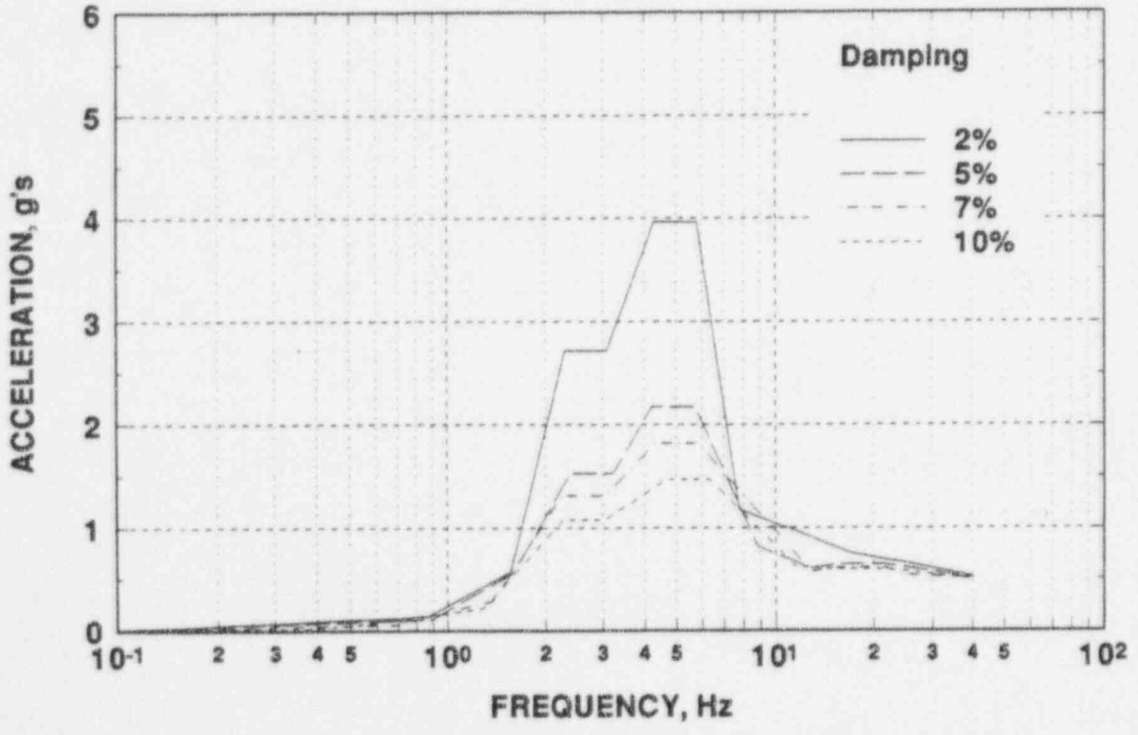

Figure 3.3 Broadened IPIRG-2 SSE actuator response spectra

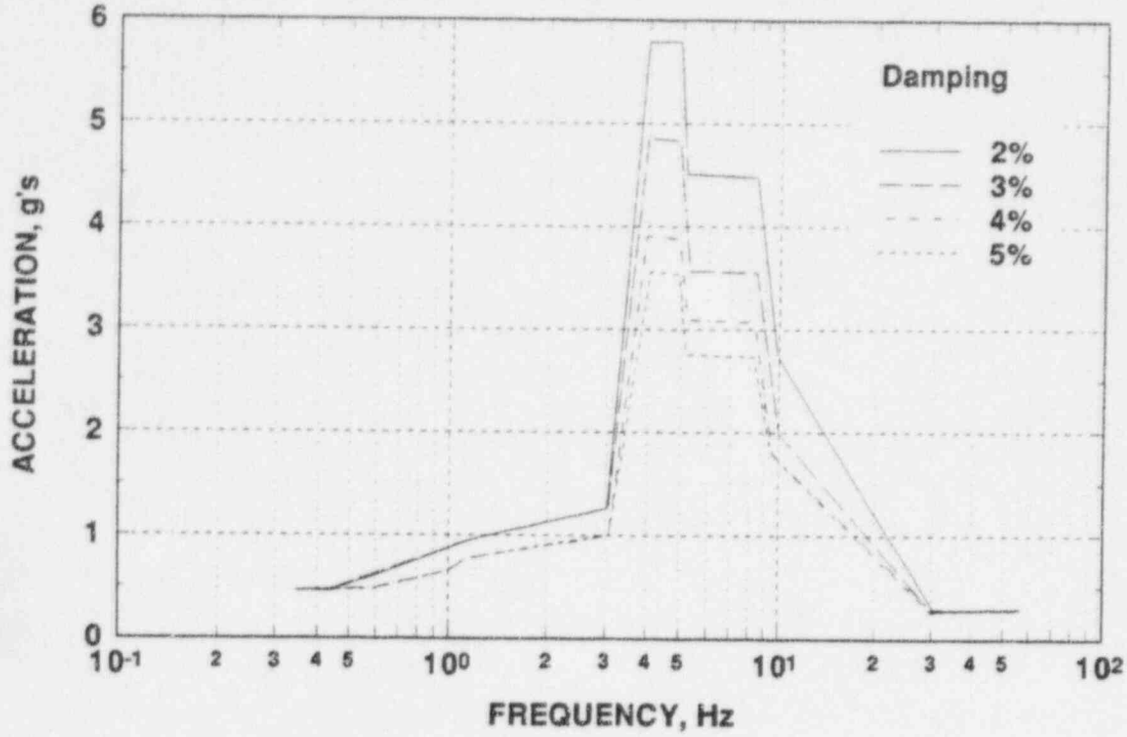

Figure 3.4 Typical SSE Floor response spectra from the South Texas nuclear plant

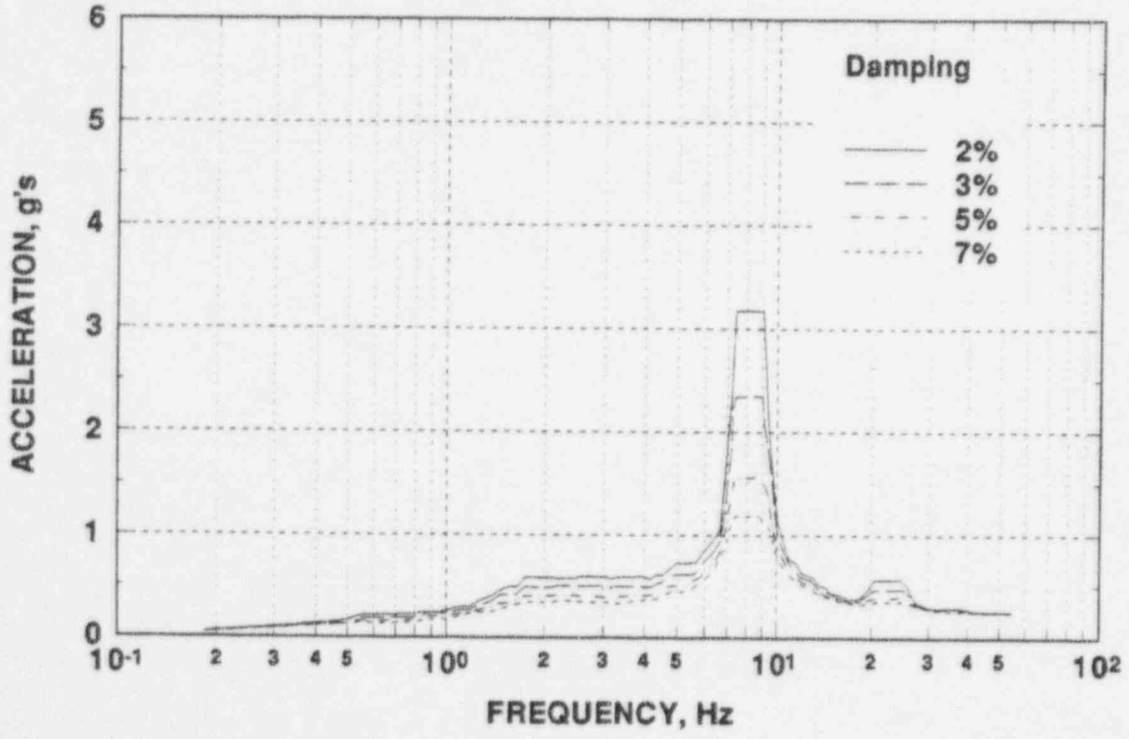

Figure 3.5 Typical SSE floor response spectra from the TVA Watts Bar nuclear plant

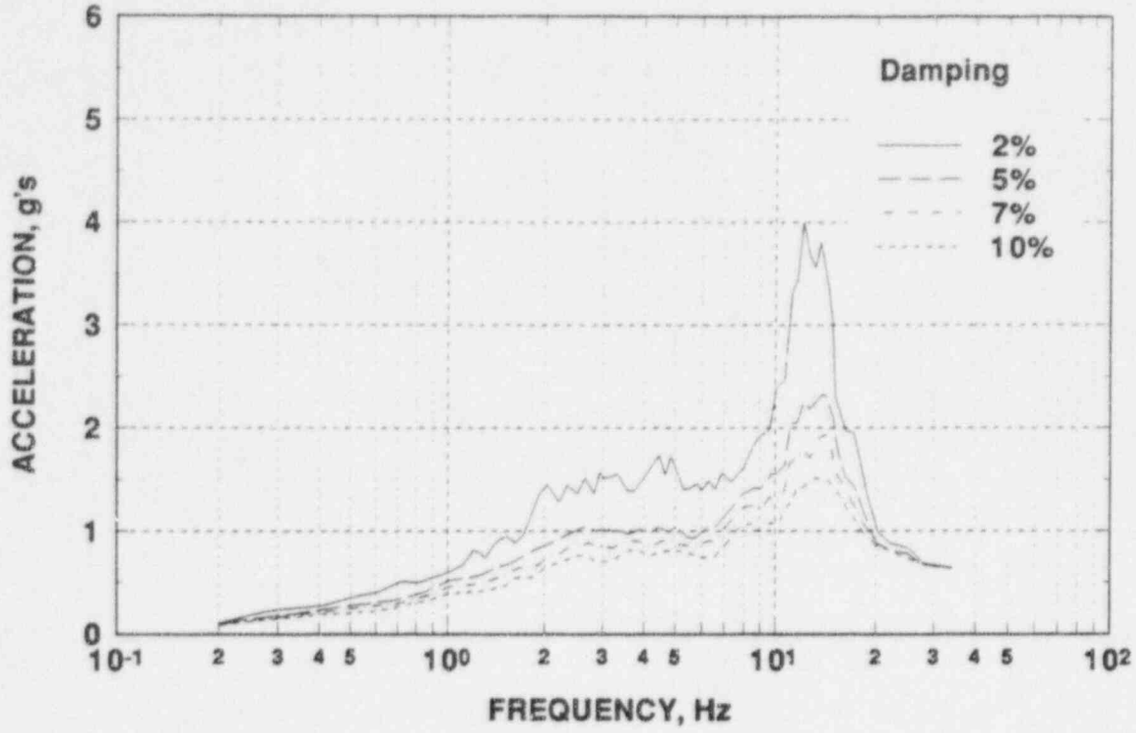

Figure 3.6 Typical SSE floor response spectra for the Westinghouse AP600 nuclear plant design

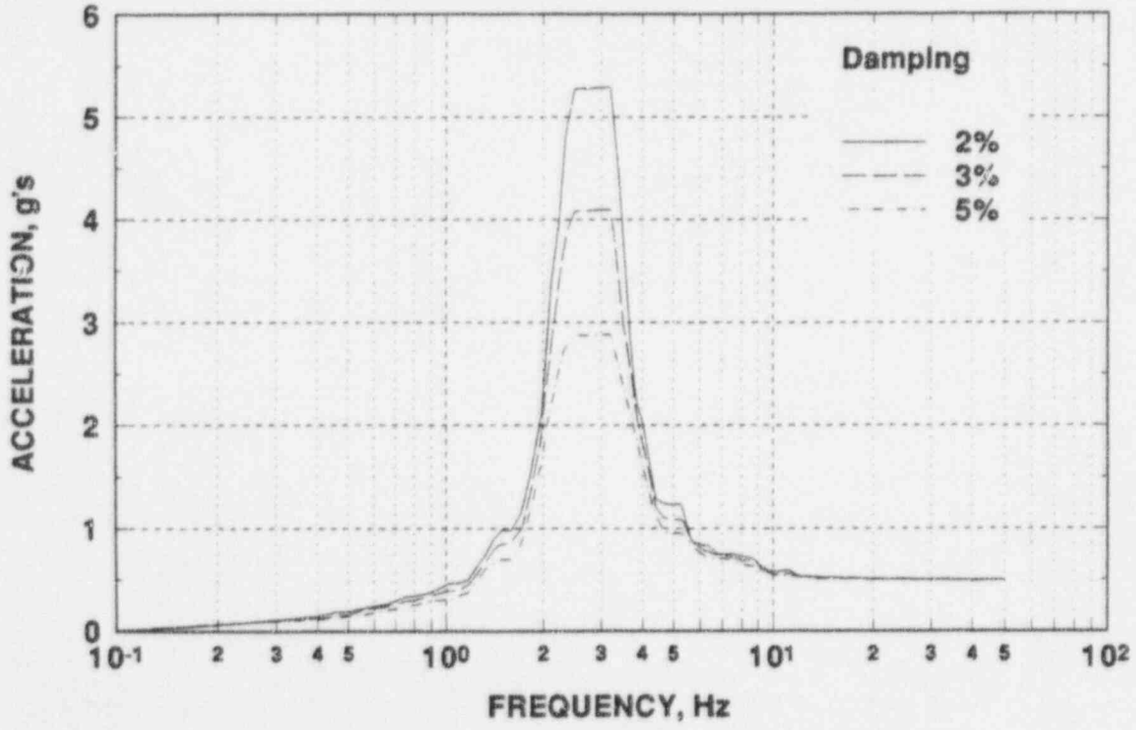

Figure 3.7 Typical SSE floor response spectra for the Advanced Reactor Corporation FOAKE nuclear plant design

3.4 Scaling to Establish Surface Crack "Test" and "Decision Tree" Loading

Scaling of the basic IPIRG-2 seismic forcing function to define the "test" and "decision tree" excitation levels involved extensive nonlinear-spring finite element calculations. Nonlinear stiffnesses were assumed for the A106 Grade B and TP304 surface cracks, the basic IPIRG-2 seismic forcing function was scaled, and time history analyses of both cracks were performed. The objective was to find one scaling factor for the "test" level excitation that could be used for both cracks. The constraint was that surface-crack penetration should occur some time during the 20-second duration of the load and preferably some time after 3-4 seconds.

Figures 3.8 and 3.9 show the available experimental records and analytical predictions for the surface cracks that were to be tested in the IPIRG-2 simulated seismic experiments. In order to accommodate the rather large range in possible maximum moment, 400 kN-m (3,540,000 in-lb) to 600 kN-m (5,310,000 in-lb), and large range in required rotation, 0.02 to 0.035 radians, a delicate balancing act between finding a suitable scaling factor and the constraints mentioned above was required. In the end, it was decided to use the SC.TNP J-estimation scheme (Ref. 3.3) predictions for ideal 66-percent deep, 50-percent of the circumference long surface cracks as the design basis for scaling the forcing function. Because of a desire to know whether or not the resulting through-wall crack would run completely around the pipe circumference after the surface crack penetrated the pipe wall (a DEGB), nonlinear-spring finite element calculations were carried out beyond surface-crack penetration. To perform these predictions, through-wall-cracked pipe moment-rotation data were needed. Figures 3.10 and 3.11 show the surface-cracked pipe and companion through-wall-cracked pipe moment-rotation curves used in the analyses.

The approach used to scale the basic seismic forcing function to the "test" level was to just try various excitation levels until a suitable level was found. Analyses were performed with both the A106 Grade B flaw and the TP304 flaw. Because the analyses become nonlinear, particularly as a flaw nears surface-crack penetration, there is no convenient way to predict how to scale the excitation for a subsequent analysis. Furthermore, the differences between the A106 Grade B flaw and the TP304 flaw are significant enough that the behavior of one flaw cannot be predicted knowing the behavior of the other flaw. To limit the amount of resources required to do the "test" scaling, "super-element" finite element models were used in which all the linear portions of the finite element pipe system model are lumped into a few selected degrees of freedom connected by the nonlinear crack springs.

Table 3.4 shows selected results of the "test" forcing function scaling analyses. Figures 3.12 to 3.15 show the nonlinear-spring finite element results at 1.25 g scaling factor. On the basis of the results shown in Table 3.4, it was decided that the "test" forcing function would be fixed at 1.25 g and that the "decision tree" excitation would be 1.38 g. Checking the effect of using the "super-element" model (super elements do not give exactly the same result as full models), the A106 Grade B flaw was found to reach surface-crack penetration at 4.01 seconds and to have no moment carrying capacity (i.e., a DEGB) at 4.05 seconds, see Figures 3.16 and 3.17. The TP304 flaw was predicted to reach 99-percent of the moment required for surface-crack penetration at 1.25 g with the full model as illustrated in Figures 3.18 and 3.19.

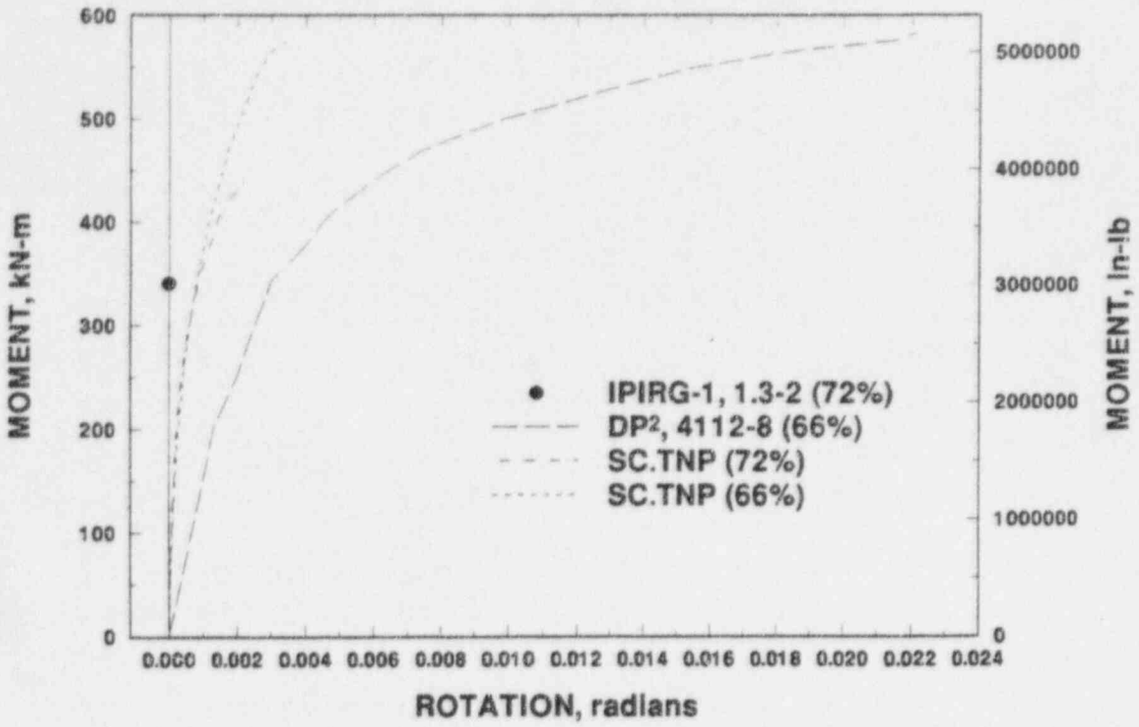

Figure 3.8 A106 Grade B surface-cracked pipe data for scaling the IPIRG-2 "test" simulated seismic forcing function

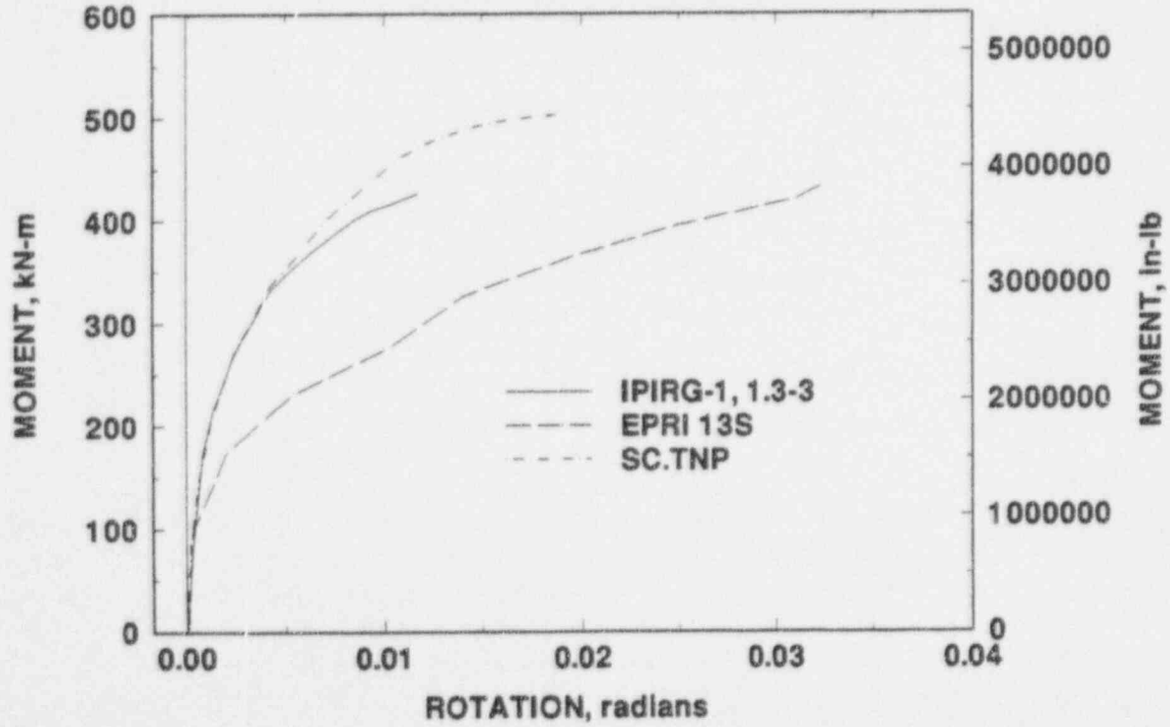

Figure 3.9 Type 304 surface-cracked pipe data for scaling the IPIRG-2 "test" simulated seismic forcing function

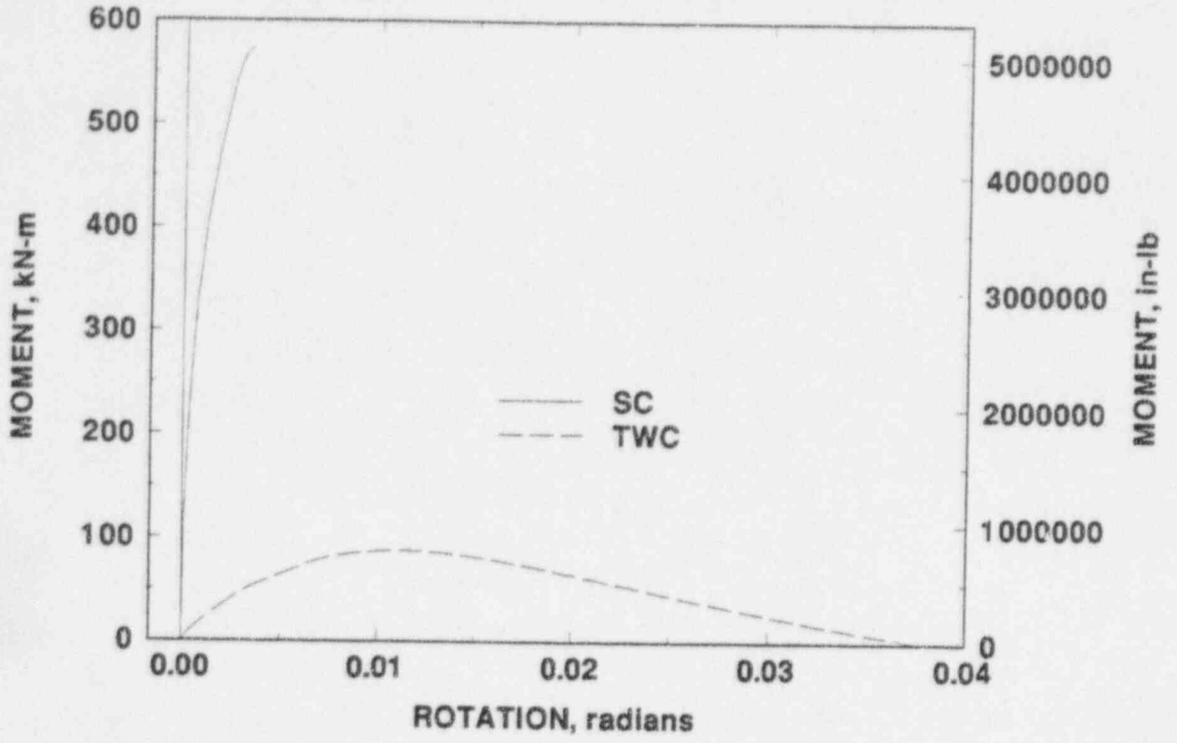

Figure 3.10 A106 Grade B crack behavior used in scaling the IPIRG-2 "test" simulated seismic forcing function

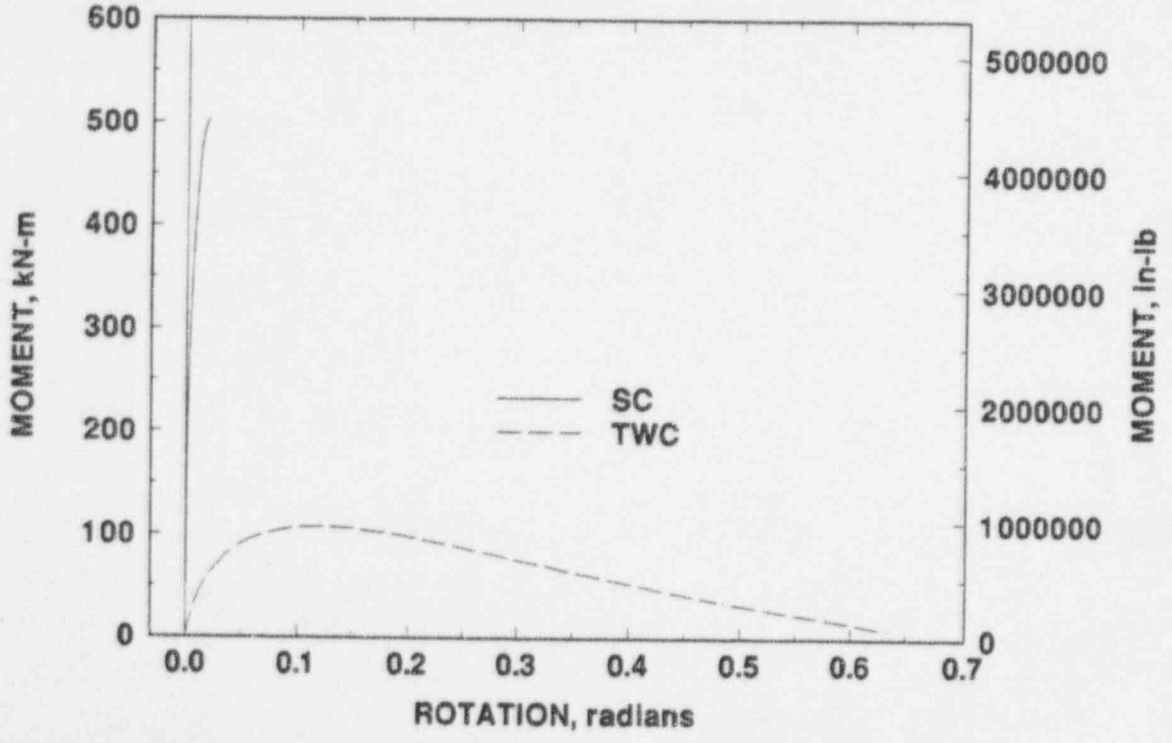

Figure 3.11 TP304 crack behavior used in scaling the IPIRG-2 "test" simulated seismic forcing function

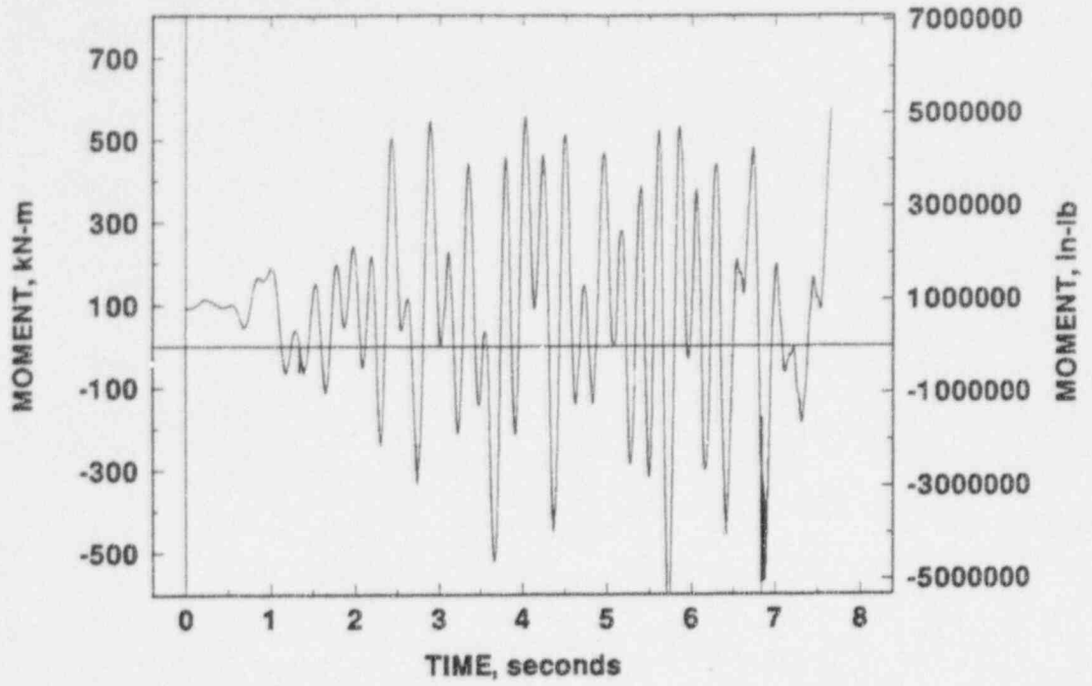

Figure 3.12 IPIRG-2 seismic forcing function scaling result for a 66-percent deep, 180-degree surface crack in base metal of an A106 Grade B pipe at 1.25 g using a "super-element" finite element model

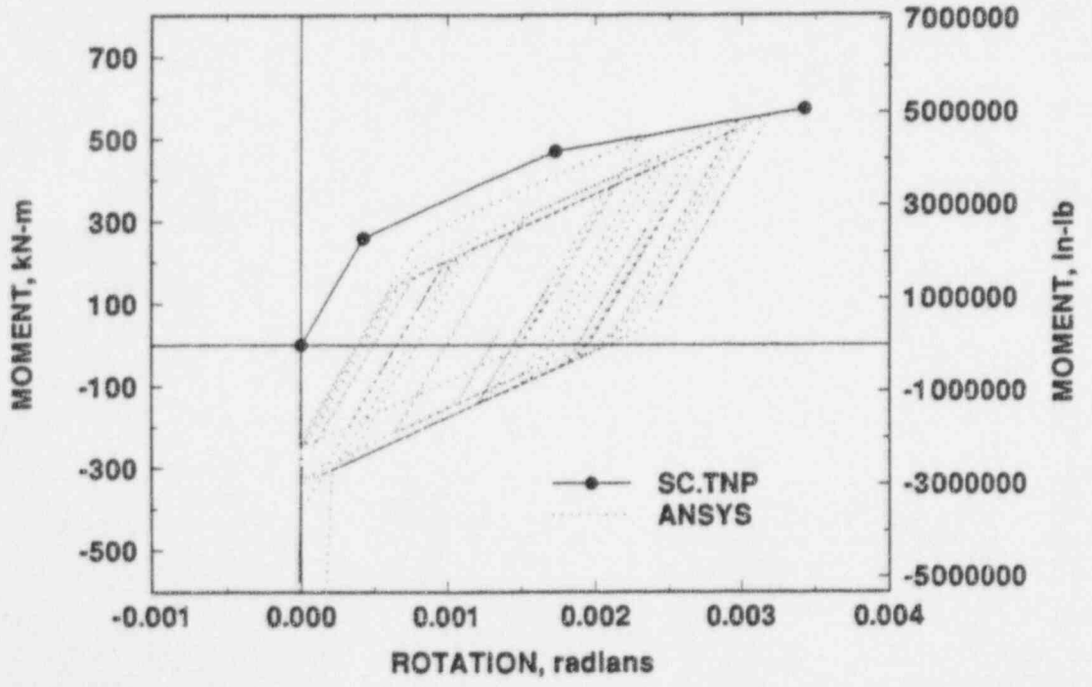

Figure 3.13 "Super-element" finite element model crack response at 1.25 g for a 66-percent deep, 180-degree surface crack in base metal of an A106 Grade B pipe in the IPIRG pipe system

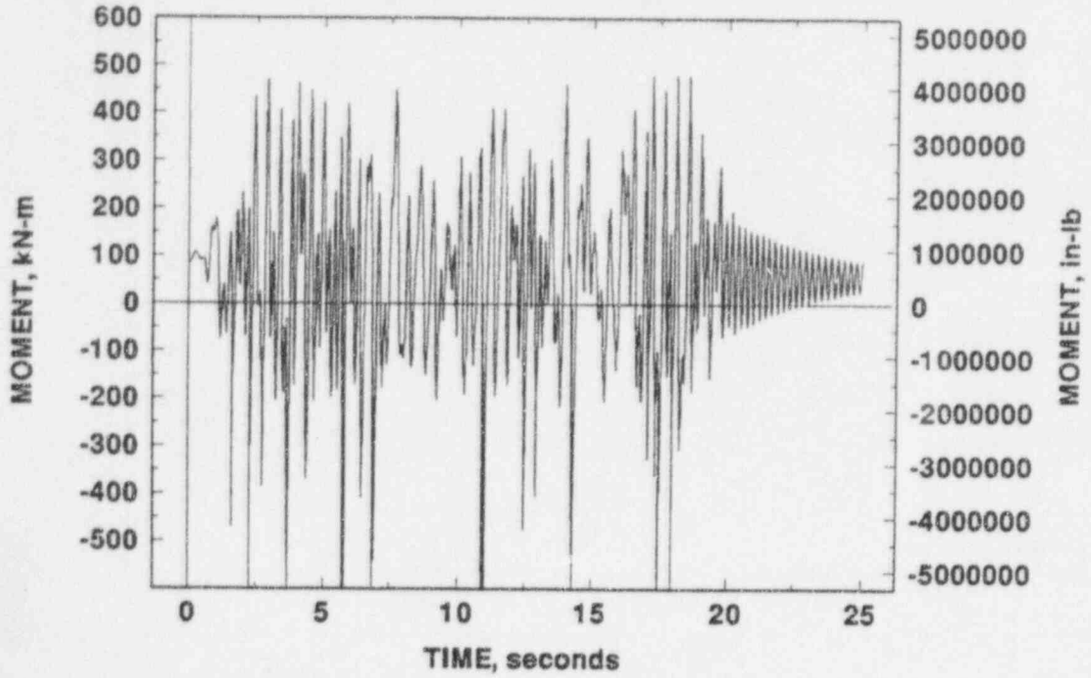

Figure 3.14 IPIRG-2 seismic forcing function scaling result for a 66-percent deep, 180-degree surface crack in base metal of a TP304 pipe at 1.25 g using a "super-element" finite element model

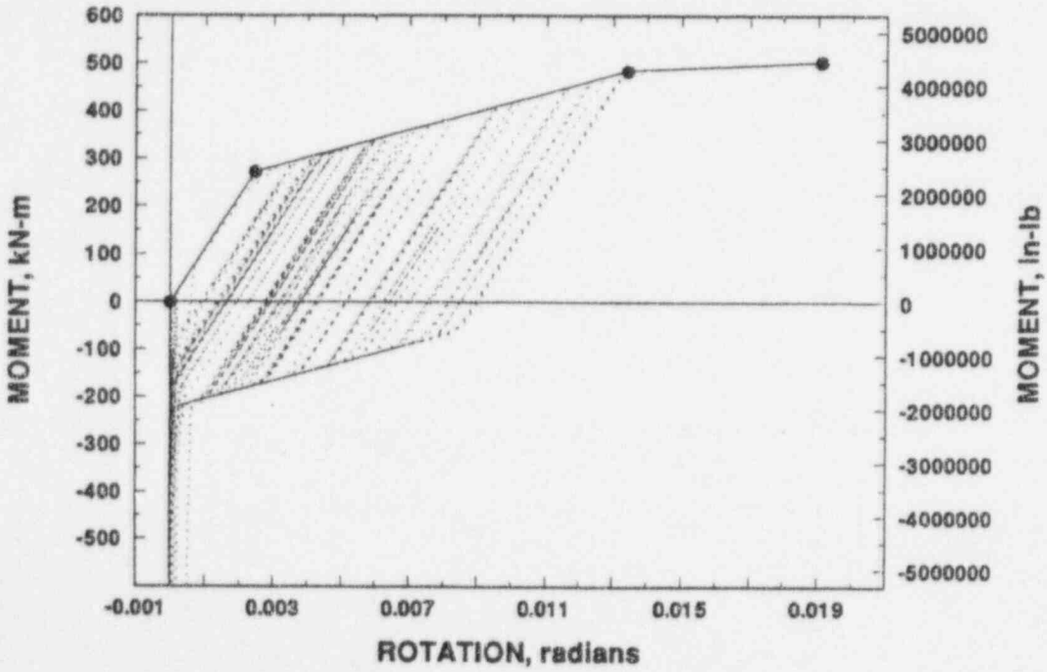

Figure 3.15 "Super-element" finite element model crack response at 1.25 g for a 66-percent deep, 180-degree surface crack in base metal of a TP304 pipe in the IPIRG pipe system

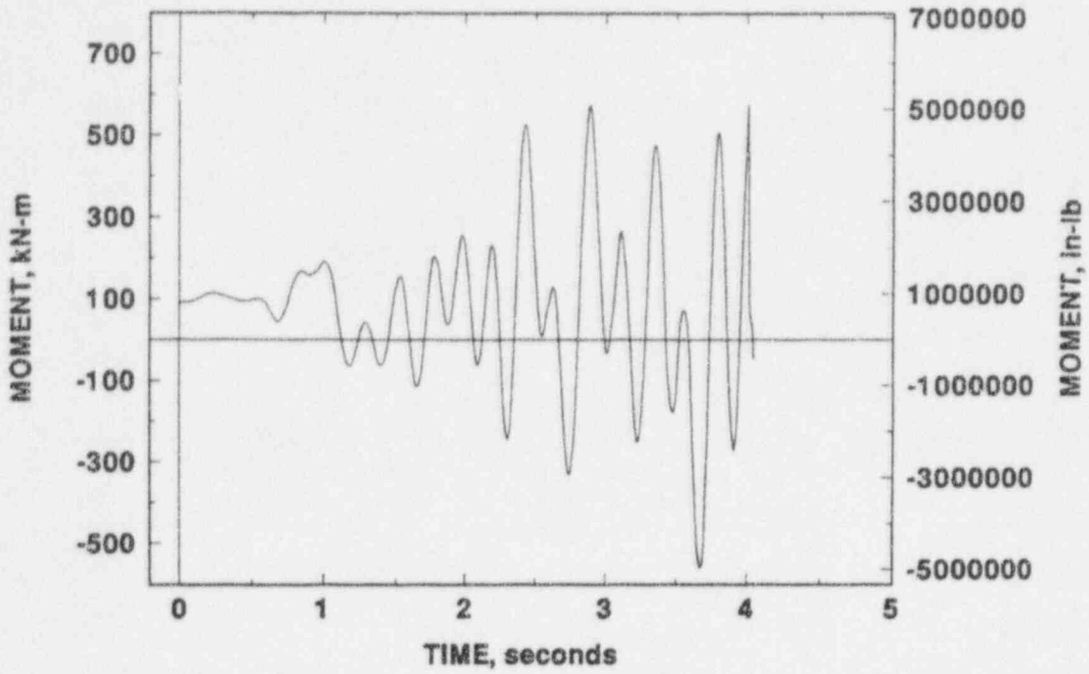

Figure 3.16 IPIRG-2 seismic forcing function scaling result for a 66-percent deep, 180-degree surface crack in the base metal of an A106 Grade B pipe at 1.25 g using a full finite element model

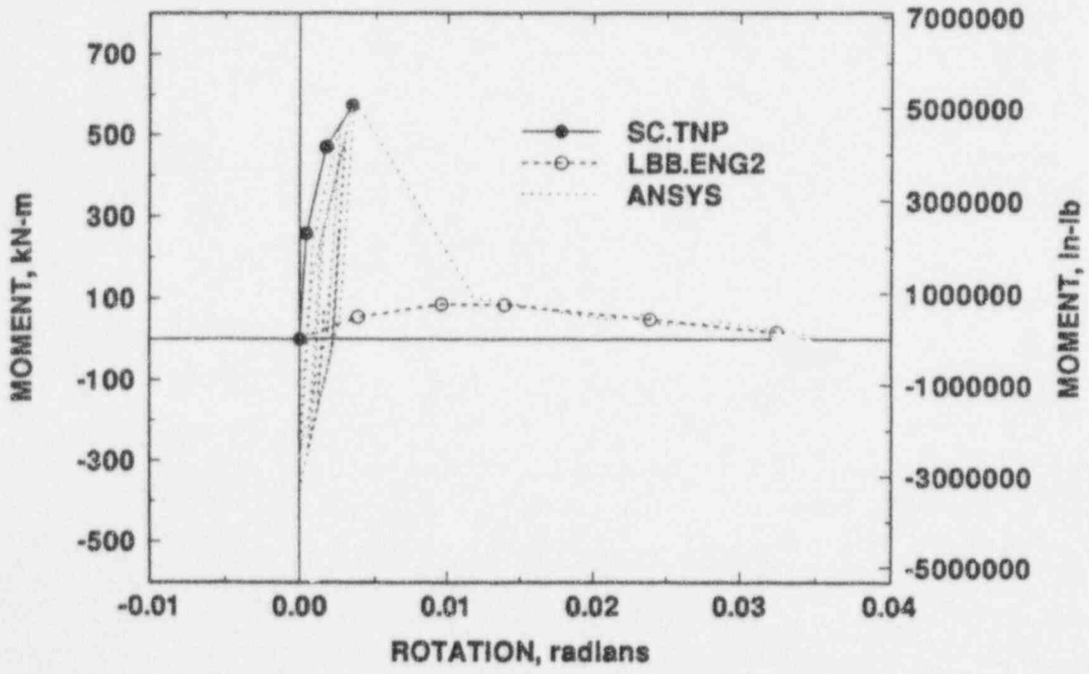

Figure 3.17 Full finite element model crack response at 1.25 g for a 66-percent deep, 180-degree surface crack in the base metal of an A106 Grade B pipe in the IPIRG pipe system

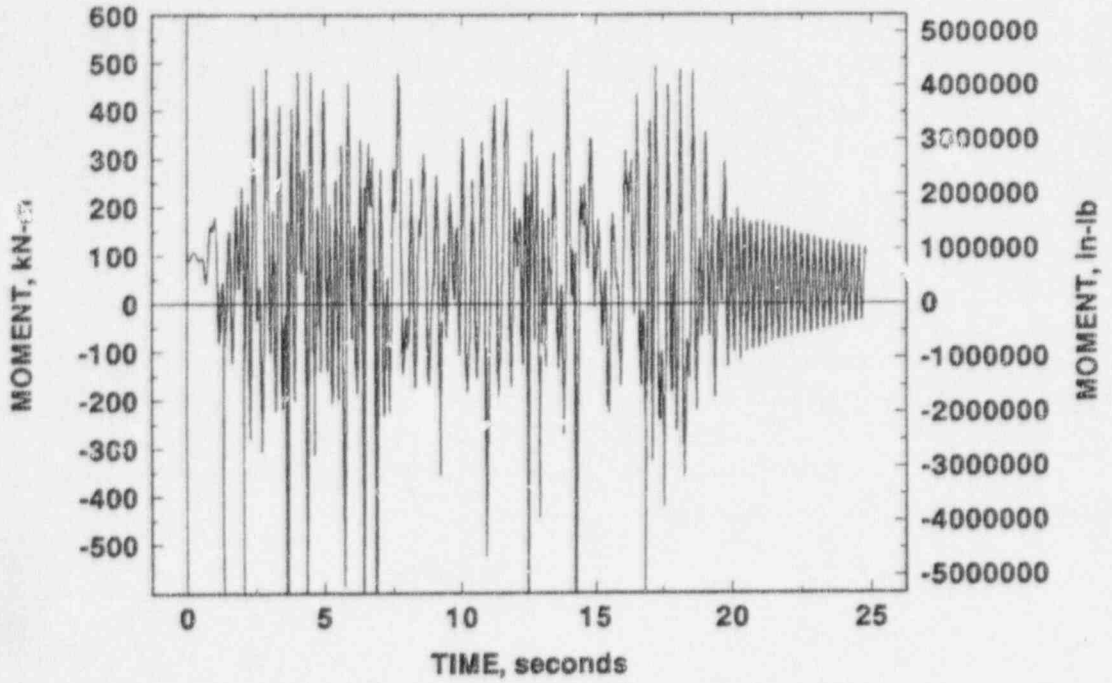

Figure 3.18 IPIRG-2 seismic forcing function scaling result for a 66-percent deep, 180-degree surface crack in the base metal of a TP304 pipe at 1.25 g using a full finite element model

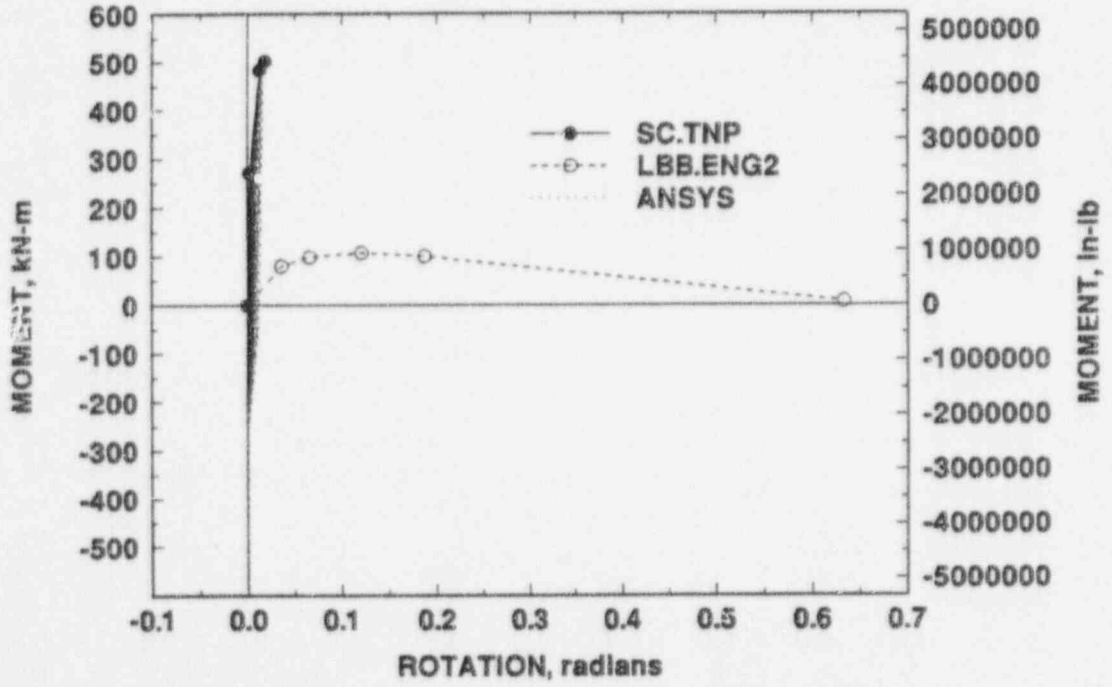

Figure 3.19 Full finite element model crack response at 1.25 g for a 66-percent deep, 180-degree surface crack in the base metal of a TP304 pipe in the IPIRG pipe system

3.5 Scaling to Establish Through-Wall Crack "Test" and "Decision Tree" Loading

The simulated seismic through-wall-cracked pipe experiment required a scaling factor different from the surface-cracked pipe experiments, because the moment-rotation behavior of the through-wall flaw was drastically different from the surface flaws. A J-estimation scheme prediction of the expected through-wall-cracked pipe behavior for a 12-percent of the circumference long crack, using the LBB.ENG2 method from NRCPIPE Version 1.4F, was the basis for selecting the flaw size for the simulated seismic and companion quasi-static short through-wall-cracked pipe experiments. The design-basis through-wall-cracked pipe moment-rotation response is shown in Figure 3.20, along with predictions and data for surface cracks either tested in the IPIRG pipe system or in related experimental programs. The moment-carrying capacity of the design-basis through-wall-cracked pipe is substantially above all of the surface-cracked pipe.

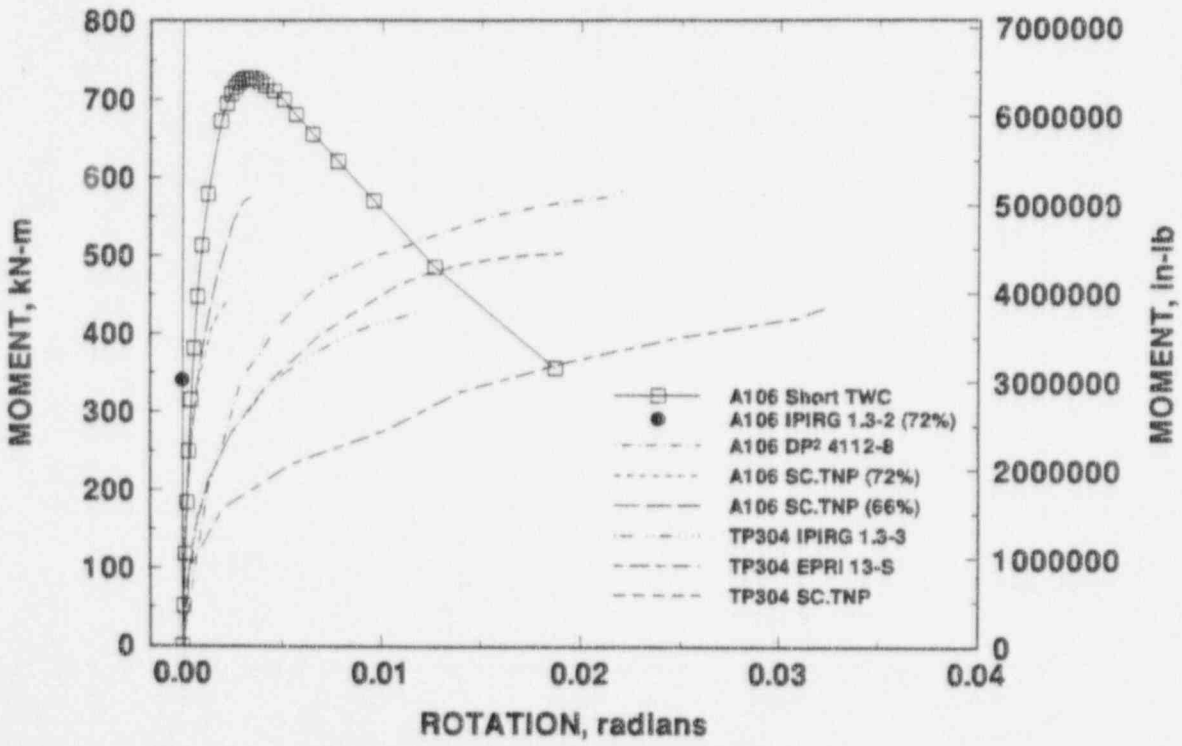

Figure 3.20 Comparison of predicted short through-wall-cracked pipe behavior and surface-cracked pipe experimental data and predictions

The limiting criterion for scaling the basic seismic forcing function for the seismic through-wall-cracked pipe was yielding of the pipe loop remote from the cracked section. Based on 288 C (550 F) stress-strain tests conducted on the straight pipe and elbow materials in IPIRG-1, the maximum allowable stress that would ensure that yielding would not occur was 380 MPa (55,100 psi). Nonlinear spring cracked pipe finite element analyses performed at scaling factors of 3.75 g,, 2.0 g, and 1.5 g excitation levels indicated that stresses remote from the cracked section met the this criterion only at 1.5 g's and below. It was, therefore, decided to fix the scaling for the short through-wall-cracked pipe experiment at 1.50 g.

Data that became available from the companion, IPIRG-2 quasi-static, short through-wall-cracked pipe experiment suggested that the moment-carrying capacity could be as high as 1.05 MN-m. The predicted moment for the through-wall-cracked pipe for the first 6 seconds of the load history at 1.50 g's, using the IPIRG-2 companion quasi-static experimental moment-rotation curve, reaches a maximum of only 747 kN-m (6,611,000 in-lb), which is well short of the maximum moment of the quasi-static experiment. However, because of the stress-based excitation limit, the 1.50 g limitation had to be adhered to. As a consequence, some amount of low cycle fatigue damage or toughness degradation would have to occur before the flaw could grow in ductile tearing.

As far as a "decision tree" level of excitation for the short through-wall crack seismic experiment, it was decided to apply a second 1.50 g loading if it was required. Consistent with the seismic surface crack experiments, the 0.2 g SSE loading was to be applied before the "test" loading.

3.6 Seismic Forcing Function Scaling Companion Analyses

Two companion analyses were performed to supplement the forcing function scaling. The first analysis determined the contribution to the crack-opening moment due to inertial loads and the stress ratio and the second analysis calculated the hydraulic oil requirements for the IPIRG pipe system servo-hydraulic system.

Throughout the conduct of the IPIRG-1 pipe system experiments, there was a concern that the loading on the crack be a reasonable mixture of inertial- and displacement-controlled stresses. In addition, it was felt that knowledge of the stress ratio was important to put the pipe test results in perspective with material property tests conducted at various stress ratios.

Although there is no universally accepted method for defining the fraction of each type of load in a combined-load test, the definition that was adopted for the IPIRG experiments was

$$I = 100 \frac{(M_t - M_{sp})}{M_t} \qquad (3\text{-}1)$$

where

I = load due to pipe inertia, percent

M_t = total moment at surface-crack penetration

M_{sp} = moment due to a static push at the actuator displacement at the time of surface-crack penetration.

The percent inertial load represents the fraction of moment applied to the test section above what would be experienced in a quasi-static test. The stress ratio, because the cycles are not constant amplitude in a seismic test, was taken as the ratio of the minimum stress to the maximum stress on the cycle at surface crack penetration. (The minimum and maximum stress values include the stress contribution due to the internal pipe pressure.) Table 3.5 lists the percent inertial load and stress ratio for the "test" level loading. The inertial load contributes about half of the stress at surface-crack penetration and the stress goes reasonably compressive.

The primary concern for the servo-hydraulic system in conducting the IPIRG-2 simulated seismic experiments was capacity of the hydraulic accumulators. The hydraulic oil demand for anything but the slowest forcing function is significantly greater than the installed hydraulic pump capacity. Consequently, the majority of oil supplied to the IPIRG pipe system servo-hydraulic system comes from accumulators close-coupled to the servo-valve. There is a limitation, however, on the duration of a forcing function due to the finite capacity of the accumulators - when the accumulators run out of oil, the actuator goes out of control. When the IPIRG pipe system was designed during IPIRG-1, the accumulator capacity was sized only for a relatively short-duration single-frequency excitation. The IPIRG-2 simulated seismic function at 20 seconds long is significantly more taxing and it was anticipated that additional accumulator capacity would need to be added to conduct the IPIRG-2 simulated seismic experiments.

Table 3.6 is a summary of the accumulator requirements for the three IPIRG-2 simulated seismic load levels. Because only 378.5 liters (100 gallons) was installed when the facility was originally built, an additional 378.5 liters (100 gallons) was installed to accommodate the seismic tests. Actuator force and stroke capacity were more than adequate.

Table 3.5 Inertial loading and stress ratio for the IPIRG-2 "test" level simulated seismic loading

Item	A106 Grade B	TP304
Percent inertial loading	60.0	52.3
Stress ratio, R	-0.53	-0.60

Table 3.6 Hydraulic accumulator demands for the IPIRG-2 simulated seismic experiments

Loading	Acceleration	Required Capacity, liters (gallons)
SSE	0.2 g	85 (22.5)
Test	1.25 g	532 (140.5)
Decision tree	1.38 g	585 (154.5)

3.7 Summary

The scaling of the basic seismic forcing function proceeded rather like the design of the function in that knowledge of nuclear plant seismic characteristics guided a number of arbitrary choices. Because of this, the resulting scaled functions seem rational. Some compromises had to be made in scaling the basic function for the "test" level loading for the short through-wall-cracked pipe to avoid damage to the pipe loop. As far as the operational requirements for applying the scaled forcing functions, additional accumulator capacity was found to be needed.

3.8 References

3.1 Olson, R., Scott, P., and Wilkowski, G., "Application of a Nonlinear Spring Element to Analysis of Circumferentially Cracked Pipe Under Dynamic Loads," in Pressure Vessel Fracture, Fatigue, and Life Management, ASME PVP Vol. 233, pp 279-292, June 1992.

3.2 Olson, R. J., Wolterman, R. L., Wilkowski, G. M., and Kot, C. A., "Validation of Analysis Methods for Assessing Flawed Piping Subjected to Dynamic Loading," NUREG/CR-6234, U.S. Nuclear Regulatory Commission, August 1994.

3.3 Scott, P. M., and Ahmad, J., "Experimental and Analytical Assessment of Circumferentially Surface-Cracked Pipes Under Bending," NUREG/CR-4872, U.S. Nuclear Regulatory Commission, April 1987.

3.4 Brust, F. W., "Approximate Methods for Fracture Analyses of Through-Wall Cracked Pipes," NUREG/CR-4853, U.S. Nuclear Regulatory Commission, February 1987.

3.5 ANSYS Engineering Analysis System User's Manual, Revision 4.4A, ANSYS, Inc., Houston, Pennsylvania, 15342, May 1989.

3.6 Rahman, S., Ghadiali, N., Paul, D., and Wilkowski, G., "Probabilistic Pipe Fracture Evaluations for Leak-Rate Detection Applications," NUREG/CR-6004, U.S. Nuclear Regulatory Commission, April 1995.

3.7 American Society of Mechanical Engineers, Boiler and Pressure Vessel Code, Section III - Division 1, Appendix I: Design Stress Intensity Values, Allowable Stresses, Material Properties, and Design Fatigue Curves pp 6-7, 24-25, 50-51, 66-67, 1989.

4.0 SUMMARY

The procedure for designing and selecting a "seismically inspired" forcing function for the IPIRG-2 simulated seismic pipe system experiments has been presented. The procedure used design tools and modeling assumptions that are consistent with nuclear plant analysis and plant design details. In contrast to typical plant design, however, the analyses are focussed on the time domain, because in the IPIRG-2 experiments we are concerned about a significantly nonlinear event, the growth of large cracks.

The objective of the study was to define the actuator motion for three load levels and to provide data for a decision on whether or not the hydraulic system accumulator capacity for the IPIRG pipe system needed to be increased. Both objectives were fulfilled. Because the methodology used to define the seismic forcing function is so closely related to actual plant design procedures and the data assumed for the analyses are quite realistic, aside from the idealizations embodied in the IPIRG pipe loop itself, the IPIRG simulated seismic test are able to be transferred to actual plant behavior.

NRC FORM 335 (2-89) NRCM 1102, 3201, 3202

U.S. NUCLEAR REGULATORY COMMISSION

BIBLIOGRAPHIC DATA SHEET

(See instructions on the reverse)

1. REPORT NUMBER (Assigned by NRC. Add Vol., Supp., Rev., and Addendum Numbers, if any.)

NUREG/CR-6439
BMI-2186

2. TITLE AND SUBTITLE

Design of the IPIRG-2 Simulated Seismic Forcing Function

3. DATE REPORT PUBLISHED

MONTH: February | YEAR: 1996

4. FIN OR GRANT NUMBER

D2060

5. AUTHOR(S)

R. Olson, P. Scott, and G. Wilkowski

6. TYPE OF REPORT

Technical

7. PERIOD COVERED (Inclusive Dates)

10/91 - 1/96

8. PERFORMING ORGANIZATION – NAME AND ADDRESS (If NRC, provide Division, Office or Region, U.S. Nuclear Regulatory Commission, and mailing address; if contractor, provide name and mailing address.)

Battelle
505 King Avenue
Columbus, OH 43201-2693

9. SPONSORING ORGANIZATION – NAME AND ADDRESS (If NRC, type "Same as above"; if contractor, provide NRC Division, Office or Region, U.S. Nuclear Regulatory Commission, and mailing address.)

Division of Engineering Technology
Office of Nuclear Research
U.S. Nuclear Regulatory Commission
Washington, D.C. 20555-0001

10. SUPPLEMENTARY NOTES

M. Mayfield, NRC Project Manager

11. ABSTRACT (200 words or less)

A series of pipe system experiments was conducted in IPIRG-2 that used a realistic seismic forcing function. Because the seismic forcing function was more complex than the single-frequency increasing-amplitude sinusoidal forcing function used in the IPIRG-1 pipe system experiments, considerable effort went into designing the function. This report documents the design process for the seismic forcing function used in the IPIRG-2 pipe system experiments.

12. KEY WORDS/DESCRIPTORS (List words or phrases that will assist researchers in locating the report.)

Earthquake, seismic, pipe, nuclear, crack, fracture, surface crack, through-wall crack, circumferential crack, time-history

13. AVAILABILITY STATEMENT

Unlimited

14. SECURITY CLASSIFICATION

(This Page)
Unclassified

(This Report)
Unclassified

15. NUMBER OF PAGES

16. PRICE

Federal Recycling Program

UNITED STATES
NUCLEAR REGULATORY COMMISSION
WASHINGTON, DC 20555-0001

120555139531 1 1AN1R5
US NRC-OADM
DIV FOIA & PUBLICATIONS SVCS
TPS-PDR-NUREG
2WFN-6F7
WASHINGTON DC 20555